Modeling and halftoning for multichannel printers: a spectral approach

Radovan Slavuj

Thesis submitted to Gjøvik University College
for the degree of Doctor of Philosophy in Computer Science

2015

Modeling and halftoning for multichannel printers: A spectral approach

Faculty of Computer Science and Media Technology
Gjøvik University College

Modeling and Halftoning for Multichannel Printers: A Spectral Approach / Radovan Slavuj
Doctoral Dissertations at Gjøvik University College 4-2015
ISBN: 978-82-8340-021-2
ISSN: 1893-1227

To those who I love and who have been with me the last 15 years ...

Declaration of Authorship

I, Radovan Slavuj, hereby declare that this thesis and the work presented in it is entirely my own. Where I have consulted the work of others, this is always clearly stated.

Signed:

(Radovan Slavuj)

Date:

Summary

Printing has been has been the major communication medium for many centuries. In the last twenty years, multichannel printing has brought new opportunities and challenges. Beside of extended colour gamut of the multichannel printer, the opportunity was presented to use a multichannel printer for 'spectral printing'. The aim of spectral printing is typically the same as for colour printing; that is, to match input signal with printing specific ink combinations. In order to control printers so that the combination or mixture of inks results in specific colour or spectra requires a spectral reflectance printer model that estimates reflectance spectra from nominal dot coverage.

The printer models have one of the key roles in accurate communication of colour to the printed media. Accordingly, this has been one of the most active research areas in printing. The research direction was toward improvement of the model accuracy, model simplicity and toward minimal resources used by the model in terms of computational power and usage of material.

The contribution of the work included in the thesis is also directed toward improvement of the printer models but for the multichannel printing. The thesis is focused primarily on improving existing spectral printer models and developing a new model. In addition, the aim was to develop and implement a multichannel halftoning method which should provide with high image quality. Therefore, the research goals of the thesis were: maximal accuracy of printer models, optimal resource usage and maximal image quality of halftoning and whole spectral reproduction system.

Maximal colour accuracy of a model but with the least resources used is achieved by optimizing printer model calibration process. First, estimation of the physical and optical dot gain is performed with newly proposed method and model. Second, a custom training target is estimated using the proposed new method. These two proposed methods and one proposed model were at the same time the means of optimal resource usage, both in computational time and material. The third goal was satisfied with newly proposed halftoning method for multichannel printing. This method also satisfies the goal of optimal computational time but with maintaining high image quality. When applied in spectral reproduction workflow, this halftoning reduces noise induced in an inversion of the printer model. Finally, a case study was conducted on the practical use of multichannel printers and spectral reproduction workflow. In addition to a gamut comparison in colour space, it is shown that otherwise limited reach of spectral printing could potentially be used to simulate spectra and colour of textile fabrics.

Acknowledgements

First, I would like expresses my deepest gratitude to my supervisors, prof. Jon Yngve Hardeberg with whom have been enjoyment and honor to walk through the various research topics and to Dr. Peter Nussbaum whose composure and structure have kept me with the two feet on the ground.

Also, I would like to express my gratitude to Ludovic G. Coppel for his contribution in research in the thesis; it was absolute pleasure to work with him. I am sure if we would work together couple of more years, we would create work would outlived us.

A beauty of Colourlab is in diversity of skills, interests and expertize. One big thanks to Dr. Marius Pedersen who led me in the image quality world and help defining one of the two main goals of the thesis. It is my desire to express special gratitude to prof. Phil Green who has been one of the main reasons why I am in position to write this text. To other authors on the publications included in the thesis I want to thanks and congratulate on a good work, so thank you Kristina, Melissa, Paula and Steven.

Working within Marie Curie CP 7.0 project was unique experience and I was fortunate to be part of it. The European Council ITN and Marie Curie foundation is one of the European finest ideas and investments. As the Colour Printing 7.0 is the EU funded project I would like to express my personal gratitude to the Marie Curie foundation for making all this possible. Special thanks to all industrial partners involved around CP 7.0, from my side, special thanks to Caldera for providing a RIP, it meant a lot.

I must emphasize at this point how important have been for me to be a part of CP 7.0 family. To whole CP 7.0 team, the supervisors for leading us and colleagues for all the time spend together, one big thank you and best of wishes for all. Therefore, thank you Aditya, Jon, Philipp, Jeremie, Ole, Carinna, Maria, Daniel for guidance and Teun, Paula, Sepideh, Steven, Melissa, Ludovic, Atiqur, Srirkrishna, Jana and Irina who all made these fantastic three years of my life.

With the danger that I miss somebody, I will just say that it was the pleasure to work in Colourlab and with all his members. Therefore, to you: Sony George, always smiling always around, Aditya but this time as a true friend, Peter for being kind and available, prof. Ivar Farup for his inputs on mathematical problems, Steven for being a friend and always helpful, Ping for all discussions, Kostas for a dash of south on the far north, Irina for joyful time and smile, Xingbo and Raju for being a good neighbours, Sun for being a good pupil, Thomas for being Thomas, Kiran and does not matter for your betrayal of Colourlab, to all Hypercept guys and all those that have transited through Colourlab, to you all, one ☺ and thanks. Being in Norway was quite an experience that can only enrich my future.

To Irma and Sesum who helped with tedious language corrections and 3D drawings. Thank you for unconditional support. To my love last three years and hopefully many more to come. And finally, to my family, for never giving up and believing impossible, I could only have an admiration.

Radovan Slavuj

The Publications

Seven papers are included in the thesis. These papers constitute the core of the thesis and are regarded to be relevant for thesis' topics and discussions. Other work done and relevant for the thesis is included in Related Papers section.

List of Included Papers

Paper A

Slavuj, R., Nussbaum, P., and Hardeberg, J. Y., **Review and analysis of spectral characterization models and halftoning for multi-channel printing**, In Proc. IARIGAI, 'Advances in Printing and Media Technology', Vol. XL, pp. 265-275, Chemnitz, Germany, 2013.

Paper B

Slavuj, R. Coppel, L. G., Olen, M., and Hardeberg, J. Y., **Measuring or Estimating Neugebauer Primaries for Multi-channel Spectral Printing Modeling**, In SPIE Proceedings: Measuring, Modeling, and Reproducing Material Appearance, Editor(s): Maria V. Ortiz Segovia; Philipp Urban; Jan P. Allebach, Vol. 9018, SPIE Electronic Imaging, pp. 90180C-1-90180C-8, San Francisco, CA., 2014.

Paper C

Slavuj, R., Coppel, L. G., and Hardeberg, J. Y., **Effect of ink spreading and ink amount on the accuracy of the Yule-Nielsen modified spectral Neugebauer model**, In SPIE Proceedings: Color Imaging XX: Displaying, Processing, Hardcopy, and Applications, Editor(s): Reiner Eschbach; Gabriel G. Marcu; Alessandro Rizzi, Vol. 9395, SPIE Electronic Imaging, pp. 93950E-1-93950E-6, San Francisco, CA., 2015.

Paper D

Coppel, L. G., Slavuj, R., and Hardeberg, J. Y., **Modelling coverage dependent ink thickness in ink-jet printing,** submitted to Applied Optics.

Paper E

Slavuj, R., and Pedersen, M., **Multichannel DBS halftoning for improved texture quality,** In SPIE Proceedings: Color Imaging XX: Displaying, Processing, Hardcopy, and Applications, Editor(s): Reiner Eschbach; Gabriel G. Marcu; Alessandro Rizzi, Vol. 9395, SPIE Electronic Imaging, pp. 93950I-1-93950I-13, San Francisco, CA., 2015.

Paper F

Slavuj, R., Coppel, L. G., Ciortan, I., Nussbaum, P., and Hardeberg, J. Y., **Print quality and color accuracy of Spectral and Colorimetric reproduction using Multichannel DBS halftoning,** submitted to the Journal of Print and Media Technology Research.

Paper G

Slavuj, R., Marijanovic, K., and Hardeberg, J. Y., **Colour and spectral simulation of textile samples onto paper; a feasibility study**, Journal of International Colour Association, Vol. 12, pp. 36-43, 2014.

List of Related Papers

Coppel, L. G., Le Moan, S., Slavuj, R., Elías, P.Ž. and Hardeberg, J. Y., **Next generation printing – Towards spectral proofing**, In Proc. IARIGAI, 'Advances in Printing and Media Technology', pp. 19-24., Swansea, UK, 2014.

Slavuj, R. and Green, P.J., **Method to estimate spectral reflectance from camera RGB values**, Colour and Visual Computing Symposium, pp. 120-127., Gjøvik, Norway, 2013.

Contents

PART II

Included Papers

Part I

Introduction

Chapter 1

Introduction

This section explains the underlying motivation of the thesis, set the goals, defines the means to meet the goals, introduces the methodology and provides an outline of the rest of the thesis.

1.1 Motivation

A multichannel printing appeared first in offset printing where for various needs and purposes, additional ink units were installed in line with process inks. However, only recently in printing time scale this technology was realized on ink-jet printers. To achieve highest possible quality and colour range, today's high end ink-jet printers have about 12 inks. Largely in scientific community, the multichannel ink-jets have been utilized in spectral reproduction with more or less success. A spectral reproduction aims at reproducing an acquired spectral reflectance of an object. Prior to the printing, input spectral reflectance is processed to a binary map which is then interpreted by the printer. An input spectral reflectance signal is a multi-dimensional vector (e.g. of 31 dimensions) is approximated with a seven dimensional vector (assuming that multichannel printer has seven independent channels or seven degrees if freedom). The approximation is performed with printer model and its inverse. This process computes ink amounts or the intensities of each channel that after mixed and printed will produce the closest possible resemblance of the input spectral reflectance. The resemblance of a two objects observed next to each other is expressed as how close in colour they appear to a human observer. If no difference in colour is observed under one illumination it is said that two objects match in colour but if they continue to match in colour when illumination is changing, it is said that two objects are spectrally matched. Absence of spectral match is manifested as unproportioned change of colour of the two objects with the change of illumination and is called metamerism.

Metamerism is common occurrence in metameric reproduction workflow. There the aim is to accurately reproduce colour under one illumination. Although this is the commonly used, widely spread reproduction system this is still its major limitation. On the other hand, a spectral reproduction workflow aims to accurately reproduce spectral reflectance which will in return remove the metamerism problem.

The advantage of using a multichannel printers in spectral reproduction workflow (in contrast to conventional four-channel CMYK printers), is that higher possibility exist to reproduce the spectral reflectance signal. However, increased number of process inks raises challenges of controlling the printer and builds up complexity of the processing multi-dimensional input-output. These challenges are taken as goals of the thesis where by applying and improving methods, models and algorithms that have been successfully applied in four channel printing, solutions might be found.

By custom modifications of existing printer models and halftoning algorithms, new printer model and halftoning methods have been proposed. A desired outcome of the research is to create a spectral reproduction workflow using multichannel printers that will be accurate, simple to use, fast to compute and of high image quality.

The colour accuracy is quantified with some of the colour difference formulas but for large colour patches (corresponding to the viewing angle of colour perception). Therefore, printer model transformations on the complex image are pixel wise processing. On the other hand, modern halftoning is block processing operation that process a set of pixels as it runs. The metric applied to colour modelling and metric applied to halftoning do not correlate well. One could also evaluate a smoothness of a colour model transformation or a banding process of the separation but is it generally attributed that halftoning is the main responsible for image quality of the reproduction system. To add to this problem is the fact that colour management is developed with very little concern about halftoning and vice versa. The role of halftoning is to control grey levels of a binary printer by converting a continuous tone signal into high frequency pattern. A goodness of a halftoning algorithm is in a quality of the high frequency pattern that is quantified through the ability of Human Visual System (HVS) to perceive it from certain viewing distance. Many halftoning algorithms have been developed for spatial dot distribution (applicable to a single ink-channel) but few are effectively used for the problem of channel interaction in colour printing. Although channel independent halftoning (where each ink-channel is halftoned separately and then merged unconditionally with other ink-channels) can be used in colour printing, the quality is compromised by uncontrolled, random channel overlapping frequencies that eventually form a low frequency pattern which is visible to HVS. As ink mixing in printing is an additive colour mixing process and as a white paper is the most used printing substrate; the ink-channel overlaps are easy to spot due to its high contrast against the white paper. To tackle this problem, an improvement of a colour halftoning is leaning toward channel dependent algorithms that are made to avoid ink-channel overlaps as much as possible. An ink-jet multichannel printer, due to its large colour gamut, is the state of the art in high quality colour printing. The channel overlapping in multichannel printing is similar halftoning problem as in four colour printing, but to far greater scale. While there is only one four colour combination of a CMYK printer, there are 35 different four channel combinations in seven channel CMYKRGB printer. Very few efforts in the literature have been made to solve the practical issue of halftoning for multichannel printing and channel independent approach has been prevailing one used in practice.

1.2 Thesis goals

The major goal of the thesis is to improve and develop spectral printer model and halftoning for multichannel printing. There are three requirements set in meeting this goal: the model must be accurate, it must be simple to use and should not need too many resources. The entire reproduction system including colour separation and halftoning must preserve expected image quality.

To improve accuracy of the spectral printer model, an effort will be directed toward improvement of a channel linearization process, the model calibration process (e.g. printing or estimating targets) and addressing dependence of the halftoning method on the accuracy of the model.

Second goal is to make model calibration simple and with the least possible resources used, especially in ink. Currently, if one wants the most accurate model for e.g. seven channel ink-jet printing system, around 16 000 patches need to be printed. Printing these patches would deplete ink in cartridges close to maximal level. When ink cartridges are changed, the new model must be build. Therefore, the resources usage plays a significant role in model calibration.

As the colour or spectral reproduction workflow is designed and evaluated on the basis of colour difference formula which is derived from the measurements of large colour patches, transformations of complex images are not in relation with model accuracy. It is expected that models have some error of estimation and it would be very difficult to determine how these spatially distributed errors would affect overall image quality. The image quality of the reproduction workflow is usually attributed to the goodness of the halftoning algorithm but overall image quality could be a function of both separation and halftoning process. Therefore, it would make sense to observe image quality of the spectral or colorimetric workflow as the combined effort of the gamut mapping, separation and halftoning process. It is desirable that image quality could be controlled or improved after separation process as it can be very complex process by itself. Therefore, a development of post-processing halftoning method also is one of the goals of the thesis. It is also important that such halftoning method operates in multichannel environment so it could be applied on multi-spectral reproduction workflow as well.

1.3 Research Questions

The light-ink-paper interaction is a complex process where both paper and ink are not of homogeneous structure. In order to model the light behaviour when interacted with such material, one would need an enormous computational power and models that could simulate all light interactions. However, this area has been and still is one of the most explored areas in printing. A half century old ideas derived for single colour or multiple colour printing are still explored, modified, improved and upgraded.

In practice, mathematical models are preferred due to its simplicity of calibration and implementation where complex light-ink-paper interactions are overlooked. These models can also be very computationally intensive and in most cases reasonably accurate.

When modelling a printer, it is device itself, its ink-set, used substrate, halftoning, ink limitation, calibration, etc. which are all modelled, and therefore the model is a function of all these parameters. Every printing technology has its specifics, offset printing has thick dense inks, laser technology has a powder as a colourant, ink-jet has fix dot size, UV curing

machines could print on any material, etc. The same empirical models can be and are used to model all these different technologies and their characteristics. A multichannel printing has many unique characteristics but many challenges where most of the conventionally used techniques might not be applied successfully. All research questions asked and goals that are defined here are in the domain of multichannel printing. The research questions for which the thesis will aim to provide an answer are:

- Could we make the empirical models more accurate (e.g. to better correlate with measurements)?
- Can accuracy be increased by aiming to model specific physical phenomena?
- What modifications need to be made to the models to account for specific ink-mixing?
- What has to be done to remove negative consequences of the light-ink-paper interaction so the image quality of the print can be improved?

Subsequently, the research goals become:

- Maximization of the printer model accuracy,
- Maximization of the print quality,
- Minimization of the computational time and resources used for calibration of a model and halftoning.

1.4 Outline of the thesis

The thesis is organized in the following manner: first there is a general division to the introduction part (**Part I**) and the included papers (**Part II**). Secondly, the introductory part is split into five sections. The theoretical background on the material included in the thesis is presented in **Section 2: Background.** The **Section 3: Summary of included papers** follows where papers are presented and related based on their scope. The summary of each included paper is provided as well in this section. In the **Section 4: Discussion**, the included papers are put in the context where their scope is discussed. The Introduction part concludes with **Section 5: Conclusions, Contributions and Perspectives,** where the summary of the contributions is discussed together with the perspectives of future research. In the **Part II** all included papers are presented.

Background

Since antiquity people have known that eyes are the organs of sight. However, they thought that an inner fire in the eyes gives birth to the waves that lead towards objects and that people are able to see that way. The modern era of psychological optics came out with an idea that eyes are working as a pinhole camera. The main difference is that instead of having a sensor, the human visual system forms images in the visual cortex of the brain. Today it is perfectly clear that there are cones and rods inside eyes which are photo-sensitive. Captured photo signal is transported further to visual cortex in the brain. Cones could be divided into 3 categories, by their sensitivity to different wavelength: long (L), medium (M) and short (S), otherwise called red, green and blue. Their population in the eye (retina) is not proportional. The actual ratio of the cones L: M: S is 10:5:1 which gives us more sensitivity on long and medium wavelengths or more sensitivity on the green and red than on blue. The whole range where visual system is sensitive is between 370 – 700 nm (Hunt, 2004), which represents just a small part of electromagnetic radiation.

Visual perception depends on three parameters: the light, a surface that reflects it and observers (Palmer, 1999). If we remove any of these three parameters, visual perception does not occur. These are the parameters that constitute the CIE colorimetry, which is the metric of the psychophysical colour stimulus (Schanda, 2007). The CIE colorimetry that we know today was established through two experiments: first performed by Wright (1928) and the other by Guild (1932). From these two experiments, the so-called tristimulus functions are obtained and later used as a basis for CIE standard colorimetric observer (CIE, 1931). Deriving such functions from the set of observers was not an easy task and surely cannot be said that these functions are good representative of the global population. Nevertheless, these functions and CIE colorimetry has been major colour communication bridge since it was established.

With light additivity assumed, a colour stimulus is an integrated (over the visible range of electromagnetic spectrum) spectral reflectance of the object, spectral power distribution of the illumination and colour matching functions which place a human as an observer. These vectors integrate to three numbers (CIE XYZ). First problem with trichromatic reproduction is that input values (e.g. CIE XYZ) are computed under the fixed observation condition that assumes constant illumination and observer. This implies that if illuminant or the observer has changed, and if two stimuli with the same trichromatic values are visually matched under the given condition, the match will not exist anymore. Second problem is that the same trichromatic values could be gained from many different spectral reflectances which form a metamer set. Spectral information is therefore, the true and complete information about an object potential to selectively absorb and reflect the light. The CIE colorimetry was established upon empirical laws of light mixing and therefore it is a reasonably good representation of colour perception as long as the observation conditions are being kept the same (Schanda, 2007).

2.1 Principles of Colorimetry

This section introduces principles of trichromatic colorimetry, metamerism problem, uniform colour space and a colour difference formula.

2.1.1 Calculation of the CIE XYZ tristimulus values

The XYZ tristimulus are products of spectral power distribution (SPD) of an illuminant, spectral selectivity or reflectance of the object (can be transmittance or translucence as well), and colour matching functions (CMF). Mathematically, it is presented as:

$$X = k \int_{\lambda_{min}}^{\lambda_{max}} x(\lambda)\, l(\lambda) r(\lambda) d\lambda$$

$$Y = k \int_{\lambda_{min}}^{\lambda_{max}} y(\lambda)\, l(\lambda) r(\lambda) d\lambda \tag{1.1}$$

$$Z = k \int_{\lambda_{min}}^{\lambda_{max}} z(\lambda)\, l(\lambda) r(\lambda) d\lambda$$

where CIE XYZ values are gained through the integration over visible spectrum. The xyz (λ) are CIE 1931 CMF, l (λ) is SPD of the illuminant, and r (λ) is the reflection of the object. Constant k is a normalizing factor that scales to the range of 0-100:

$$k = \frac{100}{\int_{\lambda_{min}}^{\lambda_{max}} y(\lambda) l(\lambda) d\lambda} \tag{1.2}$$

Simple explanation is that CIE XYZ is the stimulus that Human Visual System (HVS) would observe or 'that what is to be seen'. Also calculation can be approximated as a sum and subsequently be represented in:

$$X = k \sum_{i=1}^{N} x\,(\lambda_i) l(\lambda_i) r(\lambda_i)$$

$$Y = k \sum_{i=1}^{N} y\,(\lambda_i) l(\lambda_i) r(\lambda_i) \tag{1.3}$$

$$Z = k \sum_{i=1}^{N} z(\lambda_i) l(\lambda_i) r(\lambda_i)$$

or

$$t = A^T L\, r \tag{1.4}$$

in matrix notation. Here **t** = [X Y Z] ^{T} is a vector of tristimulus values, **A** is the matrix with CMFs, **L** is the vector of CIE illuminant or illumination source SPD and **r** is a vector of spectral reflectance.

2.1.2 Metamerism

Two objects that have distinct spectral reflectances but which integrate to the same CIE XYZ tristimulus values are known as metameric pairs (Wyszecki, 1958). The tristimulus values are calculated from the surface reflectances, the illumination and the colour matching functions. These values are used to uniquely identify object colour. Two colours are metameric if their CIE XYZ tristimulus values are the same, X1=X2, Y1=Y2, Z1=Z2, but different physical characteristics with the respect to illumination and the standard observer (Wyszecki and Stiles, 1982). Physical characteristic of an object's to selectively absorb and reflect the light is quantified by spectral reflectance. When spectral match between two objects is achieved, they will match in colour under any light and for any observer. If two objects, believed to be spectrally matched, match in colour under one illumination, but this match brakes under another illumination, the spectral match does not exist between two objects but only a metameric match.

The metamerism is all around and is hard to avoid it, but if critical colour judging of an object is performed outside of context where the object will be used, the spectral match is very desirable (most common example is a clothing object observed in store and then on the daylight).

2.1.3 CIE L*a*b* Colour Space

The CIE L*a*b* colour space is an approximation of how the HVS perceives difference between two colours (Hunt, 2004). On the other hand, the CIEL*a*b* values represent tristimulus values after adaptation of the HVS on the intensity and colour of the light (also called a white point). In simple words these values are 'what have been seen'. Therefore, CIE L*a*b* values are calculated using the previously determined CIE XYZ values:

$$L^* = 116 f\left(\frac{Y}{Y_w}\right) - 16$$

$$a^* = 500\left(f\left(\frac{X}{X_w}\right) - f\left(\frac{Y}{Y_w}\right)\right) \tag{1.5}$$

$$b^* = 200(f\left(\frac{Y}{Y_w}\right) - f\left(\frac{Z}{Z_w}\right))$$

where Xw,Yw,Zw is the white point of a CIE illuminant. The function f(α) is defined for a different light conditions as:

$$f(\alpha) = \begin{cases} 7.787\alpha + \frac{16}{116} & if\ \alpha < 0.008856 \\ \alpha^{\frac{1}{3}} & otherwise \end{cases} \quad (1.6)$$

2.1.4 Colour difference and spectral difference

There are many colour difference formulae, all specific to the colour space where their calculations are applied. In the end, whether performing Euclidian distance or angular variation they are calculated similarly: the sum of the absolute difference in all directions of a colour space. One such formula is applied on a mentioned CIE L*a*b* space:

$$\Delta E^*_{ab} = \sqrt{(\Delta L^*)^2 + (\Delta a^*)^2 + (\Delta b^*)^2} \quad (1.7)$$

where

$$\begin{aligned} \Delta L^* &= L^*_2 - L^*_1 \\ \Delta a^* &= a^*_2 - a^*_1 \\ \Delta b^* &= b^*_2 - b^*_1 \end{aligned} \quad (1.8)$$

Spectral difference on the other hand is represented as a Root-Mean-Squared-error (RMS):

$$sRMS = \sqrt{\frac{1}{N}\sum_{i=1}^{N}(r_1(\lambda_i) - r_2(\lambda_i))^2} \quad (1.9)$$

where N is the number of sampling points of the spectral reflectance vector $r_1(\lambda)$ and $r_2(\lambda)$ whose difference is calculated. This metric gives a single number which makes it good for processing purposes (e.g. optimization) but depending on a colour, it can give a poor correlate to the colour difference (Imai et al.,2002).

2.2 Colorimetric and spectral reproduction system

Colour management is the communication of the data for unambiguous interpretation of colour information and the application of colour data conversions required for the intended reproductions (ICC, WP5). Traditionally, colour management systems (CMS) have been based on tristimulus colorimetry (CIE, 1931). Spectral measurements in the colorimetric CMS are converted into tristimulus values before used in the CMS. When converting from the spectral data to tristimulus values there is a loss of information due to the dimension reduction from n-dimensional spectra to the three-dimensional colorimetric values. This loss of information can result in two colours, which are spectrally different, to give the same colour sensation under a specific viewing condition (section 2.1.2). These colours are called metamers. Example of metameric or colorimetric reproduction system is given in Figure 1.

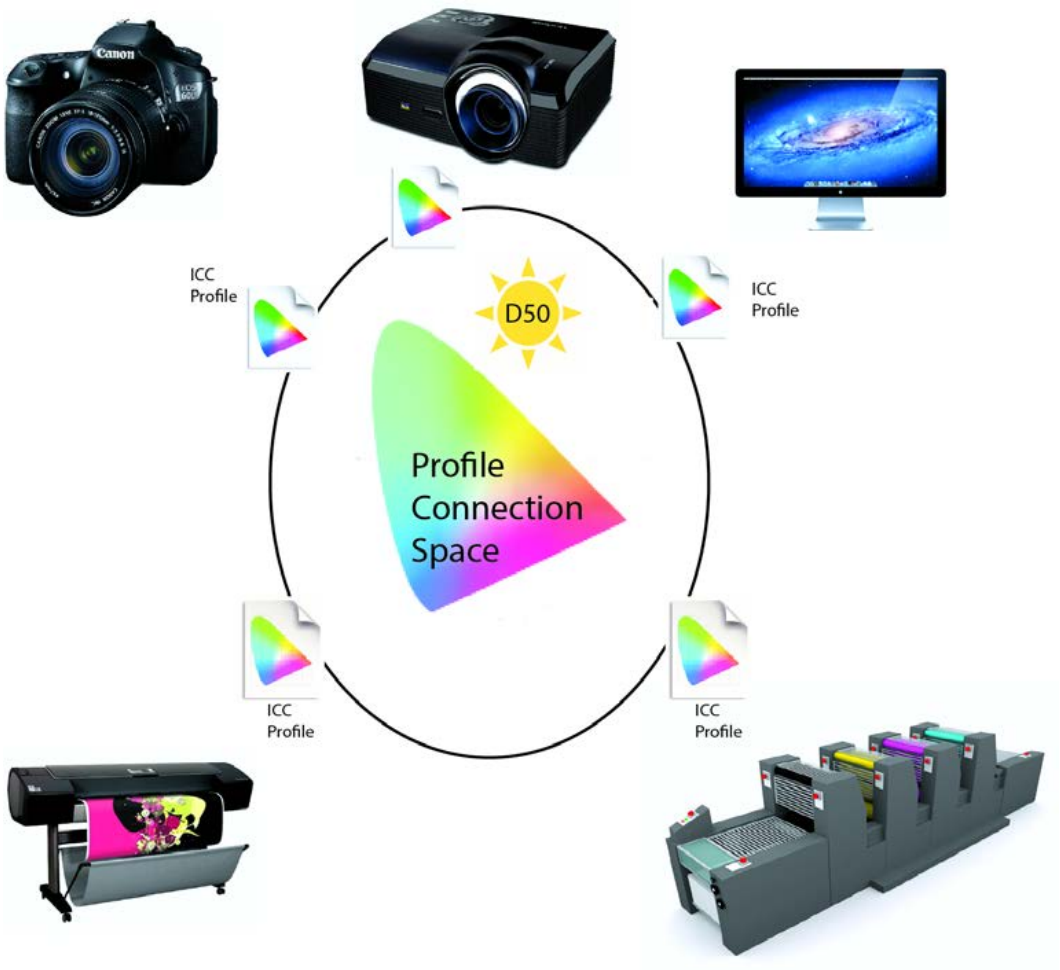

Figure 1.* Commonly used colorimetric reproduction workflow (ICC). Devices communicate via common colour space (PCS), usually CIE L*a*b* space, under the fixed illumination conditions and the standard observer (CIE Standard 1931 Colorimetric Observer).

*Redrawing of the ICC metameric (colorimetric) reproduction workflow. Image collection, specific organization (grouping of RGB and CMYK devices), showing four colour offset as conventional technology vs multichannel printer (HP z3200 PS, used in all papers in the thesis), connecting circle are original creation of the author.

Devices in the colorimetric workflow are described in a colour profiles which among many other data, stores device characterization data, calibration state and intended reproductions goal.

First benefit of using spectral colour management (or spectral reproduction workflow) is that to some extent is possible to avoid metamerism (e.g. Tzeng, 1998, Chen, 2004). This comes at the cost of computational intensity and complexity. There are variations of this system based on the desired reproduction goal (Hardeberg, 1999, Gerhardt, 2006, Urban and Berns, 2011) but its general form is presented in Figure 2.

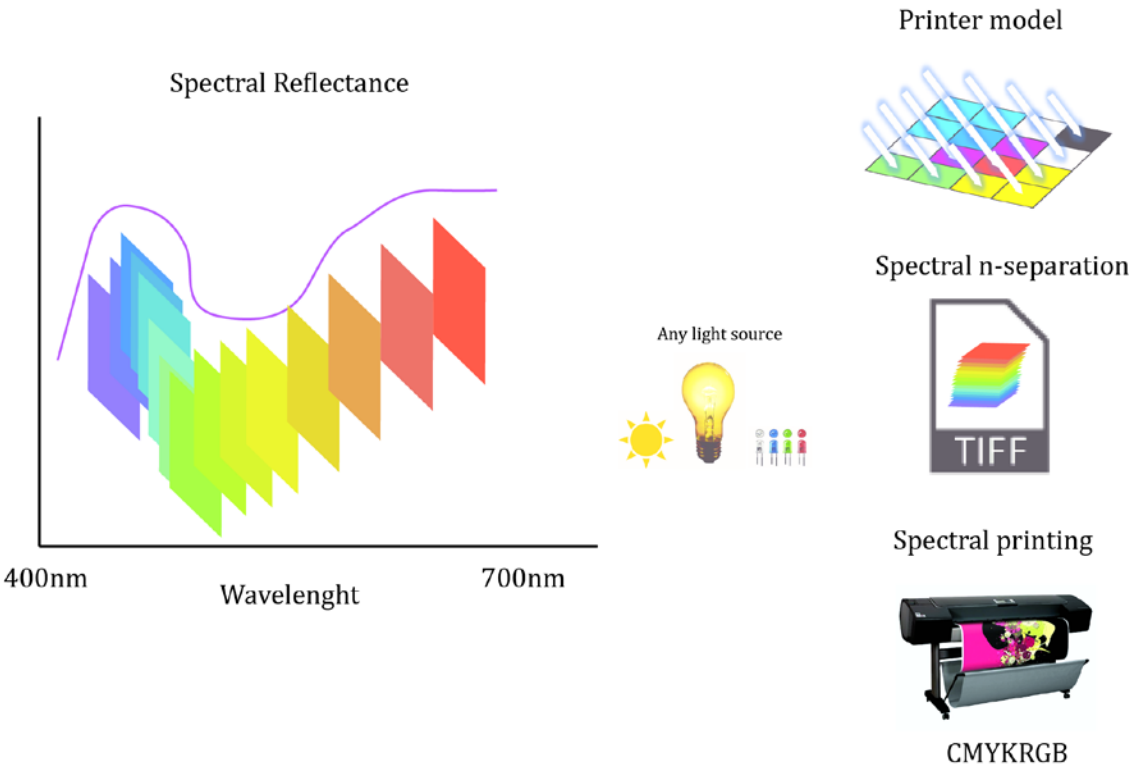

Figure 2.* Generalization of a spectral reproduction workflow. The spectral reflectance is measured with instrument or estimated with a camera. With spectral reflectance the CIE XYZ or CIE L*a*b* values under any illumination can be computed. The reflectance is estimated with the printer model while spectral separation is computed in iteration. Dimension reduction is performed from e.g. 31 of the reflectance to 7 of typical multichannel printer.

*Spectral reflectance with colour channels and organization of the images in the workflow are original contribution of the author, The printer model and TIFF image is redrawn are redrawn with the parts with original creation (e.g. multi-layer, multi-colour stock symbolizing separation process).

2.2.1 Multichannel printing

On wider scale, particularly in ink-jet printing, a multichannel printer where the CMYK + N inks are utilized as the process inks is relatively recent occurrence. In offset printing, one of the interest areas of multichannel printing is to simulate spot colours (e.g. Pantone, Inc) by using only in-machine process inks. Similar idea has been conveyed to modern day ink-jet printers that have been a standard tool for proofing (a simulation of the other printing technologies). High print quality and large range of reproducible colours (otherwise called a gamut) enables multichannel ink-jet printing to simulate a print from any other printing technology. The simulation of one printing technology or any other colour reproduction device, with a printer is called hard proofing. In contrast to soft proofing done on displays (which are somewhat limited with number of channels and spectral power distribution of their primaries), hard proofing can be achieved with two reproduction workflows: colorimetric and spectral. The latter is also called spectral printing and is discussed in following Section 2.2.2.

2.2.2 Spectral printing

Spectral printing is a reproduction workflow that takes at the input a spectral reflectance which is reproduced by mixing the printer's primary inks. Logical choice for spectral printing is to use as many colorants as possible in order to enlarge spectral variability and hence, increase the chance for accurately reproducing input reflectance. It instantly becomes clear that printers are much more flexible for spectral reproduction then the displays are. Ink-jet in particular is the versatile, multi-ink printing system where channels could be potentially altered. Other advantage of printing over displaying spectral information is in the smoothness and broadband shape of the inks reflectances while display primaries have very spectrally selective, usually RGB primaries. Although spiky, sharp edged radiances of displays are useless for spectral reproduction, they generally tend to have significantly higher colour gamut (Hunt, 2004, Green and MacDonald, 2001).

The spectral reflectance dimensionality variations are based on the number of measurement points. Usual number of sampling points in the visible range of electromagnetic spectrum (e.g. 400-700 nm) is 31, assuming a 10nm sampling step. The 10nm spectral resolution has proven to be sufficient for spectral printing purpose owning to the smooth reflectance curves of the inks (e.g. Kang, 1999, Finlayson and Morovic, 2001). Currently, the most convenient tool to use for spectral printing is a multichannel printing system. In reduction of dimensionality from 31 of the spectral reflectance to e.g. seven of the printer, an amount of information is lost which leads to following two assumptions: the inks on the multichannel printer are not optimized for spectral printing (Hunt, 2004, Alsam and Hardeberg, 2004, Urban and Berns, 2011, Morovic et al., 2012, Slavuj et al., 2014) and the number of inks and spectral variability is not sufficient for printing spectra of most of the real world objects (Morovic, 2013, Urban, 2013). The key part of the spectral printing workflow is the spectral printer model. These models provide an estimate of the printer output while calculated in inverse direction, an ink mixture needed to reproduce input reflectance. Spectral reproduction workflow will be prevailing one used in thesis with multichannel printer as a tool.

2.3 Spectral Printer modelling

The first printer model for monochrome printing was introduced by Murray (1936) on the basis of the work of his colleague, hence the model has Murray-Davis (MD) name. Model assumes that the reflectance R_λ of the certain area is the product of the relative coverage of ink a_i, paper $(1 - a_i)$ and reflectance of the ink $R_{\lambda,i}$ at full coverage:

$$R_\lambda = a_i R_{\lambda,i} + (1 - a_i) R_{\lambda,i} \tag{2.1}$$

The dot area coverage could be described as theoretical and effective dot area coverage. The former is the digital information sent to the printer and latter is the real dot on the paper. During printing process, ink penetrates to the substrate and phenomenon of dot gain occurs. It is called physical or mechanical dot gain as it is caused by printing system (contact or non-contact) and is resulting in physical spreading of the ink as it deviates from the desired shape. In order to calculate effective dot area one must invert the MD model:

$$a_{eff} = \frac{R_{min,meas} - R_{min,p}}{R_{min,i} - R_{min,p}} \tag{2.2}$$

where subscript p is the reflectance of the substrate (paper), i is the reflectance of the primary ink and R_{min} is here to denote that the calculation is not performed with whole reflectance curve. Rather, it takes minimum value of the reflectance as it is the one that will be most affected with the dot gain. The estimated factor a_{eff} is the scaling factor for the input reflectance that translates the reflectance of primary ink after dot gain. If we are interested in how our dot gain is influenced by the change in spectra, we can rewrite the equation to a matrix calculation using least squared minimization:

$$a_{eff} = R_{m,p} R_{i,p}^T \left(R_{i,p} R_{i,p}^T\right)^{-1} \tag{2.3}$$

Here, $R_{m,p} = R_{meas} - R_p$, $R_{i,p} = R_i - R_p$, where R_{meas}, R_p and R_i and are row vectors with spectral data. Other type of dot gain that MD model doesn't account for is optical dot gain. This phenomenon occurs due to the light scattering within the substrate. This implies that substrate near the dot does not have same reflectance value as pure substrate. It is actually a combination of the light that has passed to the ink filter, scattered inside the substrate and left out from unprinted area. Although this phenomenon is not necessarily unfavourable (it increases the colour gamut), it adds complexity into modelling.

2.3.1 Neugebauer model (NG)

Neugebauer extended MD model for multi-colour output by linear summation of the product of tone area coverage of each colourant and its reflectance (Neugebauer, 1989):

$$R_{\lambda=} \sum_i a_i R_{\lambda,i,max} \tag{2.4}$$

The model performs interpolation using so called Neugebauer primaries (NP) as a nodes in n-dimensional space. For three colour case there are 8 NP's: substrate, cyan, magenta, yellow, red, green, blue and black (assumed when all three primaries are mixed together). Beside linearity that MD assumes, there is an assumption of randomness and independence of dot distribution where fractional dot coverage is represented by Demichel equations (Demichel, 1924):

$$
\begin{aligned}
a_w &= (1 - a_c)(1 - a_m)(1 - a_y) \\
a_c &= a_c(1 - a_m)(1 - a_y) \\
a_m &= (1 - a_c)a_m(1 - a_y) \\
a_m &= (1 - a_c)(1 - a_m)a_y \\
a_r &= (1 - a_c)a_m a_y \\
a_g &= (1 - a_m)a_c a_y \\
a_b &= (1 - a_y)a_c a_m \\
a_k &= a_c a_m a_y
\end{aligned}
\tag{2.5}
$$

This theoretical fractional coverage could be replaced with effective dot coverage calculated with inversed MD model. The condition of randomness that NG model assumes can be satisfied by using rotated screens or stochastic patterns, where for dot-on-dot printers has to be modified (Bala, 2003).

The NP's are only measurements that are required as an input for this model, where physical dot gain can be estimated for each printing primary and can serve as the input for Demichel equations for better accuracy. However, the classical NG model does not account for optical dot gain and as that cannot provide a good estimate of printer output.

2.3.2 Yule-Nielsen n - factor

The analysis of the measured and estimated reflectance showed that optical dot gain adds to the non-linearity of the light-ink-paper interaction (Yule, 1951). Yule-Nielsen n-factor is empirically determined number to which the base reflectance is raised to the power of *1/n*:

$$R_\lambda = \left[a_i R_{\lambda,i}^{\frac{1}{n}} + (1 - a_i) R_{\lambda,p}^{\frac{1}{n}} \right]^n \tag{2.6}$$

This factor is determined through mathematical optimization, although it could be derived with simple iteration process. Exponent 1/n is transforming the reflectance space into one that is considered linear and then scaled back to the reflectance space by rising to the power on n.

There has been attempts to assign a physical meaning to the n factor (Ruckdeschel, 1978, Pearson, 1980), but most of the authors came up with one conclusion: *n=1* corresponds to the MD model, where for *n=2* it is believed that represents highly scattered substrate. However, with ink-jet printing, the effect of the dot gain is significantly higher than with other printing technology.

There is a potential caveat in the process of determining and assigning n factor. Namely, the n factor could be used to model both optical and physical dot gain, which is not the ideal situation as we are relying on a single number. Much better option will be to apply the n factor to the already corrected reflectance for the physical dot gain. When we measure the single colour ramp to provide an estimate of the physical dot gain, the measuring instrument, being the area measuring device will effectively record the optical dot gain as well. The best scenario would be to separate physical and optical dot gain, which is not trivial process (Namedanian and Gooran, 2010) and not feasible to perform every time when new characterization model is needed. Potentially, determination of the n factor could be done as a function of the wavelength. This implies that the reflectance of the area is actually dependent on the dot gain, or that ink penetration will cause the reflectance attenuation. Although this approach provides better modelling of the n factor, it is not proven that the optical dot gain is wavelength dependent (Namedanian et al., 2008). This brings back the fact that the n factor does not represent a physical phenomenon.

2.3.3 Cellular NG

The main aim of the cellular model is to increase precision of interpolation by increasing number of the sampling points and this would lead to a more accurate printer model at the end (Heuberger et al., 1992, Rolleston and Balasubramanian, 1993). More sampling points will lead to the division of the printer gamut into cells, where sampled points serve as the nodes for lower and upper boundaries of the cell. There are significant non-linearity introduced by paper ink interaction and those will reflect on interpolation precision in the process. This is in fact the main problem of the classical NG model where the cellular extension is much less prone to this.

If the dot gain has been accounted for, the sampling of the printer colour space for cellular model will than include the effective dot coverage. The search for the desired point is then performed equivalently to the inversed MD model with the exception of the end points which are in this case lower and upper boundary of the searched cell:

$$a_{eff} = \frac{R_{\lambda,i} - R_{\lambda,L}}{R_{\lambda,L} - R_{\lambda,U}} \tag{2.7}$$

Here, $R_{\lambda,i}$ denote the reflectance of the ink, $R_{\lambda,L}$ denotes node on the lower boundary of the cell, and $R_{\lambda,U}$ is the upper boundary node.

The problem with this model is that it requires high number of training (measurement) patches. This number is the function of number of levels in the sampling along single colourant (e.g. 3 for 0, 50%, 100% coverage), raised to the power of number of the colorants (channels). If we have 5 level sampling combined with 7 channel printing system we would end up measuring around 75.000 patches. Although this will provide highly accurate model it is simply not feasible bearing in mind that each change of the paper or a colourant would require new model. It is showed that by converting to the cellular model we can get improvements over classical YNSN model but to the extent of 25% in RMS spectral precision (Taplin, 2001). There have been attempts to reduce number of patches (Chen et al., 2004) and measurement intensity by estimation of some nodes. There is also an assumption

that some part of the space should be sampled with higher frequency than other. To determine what area is that, one must analyse spectral or colour error gradation throughout the printer space. There is also an issue of the cells search for interpolation process. As the printing relies on the metamerism to produce colour match, there are multiple cells that can map to the same colour. To obtain the 'right one', one must set a condition for optimization process that is based on the particular requirement of the model usage. This constraint can be spectral difference or metamerism minimization as well as the colour difference under specified illuminant.

2.3.4 SN based models: improvements and extensions

There have been many attempts and improvements to the Neugebauer model and its extensions: YNSN and cellular. With assumption that ink spreading is not the same on paper and superimposed on another ink (Emmel and Hersch, 2002) the proposition is made to use calibration curves for each two and three colour overprint. This helps the model to perform better but requires additional measurement especially when it is applied to multichannel system. In fact, each two or more colour NP would have its own calibration curve and this is what makes this model similar to the cellular approach. Multiple attempts were also made to estimate the parameters for the NG model such are dot gain, n factor and primaries (Abebe et al., 2011, Agar and Allebach, 1998, Balasubramanian, 1999, Zuffi et al., 2005). Especially the physically non realizable primaries were addressed (where more than four colours need to be printed on an area) and although not printable, these NP's are very useful for sampling of the space for interpolation.

2.3.5 Inverse YNSN

As YNSN, due to the high non-linearities caused by dot gain (both optical and mechanical), is analytically non – invertible, numerical methods of mathematical optimization must be employed for such operation. There, the optimization routine subsequently calls YNSN forward model to give an estimate for input for a cost function (usually colour or spectral difference) that should minimized.

2.3.6 Continuous tone model: Kubelka- Munk model (KM)

Many types of colouration systems have used this model for prediction of the colour mixture. It is also widely used for various purposes in graphic arts where primarily halftone systems are usage. It is assumed that most of the scattering comes from the paper and therefore the single constant KM (Kubelka and Munk, 1931) theory was considered to be very useful for halftone printing. It bases its approximation by considering ratio of scattering and absorption coefficients of the mixture:

$$(K/S)_\lambda = \frac{(1-R_\lambda)^2}{2R_\lambda} \tag{2.8}$$

Where R_λ is the spectral reflectance of the mixture, K is the absorption coefficient and S stands for scattering coefficient. To use this model for halftone printers, K/S factor is calculated for each ink at maximum coverage and for the paper:

$$(K/S)_{\lambda,i} = (K/S)_{\lambda,i,max} - (K/S)_{\lambda,p} \tag{2.9}$$

For multichannel case, the previous equation can be expanded:

$$(K/S)_{\lambda,mix} = (K/S)_{\lambda,p} + \sum_i c_i (K/S)_{\lambda,i} \tag{2.10}$$

Where c is the weighting on the unit K/S and is based on the concentration of the ink. In the K/S space, the additivity of the mixture is assumed and it is the space where the reflectance is behaving in linear manner. This fact was used by Chen et al. for the model inversion where he used K/S space instead of the ink space where this linearity does not stand. Also, inversion of the model can be done analytically and it is straightforward process:

$$R_\lambda = 1 + \left(\frac{K}{S}\right)_{\lambda,mix} - \sqrt{\left(\frac{K}{S}\right)^2_{\lambda,mix} + 2\left(\frac{K}{S}\right)_{\lambda,mix}} \tag{2.11}$$

There is also the cellular version of the KM model that performs the same operation like cellular NG model and also requires intermediate steps for measurements. The interest in using KM model is particularly strong in estimation of the physically non-realizable primaries that are needed for good space sampling and later interpolation. Also, estimation of the primaries can be used to reduce number patches needed for cellular NG model.

2.4 Halftoning

The human eye cannot differentiate between individual points with resolution of 60 L\cm = 150 LPI (0,167mm dot size). It integrates over the surface so if there are fine enough dots, the eye would not be able to see any difference from continuous tone. On this fact relies halftone printing. To produce a good colour halftone one has to place coloured dots so that the following specifications are optimally met:

- The placement pattern is visually unnoticeable.
- The local average colour is the desired colour.
- The colours used reduce the notice-ability of the pattern.

Halftoning is method of simulating continuous tone images with binary devices such are most of today's printers. There are two approaches: one achieved with varying the size of dot and other with varying the dot placement frequency at a particular area. The former correspond to AM (amplitude modulated) raster and latter to FM (frequency modulated) halftoning (Figure3).

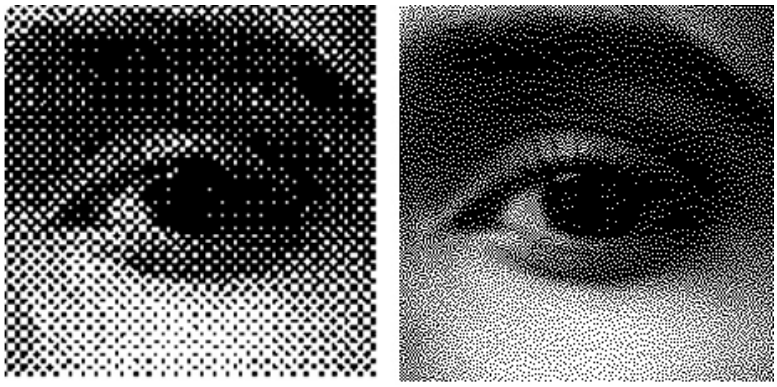

Figure 3.* The AM (left) and FM (right) dot placement structure.

The FM screening is also called stochastic screening due to random distribution of the dots. There is also a possibility to combine AM and FM halftoning into hybrid approach. In this case, part of the image with dark and light areas would be halftoned using AM raster, while mid-tone areas would be covered with FM. Having the more isolated point, FM halftone structure is more sensitive to dot-gain. Dot gain is random individual dot increase in size and comes as a result of interaction between colourant and surface.

Chemistry and physics of the colorants and surface play major roles in this process. Overlapping of process colours might provide different results depending on the extent of the overlap and on the physics of the ink itself. Namely, inks are not ideal, and will produce different colours depending on their interaction with other inks. This is almost impossible to avoid in FM screening, while the AM type is less sensitive as there is no so much overlap. Registration plays the major role in this process and a common solution would be to expose separations under different angles. This would solve the problem in the case of AM (clustered dot screens) but will still remain a problem with the FM type.

The gray level of a particular area can be simulated either with high frequency FM halftones or with large dots using AM screening. As some printers can vary the amount of ink layer on the surface and therefore to vary the intensity of an individual dot, the number of reproducible gray levels can increase greatly. Accordingly, colour gamut increase is expected with this feature. Screening of different separation is usually done in different angles. Rotated screens produce moiré pattern that is, at its best, twice as large as the pattern for an individual screen. Rosette is a type of moiré and represents all possible overlaps between colorants (Figure 4). CMK separations under 30° relative to each other will show most of the rosettes and more GCR is applied, more likely to result in rosettes.
colour. This is to great extent reduced with higher resolution used for printing, but not completely eliminated. Bad registration could also cause rosette.

*Halftoning on the image result of authors adaptation of the Matlab functions of the halftoning Toolbox from (Monga, Univeristy of Texas – Avalible at [half_tol_tex] , image taken from Linkoping University halftoning toolbox.

Figure 4. Moiré and rosette pattern formed as two high frequency patterns combining under different angles (from Kipphan, 2001, page 92).

There are two types of rosettes, with a hole in the centre and with a dot in the centre. In conventional printing, where there is a three colour system, yellow colour, as being the least distinctive colour is usually angled to 15° regarding magenta and cyan. Due to various factors like dot gain and miss-registration, there is interference that shows up as a result. This interference is related to image structure and makes it sometimes impossible to avoid moiré. Also, there is a rosette effect that will depend on the relative position of colour separation to each other. This is particularly true in homogenous areas covered with one

It is common for halftoning to be done per channel, and although miss-registration is possible, rotated screens should account for this. Repeatability and reproducibility also must be evaluated for a particular device in prior to the determination of halftoning strategy and formation of separation angles. If behaviour of the device is shown promising stability then dot-on-dot might be an option. For a CMY colour separations the angle orientation is usually chosen in steps 30° one colour after another, while for the 4 colour case, this shifts to 15°. As being least distinctive, the yellow separation is usually placed between two more dense separation of cyan and magenta. In the 4 channel option, yellow is positioned at 0°(90°) angle where cyan and magenta are taking 15° and 75° positions and therefore leaving 30° gap from black which is at 45°. Depending on the GCR strategy, the position of black might be taken by cyan or magenta if it is chosen to go with minimum grey component replacement.

When it comes to multichannel printing, the angles might be decided depending on the colours used for printing. Usually there are no more than 4 colours printed on a particular spot and it is up to thresholding algorithm to decide which colours to output. The strategy might therefore be the same, with light colours in between the dark ones and with 30° angle between two dark colours. If decided to continue with more than 4 colours, after positioning a light colour at 90°, the next dark colour (e.g. blue) will be at 105° and so forth. Ink-jet system is particularly sensitive to dot gain. High resolution available on these devices is almost never achievable due to this factor. Appropriate halftoning strategy should be chosen in conjunction with an ink limit control.

2.3.1 Error diffusion

Some common and widely used types of the FM halftoning structure are stochastic and error diffusion screens. Stochastic screen is the standard threshold array halftoning screen which is rather a point-based process then spatially adaptive algorithm.

Error diffusion is a FM-type adaptive algorithm, where no fixed patterns for any grey level exist. It is easy to implement and offers some advantages such as low noise and edge enhancement. These contribute to the overall image quality and therefore this algorithm is widely used. This algorithm operates on pixel-by-pixel basis where the input pixel in quantized to the one with a bit value of either 0 or 1 (Figure 5). Threshold value is therefore set to ½. The quantization function could also give a multibit output for printers that can vary thickness of the ink layer. Input pixels are usually in 8bit precision and there is a difference from the threshold which is conveyed to the surrounding pixels in different amounts. These amounts will depend on the filter weights which can be controlled or completely changed. With moving the error to the neighbouring pixels, the algorithm modifies values of the original but the average brightness in an image would remain almost the same. This applies to both local and global image brightness.

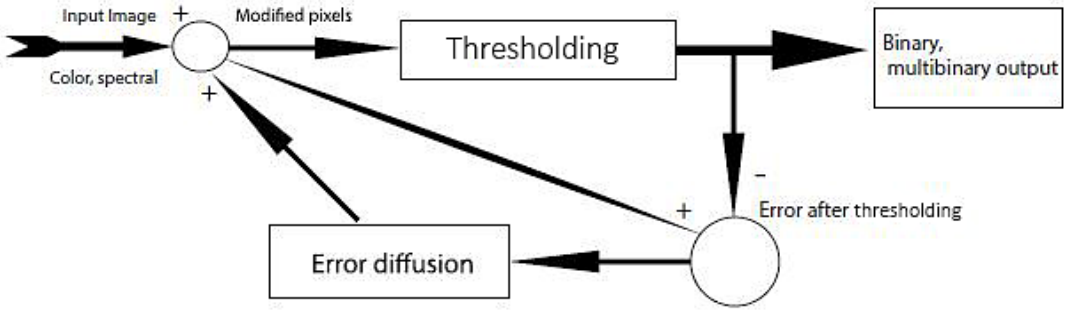

Figure 5.* Generalization of error diffusion halftoning.

The strategy to introduce colour is to halftone each channel separately. Here scalar error diffusion is not performing well due to isolated channel halftoning and later to the combination of the two. This combination will most likely induce low-spatial noise as points are randomly overlapping during printing. With luminance introduced in such way, together with colour errors and inability to account for these with calibration, the need for a better colour printing option is needed.

2.3.2 Vector error diffusion

Introduction of vector error diffusion halftoning solves the problem of the scalar approach, and although it introduces its own shortcomings, it is probably the best option available for colour printing. This vector extension of scalar ED takes a set of primary colours as threshold points. Quantization function now takes an input pixel as a vector and compares its distance from each of the primaries. All colour channels are processed together and therefore problem of uncorrelated colour channel matching is addressed this way.

*Figure 5 is the original creation of the author.

Usually, chosen colour space for this purpose is CIE L*a*b* which corresponds better to human visual system. Colour errors are that way calculated through vector differences which reduces output colour mismatch. Other artefacts that are better modelled using vector error method in CMYK printing is noise and texture which are less visible than with scalar model. Also, there is a possible extension to multichannel printing where all printing primaries can be used inside of the space where vector matching takes place.

Input pixel is transformed in either 0 or 1 value where error is distributed according to the error matrix to neighbouring pixels. These matrices are taken from scalar method and can vary in values and in size. Problems that this algorithm is facing are accumulation of the error, smearing and failure to perform well when colours are out of gamut. Going from one uniform area to the other (one colour patch to next one), the error is conveyed with scanning path and is usually absorbed at the border where artefacts of this process could be seen. Also this method, as having the same error distribution weights, is experiencing the same shortcomings like scalar model. Other option would be to use hybrid approach called semi-vector error diffusion halftoning. This algorithm requires separations divided to light and dark so the yellow colour will be put through standard scalar error diffusion while C and M will be treated together by using vector error diffusion. The threshold for CM combination is with multiple points and if the sum of these two channels is higher than 1.5, output colour would be blue. Possible application of this algorithm would be on multichannel printing where additional colours are enhancement of the primary colours combination.

2.3.3 Spectral Vector Error Diffusion (SVED)

This model represents spectral extension of vector error diffusion and it performs selection in reflectance space (Gerhardt and Hardeberg, 2008). Each pixel in an image is a vector of data expressing a colour value or spectral reflectance. Primaries for matching in this technique are reflectances of possible printer primaries (process colours, NP's). Output from this method is binary primaries (NP's) combination, gained by comparison and selected by minimum Euclidian distance from input vectors (spectral reflectances).

2.3.4 Direct Binary Search (DBS) halftoning

Direct Binary Search halftoning has been for many years the algorithm that gives the best textures and image quality (Figure 6). It started with monochrome version (Lieberman and Allebach, 2000) and then upgraded with several colour versions (Agar, 2005, Li and Allebach, 2001). It is one of the model based algorithms where HVS and printer model are taking into account when performing optimization. Optimization yields best possible dot pattern on the dot coverage area. The goodness of a printed pattern is based on visibility of its textures. In colour version this texture is dependent on colourant. This fact actually has been utilized in a colourant-based DBS (CB-DBS) halftoning algorithm. They control the quality of each colourant texture separately along with the total dot distribution. First, the dot overlapping and positions of magenta and cyan dots are decided by a monochrome DBS halftoning algorithm. Then, dot colouring is accomplished by a swap-only DBS constrained on the predetermined dot positions in the first step.

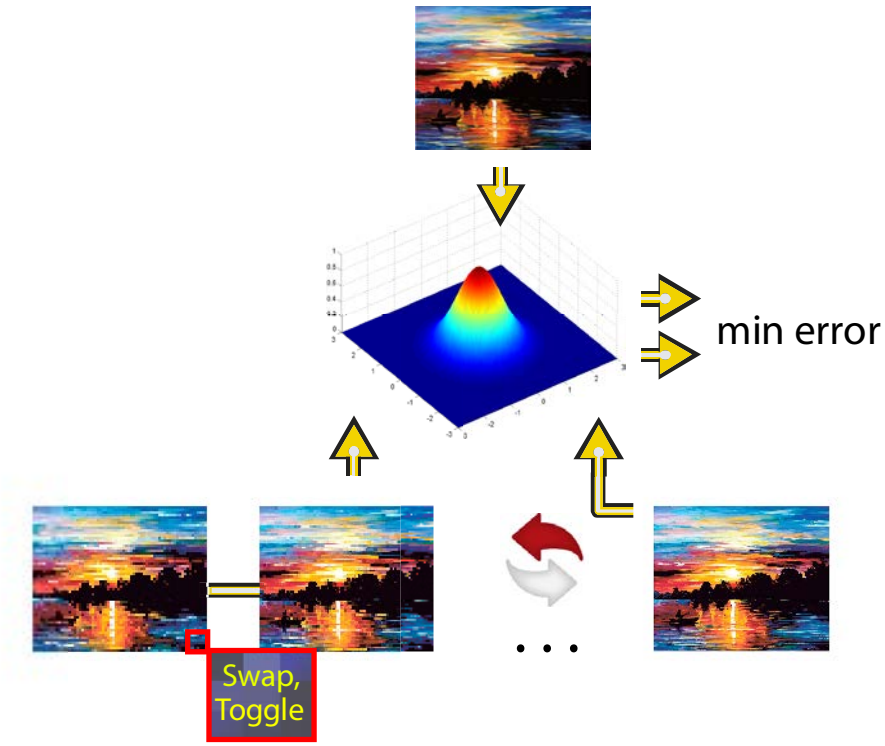

Figure 6.* Simplification of the DBS halftoning algorithm. The integration starts with initial halftone. Pixels in the block are swapped and toggled. The halftoned image is compared to the original through the HVS filter.

The benefits in this approach are:

- Uniform texture of both single and combined channels.
- Maximization of dot-off-dot.
- Reduced visibility of texture (halftoning artefacts).
- Increased colour gamut due to the controlled overlaps.

The summary and comparison of the different halftoning algorithms are presented in Figure 7.

*image (painting) taken from Slavuj and Pedersen, 2015. Processed by the author, Workflow drawed inspired by the C++ code execution for DBS algorithm, A 3D graph, resembling HVS filter, plotted on the data from the DBS algorithm, created in Matlab by the author.

2.4.5 Halftoning for multichannel printing

To this day there has been a very limited research attention dedicated toward the multichannel halftoning problem. It is a new technology, especially to the ink-jet printing. The other reason is that the conventional channel independent halftoning could be applied as well. The only two noticeable halftoning methods applied to multichannel printing are noted in Hexachrome printing (Pantone Inc.) and by Zitinski et al. (2013). These two methods are developed for the AM halftoning where for the additional channels (e.g. Orange and Green at Hexachrome system and RGB for modern day multichannel printing), the new angles are defined so they do not interfere with other process colours.

Figure 7.* Representation three types of halftoning algorithms: Original (top left), Cluster dot (top right), Error diffusion (with Floyd-Steinberg filter), and DBS (bottom right). All halftoning algorithms have their specifics. The cluster dot has good rendering of transitions in dark areas; error diffusion has sharp edges where DBS is uniform.

*image, Lena, comes from Halftoning toolbox (Monga, University of Texas), Computational for cluster dot, FS ED – custom build Matlab function, DBS, monochrome version, C++ code written by Puneet Goyal, Purdue University, Given for scientific purposes and research to Colourlab.

2.5. Discussion on the Background

This section will provide a discussion based on introduced background material. The goal of such discussion is to provide a bridge between theoretical part and the research part. Based on the motivation (section 1.1) for the research, on the research questions (section 1.3) , the goals of the thesis (section 1.2) and using defined terminology and material in section 2.1 to section 2.4, this section will give an overview of the previous research that inspired and have eventually led to the research conducted and reported in the thesis.

2.5.1 Spectral reproduction potential

The active area of discussion in the spectral printing is which error metrics to use and what kind of workflow should be established. Imai et al. (2001) gives an overview of metric that are applied to evaluate spectral reproduction. Spectral RMS (section 2.1.4) does not give an intuitive information of spectral reproduction and it is most commonly used in combination with a colour difference metric (Taplin, 2001, Gerhardt, 2005). Other researches advocate use of multi-illuminant metric (e.g. Morovic et al., 2012) where the resulting colour difference is an average over more than a hundred illuminations. This approach emphasizes a spectral reproduction's robustness in a perceptually meaningful manner. Other work suggests using an interim space such is the Lab PQR (Rosen and Derhak, 2006), a hybrid of colour and spectral space. Owning to limited spectral gamut of the commercially available printers and its ink-sets, Urban (2008) argued for a use of multi-illuminant perceptual space for spectral reproduction. Inspired with Lab PQR and multi-illuminant perceptual spaces, Le Moan and Urban (2014) computed a five dimensional space to reduce dimensionality of spectral data processing.

2.5.2 Toward multichannel spectral printer model

The key quantitative value of printer model performance is its accuracy. This difference is usually represented by colour or spectral difference metric (section 2.1.4) that numerically describes the difference between the model estimate and measured value.

There are many limitations to printer model accuracy (e.g. Wyble and Berns, 1999, Amidror and Hersch, 2000) but tradeoff between resources needed and computational time (both model training and execution time) determines its practical use (Kang, 1999, Green, 2011). Practical use of printer models is a qualitative measure and depends on application and expectations (e.g. in desktop colour application or in industrial production). On the other hand, a spectral printer model is intended for spectral reflectance reproduction (section 2.2). An accuracy of spectral printer model could be quantified in various combinations of colour and spectral difference metrics. Therefore, in absence of perceptual meaning of spectral RMS, this metric is used in combination with some of the colour difference metric. In attempt to improve a multichannel spectral printer model inversion, Gerhardt (2007) used mixed spectral RMS and colour difference metrics due to the poor correlation between these two. On the other hand Tzeng and Berns (1998) have used both colour difference and metamerism index (CIE, 15:2004) in order to select proper four ink combination while Chen et al. (2003) have used Color constancy index (CIE, 15:2004) for similar purpose. Other reason to use multiple metrics in model optimization and accuracy

reporting is due to the fact that today's printers have rather limited spectral gamut (Hunt, 2004, Urban and Berns, 2011, Morovic et al., 2012).

The prevailing problem of calibrating and using spectral printer model remains the complexity of dealing with a multi-dimensional input such as spectral reflectance. For example, a look-up table (LUT) computed on spectral reflectance as an input (e.g. 400nm-700nm, 10nm sampled), regular sampled multichannel printer space (e.g. with 3 independent channels or process inks, CMY) on the output, with only one sample per channel, would have size around 6.4 TB. Using such LUT based interpolation as the spectral printer model is not an option for multichannel printer where size to store the LUT is three times larger than three channel equivalent. Researchers in the field of spectral printer modeling have spent years on this problem. Tzeng (1999) has used a selection technique based on the contribution of the ink combination or mixture to the spectral variability of the output. On the other hand, Taplin (2001) performed an evaluation of whether three of four printer models can be used to model a six-colour printer. The selection criteria were also a tradeoff between accuracy and usability. Similar approach is taken by Slavuj et al., (2013) but with a seven channel printer where findings confirm that some version of the Neugebauer model should be used. The landmark work by Neugebauer (1937) presented as an extension of the Murray-Davis model (both presented in section 2.3) and defined the model as a set of linear equations. The model makes an estimate by a sum of fractional areas covered by all the colorants at full tone and further on performs a multi-linear interpolation to locate a point. In various forms this model has been subject of modifications (e.g. Viggiano, 1983, Heuberger, et al., 1992, Bastani, 1996, Balasubramanian, 1999, Emmel and Hersch, 2002, Hersch, 2014), improvements (e.g. Yule, 1951, Chen et al., 2004, Abebe et al., 2011, Slavuj et al., 2014) and combinations with other models (Yule, 1951, Tzeng, 1998, Hersch and Crete, 2005 Rossier and Hersch, 2010). The most effective combination with other model is Yule-Nielsen modified spectral Neugebauer model (YNSN) which improved model accuracy significantly. The Yule-Nielsen model is intended to model an optical dot gain, the phenomenon of multiple scattering of the light entering the paper substrate and exiting in various directions (Yule, 1951). As at least one direction of scattered light must go through the printed area and exit thorough the unprinted area, the appearance and measured spectral reflectance are altered. This phenomenon occurs at very small printed dots and surrounding paper areas. Difficulty arises from the fact that majority of the measuring instruments have an aperture size much larger than these printed dot areas and necessarily captures both printed and non-printed areas. In return, it is very difficult to accurately separate optical and mechanical dot gain (section 2.3) from the measurements information (Yang et al., 2001, Namedanian, and Gooran, 2010, Namedanian et al., 2013). The optical dot gain induces non-linearity of the printing process and is the main factor that limits accuracy of the Neugebauer model. Therefore, Yule-Nielsen n-factor is an empirical fit which is applied to all colorants before Neugebauer equations are executed. It is shown that n-factor gives a good fit between measured and predicted reflectance. In other words, the n-factor translates all reflectances of the colorants into the space where mixing of the colorants is assumed to be linear (as it was first assumed by Neugebauer). Overall, the YN modification of Neugebauer equations brings a twofold improvement in accuracy of the prediction (e.g. Rolleston and Balasubramanian 1993, Wyble and Berns, 2000). However there are certain limitations of this model, particularly if is to be used with multichannel printer. The n-factor is a selected value that is obtained after optimization routine computes

all possible exponents (or n-factors) that applied on spectral reflectance of the colorants give the best prediction. A problem with this approach is similar to any other data fitting model; it is dependent on the training set. In the case of YN n-factor, this dependency is on the process ink, its area coverage and substrate. This is easily demonstrated by using a training set as a test set (e.g. a cyan ink ramp is used as a training and test data set) and then the same training set but different training set (Wyble and Berns, 2000). As the YN optical dot gain phenomena is quite old idea, only recently, when growingly powerful computers are used this idea revitalized. There have been many attempts to try to assign physical meaning to the YN n-factor. The light-ink-paper interaction is very complex and n-factor is only derived to account for one isolated phenomena out of many that occur in the paper bulk. Through the years, much research has been dedicated to evaluate YN model on various test situations. Ruckdeschel and Houser (1978) analytically demonstrated that n-factor in a describes a range of substrates with values from 1 to 2 where moving toward 1 means a higher specular reflection (e.g. a glossy paper) while moving toward value of 2 the substrate is assumed to completely scatter the light (e.g. a matt paper) which confirms assumptions made by Yule (1951). They also showed that determination of the n-factor from varying dot area coverage is only valid up to the 50% effective coverage. On the other hand Pearson (1980) found from evaluation of many substrates and coverage combinations that the best average value to use for the n-factor is 1.7. The factor is further explored in YNSN model applied to multichannel printers (Taplin, 2001) for a six-channel CMYKOG and Gerhardt (2005) for a CMYKRGB printer, both with custom made inks. They both reported derivation of the n-factor with and without previous calibration of each channel. They had similar conclusion that if optimization is conducted on calibrated channels, the YNSN prediction improves. However, as they used rather different test set (Taplin used two colour overprint chart with 9 levels per channel, while Gerhardt had up to the four colour overprints with four levels per dimension). However their results suggest very different performance and while Taplin(2001) confirms findings by Wyble (1999) for two colour overprint prediction (mean ΔE^*_{ab} of 2.58 with 1.73 standard deviation and 7.7 maximum prediction error), Gerhardt (2007) has shown that on another test set (with many high coverage patches) are nearly threefold worse. It is assumed from these findings that must be another very significant dependency of the n-factor on coverage or in particular on high coverage. Other than single cell YNSN model (only one 100% colourant measured), the so called cellular YNSN model (first explored by Heuberger et al., 1992) have been used in practice. Ever since, this model has been state of the art in accuracy that can be achieved by printer model (section 2.3). The Neugebauer idea was to sample the printer space with printing and measuring the full-tone colorant outputs and each of the full-tone colorants combination. If these form a LUT, the full-tone colorants and their mutual combinations will be the nodes of the multi-dimensional LUT. Subsequent interpolation that searches for the desired value in the LUT grid (e.g. 35% cyan, 5% magenta combination) would have two nodes to calculate mid-value, one full tone C+M combination and non-printed paper as 0% ink covered area. The desired point is somewhere at the mid distance from both nodes but due to the high non-linearity, and without YN model modification, the accuracy of the predicted value is not satisfactory for many applications (Wyble, 1999, Green and MacDonald, 2002, Kang, 2004). Adding one 50% coverage node into same LUT will improve prediction of the desired

value (Tzeng, 1999, Taplin, 2001), but this will come at the cost of significantly more measurements. The rough estimate is that for a seven colour multichannel printer, with 10 samples per each channel, one would need $10^{\wedge 7}$ measurements while for three colour printer with same 10 samples per channel, around $10^{\wedge 2}$ measurements. In each case, such cellular Spectral Neugebauer (cSN) or cYNSN model would give maximal accuracy currently possible to achieve with printer models. However, the amount of ink that would have spent printing these cYNSN training patches (and probably test patches as well) for a multichannel ink-jet printer, would depleted the ink levels to the point of uselessness (when inks are changed, the new model must be build). This stress the fact that all models are dependent on the training set which is dependent on the printer, substrate, ink set, halftoning, ink limitations, etc. Unfortunately there is no a model or a method available to account for all these changes which even more emphasize the need for optimized, robust, accurate, the least measurement intensive and fast executing model still is and have been one of the most researched area in printing.

2.5.2 Toward multichannel halftoning

As it is the case with printer models, halftoning algorithms also operate on certain pre-assumption made on the printing process. The spectral and colour reproduction are concerned on reproducing desired spectra or colour. Minimal area of a colour patch is closely related to the aperture size of a measuring instrument. Even with 5mm in diameter, such measurements will include many printed dots and areas of the paper. Exactly how many dots can be captured with small aperture is depending on the printer resolution. High end ink-jet printers claim to have up to 1200dpi in each direction (HP z3200 PS). Rough calculation says that around 1800 dots is printer able to send along the aperture diameter direction. The "true" resolution is not known however but again rough calculation based on the dot gain curves (Slavuj et al., 2013) suggest that probable resolution of the print itself is around 600dpi. This resolution is still not perceivable to HVS which cannot and differentiate between individual points with resolution of 150 LPI which is roughly 330dpi (Kipphan, 2001). However, human eye is very capable to spot a low frequency pattern, which can come as a result of spatial error in high frequency dot distribution (e.g. worms of Error diffusion algorithm (Ulichney, 1987). The problem of colour halftoning comes on top of the problem of spatial dot distribution. The statement suggests that if artefacts of the halftoning occur in one channel, it is most likely to be conveyed to other channels as well.

Error diffusion, first introduced by Floyd and Steinberg (1975) has been one of the most successful algorithms for halftoning in the last half century. Even the original filter created by Floyd and Steinberg is still in use. Other important breakthrough in halftoning occurred when Pappas and Neuhoff (1992) and Anolui and Allebach (1992) have introduced a concept of a model based halftoning. The model based halftoning is an optimization heuristic that constrains printer special characteristics and interactively computes the image that minimizes perceptual error between original and halftoned image. As any optimization process (e.g. similar to the one used in cYNSN model inversion or in computing n-factor), the problem is the computational time. Although quality of the model based halftoning is the state of the art (Figure 7, bottom right image), its wider use is still questionable.

In colour halftoning, there have been attempts to deal with channel interactions. (e.g. Haneishi, et al., 1996, Shaked et al., 1996, Pappas, 1997, Lin and Allebach, 1998, Agar and

Allebach, 2000, Damera-Venkata and Evans, 2001, Lee and Allebach, 2002, Monga et al., 2007, He, 2010). Particular interesting is the work by Lee and Allebach (2002) on channel dependent colour based DBS halftoning (CB DBS) while work by He (2010), which can be seen as an improvement of the CB DBS is based on slightly different conditions. A CB DBS halftoning controls the quality of each colourant texture separately along with the total dot distribution. Authors have regarded that yellow ink, as being of low contrast to the paper, should be discarded in optimization of the halftone. The relevant channels are cyan and magenta and these should be distributed as uniform and possible and their overlaps are controlled with maximization of dot-off-dot halftoning. First, the dot overlapping and positions of magenta and cyan dots are decided by a monochrome DBS halftoning algorithm. Then, dot colouring is accomplished by a swap-only DBS heuristic constrained on the predetermined dot positions in the first step. The extension of this approach by He, suggests that yellow channel, when combined with other channels (cyan and magenta), introduces high density textures that becomes visible, so it cannot be disregarded. The author calls his method hierarchical DBS where each channel and their overlaps are sequentially halftoned based on their texture visibility. These two algorithms and those alike, are the paramount in halftoning quality. Another study has recently done that evaluate how practical are these algorithms today (Tragery et al., 2011), when GPU processing is available. They showed that for a full HD resolution image, processing time without GPU is around 2572 s, but with GPU is 127s.

Similar to the research capacity invested to a printer model research, halftoning also has been one of the most researched areas in printing. This proved point made in (Section 1.3) that printer modelling and halftoning are two most important operations in the print workflow. However, there has not been an attempt to evaluate a whole reproduction system where color management and halftoning are considered jointly. As mentioned in the (section 1.1), halftoning and colour management are developed and evaluated in absence of one another. In order to calibrate printer model, the training target is already printed with the given halftoning and it is again tested against the same halftoning. The only concern on channel interaction is that Neugebauer model, if used with Demichel probability model (Demichel, 1931), will depend on the given halftoning even though the model is calibrate for that halftoning (Slavuj et al., 2013). The dependency of the Demichel model on different superposition conditions was explored by Amidror and Hersch (2000) based on the work by Rogers (1998) who conducted limited study with single channel evaluation. They have evaluated whether Demichel assumptions, which they conclude to work only on one unique channel overlapping conditions, stands for rotated screens and stochastic halftoning. Oztan et al., (2000), confirms finding of Amidror and Hersch for different halftoning conditions; that is, dot-on-dot, dot-of-dot, rotated screens and stochastic, the Demichel model cannot be used with first two conditions where statistical independency of each channel does not exist, and that the closest to the assumptions made by Demichel, is a rotated screens. In Slavuj et al., (2013) Spectral Neugebauer model applied on multichannel printing was tested with two halftoning: channel independent: Floyd Steinberg Error Diffusion (Floyd and Steinberg, 1978) and simulated rotated screens (simulated stands to mark that ink-jet are natively a FM device as it cannot alter size of the dots). The angle chosen for RGB channels was around 7° from their complementary CMY channels. It is

found that performance of the SN model with rotated screens is noticeably better than with channel independent FM halftoning which suggested that there were more dependencies of the SN model than calibration and dot gain compensation (also very different for different halftoning). Another halftoning and colour management concatenation was done by Kawaguchi et al., 1998. They have utilized VED halftoning (section 2.3.2) in a spectral reproduction workflow. However they claimed that processing full spectral reflectance information would be too complex so they have taken the dimension reduction approach. Such reduced dimensionality of the input signal they applied to VED worked well and even better then with conventional colorimetric workflow. Later, Gerhardt and Hardeberg (2005) will build upon that work but will define a new set of primaries, the spectral reflectance of the NPs. They regarded a SVED (section 2.3.3) to be more suitable as an inverse model plus halftoning and all the halftoning manifestations (error accumulating, banding, noise), they tried to solve by modifying input spectral image (although they also experimented with different filters). This was an example how different are colour management and halftoning but also how dependent are on each other.

Chapter 3

Summary of included papers

This section provides an overview of the scope of the included papers and the summary of each of them. The section starts with introductory part where the scope of the papers is graphically presented.

3.1 Introduction

The general objective of the thesis is to evaluate, improve and create a new spectral printer model and halftoning for multichannel printing. Goals that for such spectral-multichannel reproduction workflow should achieve are: colour accuracy, practicality, high speed of processing and good image quality of the output.

The core of every reproduction workflow is the model made estimation of the input signal. Starting point in reproduction workflow is a colour patch measurement or an image acquired by measuring instrument or a camera (spectral or colour). Input signal is then transformed through a gamut mapping, the model estimate and halftoning. All these operations (and many more in between) could be summarized in one word as 'transformations' of the input signal.

Transformations are generally separated in: spectral - colour transformations (e.g. from source image colour space to destination – printer space), and transformation of the model estimated tone value (expressed as dot area coverage) into a binary map via halftoning. It is taken that these two transformations are most important for any reproduction. This is somewhat universal assumption one can make about printing, whether printing is with monochrome printer, four channel CMYK device, or some of the multichannel printing device. Colour or spectral transformations (e.g. forward model and separation) are responsible for colour accuracy of a printed area while halftoning determines spatial distribution or the size of the dots within the same area. Therefore, halftoning is then responsible for achieving the average colour (tone) of the halftoned area. On the other hand, the goodness of halftoning algorithm is also quantifiable through the quality of textures, expressed as some of the image quality metric. The texture has higher image quality score if it hardly perceived.

Therefore, to say what a good quality print is, one must go through all transformations and report their colour accuracy and image quality. Unfortunately, these two metrics do not correlate very well considering that one works on pixels and other on whole image. Also, the spectral-colour transforms and halftoning algorithms are designed separately and in absence of one another.

Consequently, in this thesis both colour accuracy and image quality are acknowledged as important reproduction goals. In order to summarize findings of included papers, the problem is divided into: model - based transformations, halftoning transformations, and other processes of a reproduction workflow (e.g. acquisition - measurements, gamut

mappings, image processing operations, etc. To model ink-substrate-printer combination, following steps must be followed: linearization-dot gain compensation step, model calibration (e.g. synthesis and printing of a model's training set of patches), and model execution where an estimate accuracy is evaluated on the target data set. Printer models are always bi-directional where in forward direction output is estimated from known or computed ink combinations (printer space-signal space), while in an inverse direction dot area coverages are estimated (signal space-printer space). These dot area coverages, when printed and measured, should correspond to the measurements of the input signal. If the model was linear, it could be easily inverted. However a complicated light-ink-paper interaction printing process is highly non-linear and complicates printer model inversion. A better understanding of light-ink-paper interaction leads to the discovery of an underlying physical phenomena where usage of physical models is. Contrary to empirical model, which provides estimate from a regular sampled printer space, physical models could greatly simplify computation and inversion process.

All modelling work in the thesis is based on the Neugebauer linear equations. As the thesis is only concern about the spectral reproduction, a Spectral Neugebauer (SN) model is used. These equations are applied to linearized data (dot gain compensation in printing) and represent fractional contribution of each of the Neugebauer Primaries (NP) into a halftone colour mixture. The NPs are printed as a colour patches and measured with spectrophotometer.

Therefore, improvements on SN model are suggested in terms of improving the accuracy of computed curves for physical and optical dot – gain (Paper B and Paper C), the NPs estimation method (Paper D). The Paper A, Paper F and Paper E are concerned with the spectral model and halftoning relation; the model accuracy and image quality when used with different halftoning algorithms and methods. The work with halftoning and modelling has also led to a new halftoning method (Paper F) which is specific for multichannel environment.

Figure 8 shows published papers and how their scope interleaves. Capital bold letters represent included papers and their scope within reproduction workflow. Some papers are investigating more than one problem which is marked with their balloon overlapping with that area. Modelling part has four papers included; two are concerned on calibration of the model (Paper C and Paper D), one paper addresses creation of the training set of primaries by estimation (Paper B), while three more papers are related to halftoning and modelling. One paper is a general one (Paper A), published to provide an insight toward a new possible research directions, but is also concerned with accuracy of SN multichannel printer model when combined with different halftoning (Paper A). Another paper aims at finding a trade-off between colour accuracy of a spectral and colorimetric workflow on one side and image quality on other (Paper F). With different halftoning algorithms applied the image quality of whole reproduction workflow is a combined quality of a colour management and halftoning (Paper F). One of the halftoning algorithms is applied in evaluation of Paper F, is previously developed post-processing halftoning method that improves quality over channel independent halftoning (Paper E). Improvement is achieved by utilizing all process inks of a multichannel printing system in order to replace otherwise unwanted CMY overlaps. One paper is concerned on the application side of multichannel – spectral printing (Paper G). This was a case study of usability of such reproduction systems in simulation of textile fabric colour.

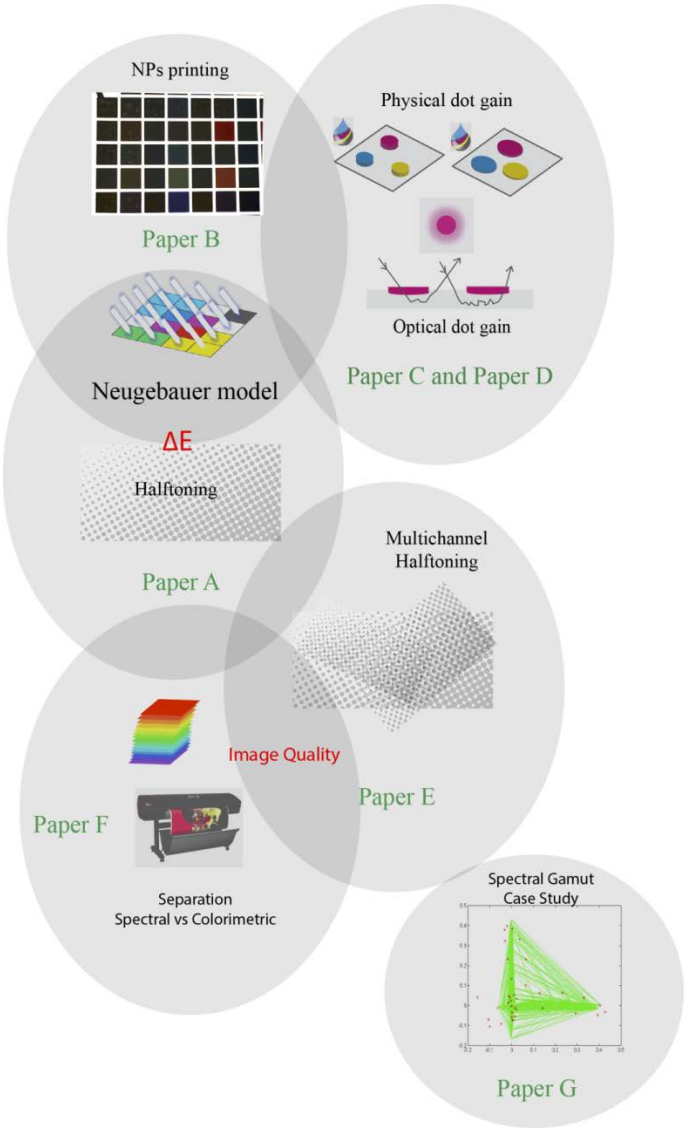

Figure 8.* Scopes of included papers in a reproduction framework.

*Physical dot gain, optical dot gain drawings are authors (used in Slavuj et al., 2015, EI – presentation), NPs printing Image taken with the camera in the lab, Neugebauer model – redrawn from Urban, Spectral Reproducion workflow presentation, halftoning-created pattern in Adobe Illustrator by author, same for multichannel halfotning, simulation of the spectral separated space is an authors original creation, spectral gamut figure taken from Slavuj et al., 2014, JAIC.

3.2 Paper A - Review and analysis of spectral characterization models and halftoning for multi-channel printing

Overview: The first aim of the papers is to provide a comprehensive review of spectral halftone printer models and a continuous tone ink mixing model. The review is primarily concerned with the spectral printer models that can be applied in the multichannel environment. Second aim of the paper is to evaluate dependency of Spectral Neugebauer (SN) printer model on the different halftoning methods (e.g. AM vs FM).

The review of the printer models starts with simple, single colour Murray-Davis (MD) model (Murray, 1926) which is usually used for a single channel dot - gain computation. The extension of MD model to multi-colour resulted in Neugebauer (NG) equations (Neugebauer, 1938). The NG model uses a Demichel probability model (Demichel, 1924) to estimate fractional area covered with one of the Neugebauer Primaries (NPs). In its original form, the NG model is not a sufficiently accurate and some of the improvements are usually used. One of the extensions of the NG idea is the YN optical dot gain compensation (Yule and Nielsen, 1951). The so called YN n-factor is an empirical factor which is obtained through the iteration and by finding local minima of the colour difference or spectral RMS as an objective function. All mentioned models by now are also called empirical models and they are based on the training set of data of the regularly sampled printer space. After model has been trained or calibrated, a look-up table (usually the case in the ICC colorimetric workflow) can be build is where intermediate points are estimated with a multi-linear interpolation. The performance of these models is therefore dependent on the number of measured patches and their proper selection.

Different approach to modelling ink mixtures is taken by the physical models, such as the Kubelka-Munk (Kubelka and Munk, 1931) model for continuous tone mixing. This model comes as very useful for estimation of non-printable or hardly printable high coverage training set of patches. This problem enlarges in multichannel printing where the artefacts such as bleeding occur when ink amount exceeds the substrate's absorption potential.

The Second aim of the paper was to evaluate the accuracy variation of the NG model when calibrated for different halftoning method. This was evaluated for rotated screens AM halftoning and for Stochastic FM halftoning.

Motivation: The aim of this work was primarily to search for the state of the art in printer modelling and to find one which is applicable to multichannel printing. The rich body of literature exists for colour and spectral models and halftoning algorithms. However, a comprehensive review of spectral printer models specific for multichannel printing was not available. The most widely used model around and in the thesis is based on Neugebauer linear mixing halftone model. This model was the best candidate to use in halftone multichannel printing environment. The second goal of was to evaluate a compliance of the models with halftoning methods. Also, halftoning and its relation with YNSN model was unclear and perhaps, the potential track toward something new was sought.

Results: As the goal was to familiarize, review and select models for the future use, the results are only presented for the second aim. Therefore, different halftoning will produce significantly different dot overlaps. Furthermore, it is known that AM is more prone to the optical dot gain than FM due to isolated dot placement. This would require halftone specific determination of the YN n- factor. However, even after specific n-factor has been calculated,

there is still a difference in accuracy of the YNSN for AM and FM halftoning. In order to account for the difference in halftoning channel overlap, one must look whether Demichel equations do hold for all channel superposition.

Conclusion: The Neugebauer linear equations are a good candidate to be used to model the multichannel printer. However, the paper, ink set, halftoning, ink limit all must be fixed and new model must be made every time when some of these parameters are changed. This is the general problem of the empirical models such as the Neugebauer model. One of the limitations of this model is in its dependency of different halftoning, where for rotated AM screens the model performs better than when used with the stochastic FM screens. This dependency is mainly due to the Demichel probability model which stands only for specific superposition case.

3.3 Paper B - Measuring or Estimating Neugebauer Primaries for Multi-channel Spectral Printer Modelling

Overview: The Neugebauer linear printer model estimates the output by linear addition of so called Neugebauer Primaries (NPs). These primaries become the new building blocks (in contrary to using only the process inks as primaries) which represent all primary inks, and every possible combination thereof. For a seven channel printer (e.g. with CMYKRGB ink set) there are many four, five and six channel overprints, where each channel is of full-tone (e.g. 100% ink coverage). Majority of substrates could absorb up to 300% of ink per area which suggest that many of the NPs are not printable without artefacts.

Non-printable NPs was the main problem that following paper has addressed. The NPs for standard SN model are full-tone overprints. A common solution to non-printable NPs is to estimate them using a continuous tone model for ink mixture. In this work, a KM model is used to estimate the reflectance of the Neugebauer primaries. Additionally, the KM model is compared with the DORT2002 (Edström, 2004) angle resolved model that also estimates scattering and absorption coefficients of the ink mixture. We conclude that DORT2002 does not offer significant improvements over KM in the estimation of the NPs, but a significant improvement is obtained when using a simple surface scattering model. This model is proposed in the paper. When estimated NPs are used as inputs to the SN model instead of measured NPs, it is found the SN model performs the same or better in terms of colour difference and spectral error. If the mixed measured and estimated NPs are used as inputs to the SN model, it performs better than using either measured or estimated NPs.

Motivation: Since most substrates are limited in their capacity to absorb the large amount of ink, it is not always possible to print all colorants combinations necessary to print NPs, particularly ones for multichannel printing. A common solution is to estimate the non-printable Neugebauer primaries from the measurements of primary colorants in the printer with the KM optical model.

Results: Results suggest that for the purpose of estimation of the NPs, it is sufficient to use KM model. The advantage of DORT2002, beside its capability to simulate different measurements geometries, is limited for this purpose and only slight increase in estimation accuracy is achieved with expense to computational time and complexity. In fact, accuracy of the estimation could be increased otherwise; by using a simple surface reflection model which essentially counts for printing on top of the black ink. Namely, if an ink (e.g. cyan or magenta) is printed on top of the black patch, only scattering (S) coefficient varies, while absorption (K) is 1 and comes only from the black ink (or other high density ink mixture).

Conclusion: In this work, a printing of the Neugebauer primaries on different substrates and the influence of ink limitation were evaluated. Very limited number of substrates is capable of absorbing the high ink amount needed for multichannel printer characterization. However, it is found that printing with the maximum ink amount is not necessary as there is no difference in spectra of the NPs when printed with different ink limits. The one

noticeable fact in the evaluation of the effect of the ink limits is that the large ink amount can lead to artefacts that influence the performance of the SN model. We have found that using DORT2002 or KM model there is no significant difference for the estimation of the primaries. The proposed surface scattering model significantly improves estimation with either KM or DORT2002. In fact, with surface reflection model, the DORT2002 outperforms KM model. The findings also suggest that the SN model performs the best when used with a mixture of measured and estimated NPs.

3.4 Paper C - Effect of ink spreading and ink amount on the accuracy of the Yule-Nielsen modified spectral Neugebauer model

Overview: During the calibration of the YNSN model, one needs to estimate effective dot area coverages from nominal coverages and as well as the optical dot gain that is a result of light scattering in paper bulk. The steps are important in sense that the 'right' ink amount should be used so it can produce desired colour. This paper investigates a dependence of the model accuracy on the ink amount that is controlled in different manner in today's printers. It is shown that the performance of the YNSN model strongly depends on the maximum ink amount. In a cellular implementation, this limitation mainly occurs for high coverage prints, which determines the optimal cell design. For ink-jet prints, apparent (effective) coverages derived from both the Murray-Davis and optimized YNSN models show very large ink spreading resulting in that the printed dots are larger than their nominal surface coverage (dot gain). Because ink-jet printing is a non-impact printing process, this leads to the hypothesis that ink dots have a smaller thickness than full-tone ink film since the ink volume on each pixel is constant. Measured spectral reflectance curves show similar trends to those of ink film with increasing thickness, which supports the hypothesis. The lesser accuracy of the YNSN model when using maximum ink thickness can therefore be explained with the fact that the patches with lower coverage have a mean ink thickness very different from that of the full-tone patch. This observation implies that the Yule-Nielsen n-factor is accounting for varying ink thickness that results in non-linear relationships between the spectral reflectance at different ink coverage. This can partially explains why the n-factor is often determined as being different for different inks on the same substrate.

Motivation: Calibration of the printer is important step toward achieving accurate reproduction. It is well known that dot gain effect, whether mechanical or optical, induces a non-linearity which is usually modelled by using an empirical fit. The YNSN model for bi-level printers assumes dots of equal thicknesses. The physical dot gain of each channel is usually computed with the MD model while the YN n-factor is computed to account for the optical dot gain. As it is hard to separate optical and mechanical dot gain from the measurements, the reflectance measured from the sample represents the one which combines reflectance of ink, and the optical dot gain which describes scattering in paper bulk. This is one of the reasons why empirical models are preferred to model optical dot gain. However, the empirical models that are used to model a physical phenomenon could not make a claim that they count for only one physical attribute of light-ink-paper interaction. This was the reason why the YN n-factor was never physically explained, although many research efforts were dedicated to it (e.g. Pearson, 1980, Arney et al., 1996, Shiraiwa and Mizuna, 1993). This paper on the other hand, tries to predict n-factor from various coverages in order to prove that it depends not on coverage but on the ink thickness which is a function of the coverage.

Results: The results show that the performance of the YNSN model is strongly dependent on the choice of maximum ink coverage, while the model performs very satisfactory when

the maximum ink coverage is restrained to around 85-90%, which is almost equivalent to using 100% maximum ink coverage with less ink amount. Namely, this is to say that what appears as a full-tone is not real full-tone, but optical dot gain makes it appear as full-tone. This implies following: first, since the ink amount has a significant impact on the performance of the YNSN model it should be reported and discussed when evaluating the model accuracy on a sample set.

Second, when using maximum ink coverage and ink amount, a cellular implementation with two cells will perform better with a cell boundary at 85% coverage than at 50% coverage.

Conclusion: The effect of an ink spreading on the dot spectral reflectance is primarily related to the relative (predicted) and not the absolute dot gain since the dot thickness is proportional to the dot area for constant volume. This means that the effect will be greater when the dots are small and the dot gain is high. The analysis suggests that the performance of the YNSN model could be improved by accounting for the variation of ink thickness. This can be effortlessly implemented by modifying the spectral reflectance of the ink according to the ink thickness determined as a fraction of full-tone ink thickness that is directly related to the relative dot gain. This requires predicting scattering and absorption coefficient of the inks in order to relate spectral reflectance to ink thickness (Paper D).

3.5 Paper D - Modelling coverage dependent ink thickness in ink-jet printing

Overview: A simple extension of the Murray-Davis halftone reflectance that accounts for the change of ink dot reflectance due to ink spreading is proposed here. Significant improvement of the prediction accuracy is obtained for a range of paper substrates and printer combinations compared to the classical Yule-Nielsen and Clapper-Yule (Clapper and Yule, 1953) (CY) models. The results show that ink dot thickness dependency is the main factor limiting the validity of the Murray-Davis model and that the optical dot gain can be neglected when the model is calibrated for one specific printer, ink set, ink limit, halftoning and substrate. The proposed model provides a better understanding of halftone reflectance that contributes to the development of physical models for simpler and faster printer calibration on different substrates.

Motivation: The work was inspired and developed from the findings in previous two papers (Paper B and Paper C). It is not however a simple extension, but rather a new model for dot-gain determination which proves hypothesis made in Paper C. This was a rather exciting finding that could replace empirical calculation of the optical dot gain done with the YN n-factor. Also, a new model based on these findings satisfies some of the set goals in the thesis; that is, colour accuracy and reduction in computational time.

Results: Findings in this work show that by introducing an ink thickness reflectance correction estimated with modified KM model, the model outperforms YN n-factor in estimation of single ink dot area coverages. The average prediction error of the proposed model is around a ΔE of 1, while modelling with YN n-factor yields error around a ΔE of 4 for all tested substrates and dot area coverages. The dot gain curves estimated by the proposed model are including both optical and mechanical dot gain and they correspond better to measured reflectance of a certain patch. As mentioned previously, it is hard to separate optical and mechanical dot gain. It is also hard to say that n-factor counts barely for optical dot gain and that mechanical dot gain compensation curves are computed just for that phenomena. The proposed model represents a diversification from the idea of optical and mechanical dot gain separation and modelling with empirical factor. Both physical and optical dot gain depend on the dot area coverage which induces ink thickness variation. When accounted for the ink thickness variation, the estimation of the spectral reflectance curves is significantly better than what is computed with MD-YN or MD-CY combination.

Conclusion: The proposed model is a simple extension of the Murray-Davis (MD) model where the reflectance of the inks dots is estimated from their thickness through the surface reflection corrected Kubelka-Munk (KM) model. The thickness of the dots is directly related to the difference between apparent coverage and nominal coverage, since a dot that gets twice as big needs to be half as high in order to keep ink volume constant. At a given nominal coverage, complete ink spreading occurs and the halftone is modelled as an ink film where thickness is proportional to the nominal coverage. This model leads to a drastic

increase of the prediction accuracy, when compared to the Yule-Nielsen (YN) and the Clapper-Yule (CY) models.

3.6 Paper E - Multichannel DBS halftoning for improved texture quality

Overview: The paper aims to develop a method for multichannel halftoning based on the Direct Binary Search (DBS) algorithm (Lieberman and Allebach, 2000). The specifics and benefits of multichannel printing are integrated into the halftoning method in order to further improve texture quality of DBS and to create halftoning that would suit multichannel printing. Originally, multichannel printing is developed for an extended colour gamut. At the same time additional channels can help to improve individual and combined texture of colour halftoning. It does so in a similar manner to the introduction of the light colours (diluted inks) in printing. Namely, if one observes Red, Green and Blue inks as the light version of the M+Y, C+Y, C+M combinations, the visibility of the unwanted halftoning textures can be reduced. Analogy can be extent to any number of ink combinations, or Neugebauer Primaries (NPs) as the alternative building blocks. The extended variability gained from the set of NPs could provide many practical solutions and improvements in colour accuracy, image quality, ink saving, etc. This could be done by selection of NPs per dot area location based on the constraint of the desired reproduction. Replacement with brighter NP at the location could induce a colour difference where a tradeoff between image quality and colour accuracy is created. With multichannel enabled DBS haftoning, we are able to reduce visibility of the textures, to provide better rendering of transitions, especially in mid and dark tones.

Motivation: How to define a halftoning strategy for multichannel printing? Is it the one which somehow needs to accommodate all used channels or is it a multiple three or four channel problem? What would be the quality of such halftoning? In this work we tried to answer all this questions and to offer a solution which provides a partial answer to all these questions. Therefore we used a characteristic ink set on a multichannel printing system to try to improve quality of a channel independent halftoning method. For spatial dot distribution of individual channels the monochrome DBS was selected for its high texture quality. Other halftoning algorithms such as Error Diffusion would potentially lead to artefacts (e.g. worms), and it was desirable that in further analysis only Multichannel DBS post-processing is visible. In theory, this idea was also very exciting, simple and had many implications.

Results: The multi-channel DBS idea, when applied on a four colour CMYK image, produces less visible texture by replacing or avoiding overlaps of the superimposed channels. All combinations CM, CY, and MY are taken into account and replaced with some of the RGB channels. Although this idea is readily extendable to a NP space from which many reproduction goals (such as colour accuracy or ink saving) can be satisfied, the work was concerned only on image quality improvements. It is shown that with the simple overlap replacement and in comparison with CMYK channels independent DBS, the MC DBS has higher NQM score and is less grainy.

Conclusion: In this work we have developed a framework for multichannel FM halftoning. The underlying halftoning algorithm is Direct Binary Search (DBS) whose spatial distribution of dots is proven to be the paramount for texture quality of the halftones. By using additional secondary colours, we are able to further improve texture quality through

reduction in texture visibility. Further on, we are able to provide a framework for multichannel printing and halftoning where the reproduction goals and decisions are made at colouration step on top of the dot locations distributed by monochrome DBS.

The texture visibility is evaluated through two image quality metrics that are directly applicable to halftones: NQM and Graininess. It is shown that significant reduction on luminance axis is possible when two primary overlaps are replaced with the secondary colour. The trend continues with three colour overprint (e.g. neutrals) where again the two primary colours are replaced with one secondary and then combined with third primary. Although two selected image quality metrics resemble well variation in luminance when channel replacement is introduced, they do not necessarily include all image quality attributes of a halftoning method. In future work, we will provide with more comprehensive set of image quality evaluation metrics. It should be noted here that as the number of overprints per addressable dot location exceeds three, the dot gain and physical limitation of both substrate and ink, disable any significant change in luminance and chrominance. Therefore, the physically imposed limitation guided us to limit the number of overprints to four. Similar limitation can be found in implementation of Cellular YNSN model or ink limitation algorithms.

3.7 Paper F - Print quality and colour accuracy of Spectral and Colorimetric reproduction with Multichannel DBS

Overview: The paper aims to evaluate image quality and colour accuracy of the spectral and colorimetric reproduction. Reproduction workflow starts with a spectral – colour image or a single spectral reflectance which, after series of transformations, is matched by printing specific ink combination. Ink amounts are then converted to binary map with halftoning and printed on the substrate. Spectral printing is designed primarily to match single reflectance of the patch but using it to print spectral images might lead to undesired artefacts and to a reduced image quality. Spectral separation and gamut mapping is a pixel based process which has multiple choices (metameres) per pixel, which spatially observing, produce noise. In comparison with colorimetric workflow, spectral is more accurate, precise, and flexible under multiple illuminants. In general, image quality in reproduction process is usually attributed to halftoning while in this work we observe transformations and halftoning as a unit. Different halftoning algorithms are used throughout work including previously developed multichannel halftoning method based on Direct Binary Search heuristic (MC DBS). Spectral transformations in used here involve inverse Cellular Yule – Nielsen Spectral Neugebauer (cYNSN) halftone model for estimation of the dot area coverages while colorimetric workflow (based on ICC architecture) uses a LUT for same purpose. It is shown that print quality of colorimetric workflow strongly depends on the halftoning, while spectral workflow is less influenced by that. After application of halftoning, and although colorimetric transforms have higher print quality score, spectral workflow is matched in evaluated noise, graininess and smoothness. It is also found that MC DBS improves image quality of both colorimetric and spectral reproduction workflow.

Motivation: Spectral reproduction is promising new reproduction framework. It is designed to match input reflectance by printing specific ink combination. However, already there is a significant limitation; spectra of a real world object are very different to ones of printing inks. This fact limits spectral reproduction usability and potentially leads to poor image quality in comparison to colorimetric workflow. Primarily this is because of metamerism problem as an image would be composed of selected metamers per pixel. On the other hand there is colorimetric workflow where only a single CIE L*a*b* value represents image pixel. Now this is all a transformation problem, and there were obvious questions following: what about halftoning? To what extent halftoning contributes to the overall image quality? Can halftoning improve on poor image quality of the spectral transformation (e.g. separation and gamut mapping)? These were the questions that are answered in this work and the previously developed MC DBS method is evaluated in the more 'real' situation.

Results: Results show that spectral reproduction is indeed a more accurate and precise reproduction and that by using spectral models, one gets a significant increase in colour accuracy of the reproduction. However, spectral separation has lower image quality in comparison to colorimetric separation due to rather large set of metamers for pixel that spectral has to choose from. The separation process is an optimization based forward model inversion process which is searching for specific ink combinations that has a minimal ΔE from original under two illuminants. As spectra of real world objects is significantly different from the one of inks, optimization under multiple illuminants become best one can

do (Urban and Berns, 2011). Optimizing with spectral RMS is known not to have a correlation with visual perception. If one then selects CIE illuminant D50 and illuminant A for optimization, then colour difference below 1 for both illuminants would correspond to a spectral match. However these two illuminants form different gamut and some samples might be in gamut under one illuminant but not the other. If added that this operation is pixel wise, it becomes obvious that spatially this has significant potential to create noise. By evaluation of Noise Quality Measure of the colorimetric and spectral (dual illuminant) separation, it is obvious that spectral has lower score in perceptual noise. On the other hand, one could not evaluate overall image quality performance of reproduction system just by judging model (separation) performance. Namely, after separation process has made an estimate of the dot area coverages, the halftoning determines dot distribution. Precisely halftoning was the process that has been attributed to carry image quality of the reproduction system. However in this work it is separation and halftoning combined which are judged for image quality performance. It is concluded here that although spectral separation produces more noise than colorimetric, after halftoning is applied, these differences are becoming less and these two workflows have very similar image quality score. It is suggested therefore, that colorimetric workflow is more prone to halftone noise.

Conclusion: The aim of this work was to evaluate a reproduction system quality, not separation or halftoning alone, but whole spectral and colorimetric reproduction system. The conclusions on image quality made at any step of the workflow are somewhat incomplete and they do not carry much significance to the final print. It is well known that spectral reproduction, for spectra which is within the gamut of the printer, is more flexible and accurate under multiple illuminations than it is the case with colorimetric. However, the very same principle that makes spectral reproduction better than colorimetric to a certain extent, makes it also more problematic once it comes to print complex images. It is true that both are designed to have highest accuracy of reproduction for a large colour patch, but specific design of transformations, makes these two reproduction paradigms very different for image reproduction. The regular sampling of the LUT in ICC colorimetric workflow and interpolation extraction of the intermediate values is significantly different from that of optimization heuristic based spectral separation. Both workflows in this work use empirical models for estimation of the output. General rule for empirical model is that they deal with inherent non-linearity of light-ink-paper by increasing sample rate for model training. According to this, spectral workflow which is in this work calibrated with 13500 patches for its cYNSN model should outperform 3000 patches calibrated LUT of the ICC colorimetric workflow. As mentioned already this is true for reproduction of the patches, which are usually observed in isolation. On the other hand, quality of the printed images is a function of spatial distribution of the pixels (or dots) and channel overlapping frequencies which are known to produce artefacts. Therefore one cannot infer that the most accurate colour reproduction would yield the best image quality. It is proven in this work that, on contrary, the most accurate reproduction (spectral) produces worse image quality output then less colour accurate one (colorimetric). It is also shown that previously developed MC DBS is a suitable halftoning solution for both colorimetric and spectral workflow.

3.8 Paper G - Colour and spectral simulation of textile samples onto paper; a feasibility study

Overview: This study has investigated how the growing technology of multichannel printing and area of spectral printing in the graphic arts could help textile industry to communicate accurate colour. In order to reduce the cost, printed samples that serve for colour judgment and decision in the design process are required. With the increased colour gamut of multichannel printing systems we are expecting to include most of the colours from textile samples. The results show that with careful control of ink limits and with bypassing the colour management limitations imposed on printing system; we are able to include more than 90% of colour textile samples into the multichannel printer gamut. Also, we evaluated how much textile spectra we can print with multichannel printers. This gives the basis for the area of the spectral printing and where this study aims on particular application of such systems. We also conclude here that it is possible to print around 75% of all reflectance from textile colours.

Motivation: It was already mentioned that spectral reproduction is not feasible for many real world objects. In this work we conducted a case study with the real problem (metamerism in textile industry) and have offered potential solution. The multichannel printing technology has opened many new possibilities with its extended colour gamut but also has given a tool for spectral reproduction. Therefore it makes sense to evaluate whether multichannel or spectral reproduction would be suitable to improve colour communication in textile industry. Spectral reproduction would in theory tackle the problem of metamerism and if majority of textile spectra are printable, it would reduce cost of design and development of textile products.

Results: By using theoretical approach with PCA and extraction of the first seven basis vectors for the reflectance data set (textile spectra), it is found that around 75% of textile spectra is within the spectral gamut of the printer. Approach used in this paper has used rotated principal components that resemble well real world, all positive spectral reflectance. The convex hull is formed in seven dimensional space within which spectral gamut of the HP z3200 multichannel printer is contained. To verify whether target reflectance of the textile material is within the printer spectral gamut, a vector distance from the hull is calculated with *inhull* Matlab function. The results also suggest that with multichannel printing technology it is possible to print over 90% of textile colours which gives a preference to using metameric workflow for reproducing textile colours with graphic arts technology.

Conclusion: In this work we presented two alternatives for the reproduction of the textile colour onto paper substrates. With multichannel ink-jet systems, it is much more likely that we can accurately reproduce textile colours and spectra. To maximize the capabilities of these devices, the full spectral printing workflow should be established. There the maximum potential of the available inks will be used as well as the control of the individual channels. Also the colourant selection process should be performed in order to address the shortcomings that current multichannel systems have for this application. Reduced dimensionality of the spectral space of a printer leads to possibility of representing multidimensional gamut as convex hull. Approximated spectral gamut can then be

compared with reflectance transformed to the same PCA space where multiple cross sections can lead to the visualization of the spectral gamut. Spectral analysis shows that 75 % of textile colours spectra can be included in printable spectral gamut. As many of these colours (25% at least) have its metamers that maps to the same point in colour space, alternative approach to the reproduction should be used. In colour workflow, it is feasible to use multichannel printers for simulation of textile colours where in pure spectral workflow is still not satisfying.

Chapter 4

Discussion

This section put the findings in the papers in the context. Previously three goals are defined that thesis tries meet: maximal model accuracy, the least resources invested, and maximal image quality of the reproduction system; that is, modelling and halftoning.

4.1 Introduction

In order to calibrate a model for four channels CMYK printing one needs to print 2^4 colour patches. Here, the number 2 marks binary printers where two states can exist, dot or no dot and where the exponent 4 marks the number of primary inks. These patches, in one form or the other will be nodes in a look – up table which in this case is of four dimensions. On the other hand, to calibrate a model for seven channel printing system, one need 2^7 patches to build a LUT. Such constructed LUT forms a basis of conventional Neugebauer model which principal is readily applicable to both four and seven channel printing systems. However, such constructed LUT has mostly unacceptable accuracy of the estimation. Common solution for this problem is to sample more frequently in each dimension. This improves subsequent interpolation and leads to more accurate model. On contrary, increased number of samples requires significant resources to print high number of colour patches. No matter how much the number of samples is increased, there is no perfect model which is highly accurate in any part of the printer space. This has largely to do with optimization of the model with colour difference formula which is applied on non-uniform colour space. These formulas are usually derived with sampling of the colour space and from measurements of the large colour patches. A model based colour transformations are designed then to have maximal accuracy per pixel in terms of colour difference. The quality of printed images is not quantified through colour difference formulas and there is no link between colour accuracy and image quality. This problem is usually diverted to the halftoning process which needs to take care of the image quality problem.

Therefore, the aim of the thesis is improvement and development of spectral printer models and halftoning for multichannel printing which should meet following requirements:

1. Accuracy,
2. Reduction of computational time and calibration resources while maintaining accuracy,
3. Image quality should be as high as possible.

4.2 Accuracy of spectral printer models

Accuracy of printer models depends on many factors. The model is specific for the printer, its ink set, substrate, halftoning and ink limitation. Some of the uncontrolled parameters in model calibration are: repeatability of printer, printing stability, miss-registration

(particularly problematic in colour printing), measurements uncertainty, substrate and printing non-uniformity, fluorescence, temperature, vibrations, etc. It is assumed here, and throughout whole thesis that these parameters are constant and out of the scope. The major modelling paradigm used in thesis is based on Neugebauer linear halftone mixing model and its extensions. One of the concerns about this model is that all input data must be linearized so that model can make an accurate estimate. This step is done through the computation of dot – gain compensation curves. The curves are computed to approximate dots increase that result in ink's contact with the substrate and/or as a mechanical act of the printing machine. The dot gain will also depend whether dots are placed on substrate directly or on the top of another dot, a phenomena called 'dot overlap'. A dot overlap is regulated with halftoning strategies where with some (such is stochastic FM), overlaps occur randomly, while for some (such is AM), overlaps are occurring at predictable pattern. The accuracy of the SN model using different halftoning is evaluated in Paper A. The results show that accuracy of the model will depend on the choice of halftoning method, even if a halftone specific dot gain calibration is provided as the input to the model. This suggests that SN model has more dependencies on halftoning than solely on specific dot gain. Neugebauer model in its original form employs probability model that estimates a likelihood of NP occurrence in the mixture using Demichel equations. These equations are designed for regular and independent halftone screens and their superposition for colour halftoning. Depending on how strong Demichel equations hold for given halftoning method the model accuracy can be reduced or increased. This was the reason why with AM halftoning SN model has better performance than with stochastic FM (Paper A).

In its original version, the SN model performs reasonably well if data are linearized and Demichel probability model stands for all superposition conditions. However this model is empirical model which means that it accounts for physical phenomena only partially. One of these phenomena is an optical dot gain, first researched by Yule and Nielsen (Yule and Nielsen, 1951). Computation of so called YN n-factor, which is an empirical fit, is also shown in Paper A. This is widely used idea that improves accuracy of the SN mode. In some form or the other, this model has been used in each of the included papers. Although this empirical fit was designed to account for optical scattering within paper bulk, there was only very limited case where this stands and in most cases however, n-factor has no physical meaning. One of the reasons for this is that it is rather difficult to separate physical and optical dot gain from the reflectance measurements.

Ink - jet printing technology has two specific characteristics: high dot gain and a constant drop volume. If a dot of assumed constant volume, has larger dot gain, it means that ink layer of the dot must be thinner from one with less dot gain (e.g. full-tone). Subsequently, adding a constant dot ink drops on top of the full-tone area would in theory double ink film thickness of the area. Although, this is not completely true due to the different dot gain when dot is overprinted on another dot (Emmel and Hersch, 2005), it is a reasonable assumption that the optical dot gain also must depend on various ink thicknesses of the dots (Paper C). This is yet another try to assign more physical meanings to the n-factor. However, it turns out, and referred from Paper C, that n – factor is in fact strongly dependent on ink coverage, particularly at high coverages (e.g. over 80% effective

coverage). The optical dot gain dependency on coverage is known; what was not known was why? We hypothesized that optical dot gain (or it is rather better to say n-factor at his point) is a function of ink thickness variation which is a function of dot area coverage. In Paper C, it is shown that YNSN model performs badly after approximately 80% nominal coverage as reflectances of inks, estimated with MD model, becomes less spectrally selective (more flat curves). It is virtually impossible for model to estimate intermediate values even though n-factor is allowed to be large (e.g. to increase spectral selectivity of apparent reflectances). Therefore the YNSN model performs badly in this region, and that is true for its cellular extension These findings from Paper C has led to proposed extension of MD model for single ink, with correction for various ink thicknesses (Paper D). The reflectance of a tone value would depend on the ink thickness, which is a function of dot area coverage. The reflectance of the ink dots is estimated from their thickness through the surface reflection corrected KM model. Therefore, what has led from Paper C and shown in the Paper D, is an idea that it is entirely possible not to model optical dot gain with n-factor and derive with significantly better results. This represents a case where spotting physical phenomena and using physical models lead to simple and accurate solutions. First obvious benefit of such findings is that there is no need to perform optimization routine to find 'right' n-factor (which is never optimal for all inks and coverages in any case). Second, various ink thickness could be modelled with high precision using modified KM model and reflectance which is estimated this way would yield a high precision estimate for each ink and coverage. Such estimated spectral reflectance corresponds to one measured with spectrophotometer and there is no need to separate optical and physical dot gain.

One more advantage of the KM model is to estimate so called Neugebauer Primaries (NPs) as many of these are not printable (Paper B). Findings in Paper B suggest that YNSN model actually performs better when calibrated with some part of estimated primaries and that significant number of NPs should be in fact estimated.

Lastly, Paper A provides a review of a cellular YNSN, which by intermediate sampling significantly increases the prediction accuracy. This model has been implemented in spectral reproduction workflow where an inversion of cYNSN model is done with optimization heuristic on dual – illuminant metric (Paper F).

It should be noted that accuracy of transformations, that is modelling and gamut mapping, whether it is a colorimetric or spectral, would depend on how much samples are within the gamut. Now colorimetric workflow relies on metamerism, and it is rather obvious to say that colorimetric workflow suffers less from gamut problems while spectral is significantly influence by that. The example of this phenomena is given in Paper G, where an analysis of in-gamut colour and spectral of textile material is given and in Paper F which applies spectral separation and gamut mapping and compared it with colorimetric separation and gamut mapping. Therefore, the findings of Paper G suggest that around 90 % of textile colour is within colour gamut of the multichannel printer but only around 70% of spectra are within spectral gamut. In Paper F, the textile samples are measured and reproduced with spectral and colorimetric workflow and it is shown that in this case, the spectral still outperforms colorimetric in terms of colour accuracy. However, if some other sample set, e.g. artist pigments, which have less than 40% printable spectra (Paper E), the results suggest opposite, that spectral workflow is less accurate then colorimetric. The reason for this is spectral gamut mapping and separation must make much more compromises in order to reproduce the input reflectance. The same compromises that

spectral workflow must make to reproduce closest possible reflectance of the input produce image quality problem, discussed in more detail in Chapter 5 of the discussion.

4.3 Reduction of computational time and saving resources

It is expected that models do not use excess of time for computation, that require the least possible number of calibration patches and to reduce measuring time and save resources in ink and paper. If printer models are easier to make and faster to compute, its usability could be greatly improved. Therefore this section is dedicated to optimization of the printer models by having this in mind, and to demonstrate that this can be a good motive and challenge at the same time. Motive is already stated but challenge of achieving these goals is expected to be a trade-off between colour accuracy and image quality on one side and computational time and resource saving on the other.

In Paper B is shown that YNSN model calibration is very costly in terms of resources (ink and paper) and that even the model does not perform any better if 'difficult' patches are printed and measured. In fact, it is shown that by estimating these unprintable NPs, the accuracy is actually improved and resources in terms of ink and paper are saved. It is also shown that simple KM model is sufficient for estimation purpose and it is actually improved by addition of a simple surface scattering model. This model corrects for surface upon which a dot is printed. In comparison with optimization based DORT2002 radiative transfer model, using KM with surface scattering model saves computational time as well. Optimization based computational processes are known to consume time. The YN n-factor is gained with optimization by minimizing prediction difference of the YNSN model. Therefore n-factor is empirical fit that should count for optical dot gain. It is known that n-factor depends on coverage, ink and paper without knowing why. The Paper C provides an answer why this is the case and instantly it becomes apparent that a number of patches used to compute dot gain curves can be reduced. It is assumed here that n-factor, apart from many other phenomena, tries to compensate for different ink thickness which is assumed to be a function of dot area coverage. This explains dependence on coverage and ink of the YN n-factor. By proving this (Paper C) the computation of n-factor can be completely avoided by estimation a coverage dependent ink thickness. Again the KM model is used for this purpose and as in Paper D, it is shown that accuracy is increased with reduce complexity, computational time and resource saving.

Lastly in Paper E a multichannel halftoning method is introduced which replace two channel dot overlap and reduces visibility of texture that way. Although this is primarily image quality concern, the overlap replacement is a post-processing operation that takes just a fraction of time from that of complicated optimization for ideal channel alignment such as majority of iterative colour halftoning algorithms.

4.4 Image quality

The quality of the reproduction is determined by spatial distribution and interaction of pixels in the image or dot covered area (e.g. colour patch). It is the feature that has been solely attributed to the halftoning as this operation spatially organizes dots to reproduce desired tone value at the given pixel or coverage area. Although it is possible to quantify

image quality of colour and spectral transformations (e.g. separation process), these evaluations are usually performed as a simulation and in absence of halftoning.

What is a halftoning method for multichannel printing, how an evaluation of the multichannel printing quality is defined, and what kind of halftoning is used with what type of transformation (e.g. spectral or colour), will be the topic of this section.

Firstly, what is the halftoning strategy or method for multichannel printing? Logical answer to this question would be that multichannel halftoning is a multiple four channel halftoning problem and that it is considered as true in this work as well. The reason is simply that ink and paper have their limitations (e.g. ink absorbance by a substrate) and that the limitation is reached with using up to four channels. Mixing more than four channels leads to artefacts on most substrates and does not provide any more spectral or colour variability (Paper F). On the other hand, multiple four colour combinations increase complexity of the halftoning operation as many different dot overlaps can occur. Dot overlap between different channels is one of the greatest concerns in halftoning and in print quality. In Paper E, we use a multichannel printer CMYKRGB configuration (standard with many different ink-jet manufacturers) to try to tackle problem of dot overlapping by replacement of each C,M and Y overlap with some of the R,G, and B channels. The overlap replacement is performed with binary images which make this process faster.

Spectral reproduction workflow aims to reproduce input reflectance with specific ink combination. Because of phenomena of metamerism, for each input reflectance (e.g. per pixel), there is a set of reflectances that would produce the same colour. Even greater set of reflectances can be mapped within 1 ΔE range, which leads to concept of 'paramer'. As this process is pixel based, and therefore disregards the neighbourhood area, noise is most likely to be induced spatially. In Paper E, this idea is extended to a reproduction workflow, and it is sought to evaluate image quality of the reproduction system by applying different halftoning after spectral or colorimetric separation. It is shown that if neighbourhood based halftoning (e.g. Error Diffusion) is applied on noisy spectral separation images, the artefacts such as banding are produced. No such artefacts are noted with DBS halftoning. Even more, if the MC DBS post-processing (Paper F) is used with either colorimetric or spectral reproduction workflow, the image quality is improved.

Chapter 5

Conclusions, Contributions and Perspectives

This section will conclude the discussion by providing a summary of the contribution of the included papers. Furthermore, it will provide an overall conclusion of the thesis and give a perspective for the future work.

5.1 Summary of the contributions

This section is an overview of the contributions of each individual included paper. The main goal of the thesis has been discussed in previous section while this section will look closely to the contribution of each included paper.

- **Paper A**: The contribution of this work was to provide a comprehensive review of spectral printer models for multichannel printing. In addition, an analysis of SN printer model accuracy as a function of halftoning was performed, addressing dependencies and limitations of the Demichel probability model as the input to the Neugebauer equations. The analysis in the papers confirms previous findings of Rogers (Rogers, 1997) for two colour printing and of Amidror and Hersch (Amidror and Hersch, 2000) and for four colour printing.

- **Paper B**: In this work we contributed to research on the SN modelling by introducing the DORT2002 model to estimation of the Neugebauer primaries. The model has been modified to work for ink mixture by fixing the scattering parameter to zero which leads to the single constant estimation process. Also a surface reflection model is introduced which simplifies and increases the accuracy of the estimation of an ink mixture. Finally, the findings of Abebe et al. (2011) that YNSN model works better when used with mix of the estimated and measured NPs is also confirmed here. This fact is even more emphasized is in multichannel printing environment where many of the NPs are not printable without significant artefacts.

- **Paper C:** This paper conducted an analysis of the YN dependencies on the dot area coverage as a function of ink thickness. The conclusion is that YN n-factor strongly depends on what is assumed to be ink thickness variation as ink spreading on the paper. Such conclusion opens up a new perspective in optical dot gain modelling; a phenomenon that has been subject of many research efforts(e.g. Yule, 1951, Ruckdeschel and Houser, 1978, Pearson, 1980, Wyble, 1999, Taplin 2001, Gerhardt, 2005) The findings provide a partial explanation why the YN n-factor varies for different inks and different dot area coverages. The spectral reflectance depends on the ink concertation (as a function of pigment concentration) in the dot coverage area, and that n-factor cannot count accurately for these differences. Therefore the

findings in this work has led to the new approach in modelling the both optical and mechanical dot gain in printing and this has been more explored in Paper D.

- **Paper D:** With findings from previous paper an extension of the single channel MD (Murray-Davis, 1931) model is proposed. Proposed model therefore estimates single ink, coverage dependent spectral reflectance by neglecting YN optical dot gain but accounting for it with ink thickness reflectance correction. Previously it was found (Paper C) that YN n-factor is a strong function of the ink thickness variation. The model counts for physical characteristics of an ink through the absorption coefficient and ink-thickness modified spectral reflectance. From the coefficients the spectral reflectance is estimated with modified CY (Clapper and Yule, 1953) model. This extension differs from earlier extensions such as the one from Arney et al., (1995) in which both R_i and R_s varying with coverage due to optical dot gain. This brings a coverage dependent ink spectral reflectance correction which is otherwise approximated with YN n-factor. It is shown that with proposed model, an accuracy of computation of the dot gain calibration curves and optical dot gain is improved three fold on average against classical YN model. The explanation for these improvements lays in the fact that YN model assumes equal ink thickness of the dots for all coverages which is almost never the case and which is shown to vary with coverage in ink - jet printing. This is a perspective and exciting new findings which give a new look to very old problem that has been driving much research (Section 2.5.2) in the last half century.

- **Paper E:** The work addressed a problem of the multichannel halftoning and has proposed a new method which is based on the DBS halftoning. The method improves image quality by reducing a texture visibility utilizing RGB channels for replacement of the CMY dot overlaps. With replacement, the need for computationally expensive iteration based dot-of-dot algorithms is reduced, while optimal distribution of each channel is maintained. Also this method is one of the first solutions (adaptations) for multichannel halftoning.

- **Paper F**: The work conducted a comprehensive comparison between colorimetric and spectral workflow in terms of colour accuracy and image quality. These two rather similar workflows show different performance when evaluated for these two reproduction goals. Both workflows are combined with different halftoning so that both separation and halftoning are evaluated for image quality. Also, previously developed MC DBS is applied in spectral reproduction workflow with expectation of improved image quality. By using MC DBS post-processing halftoning method image quality of both colorimetric and spectral reproduction workflow improves.

- **Paper G:** This study has investigated how the growing technology of multichannel printing and area of spectral printing in the graphic arts could be applied in simulation of the textile colour and spectra. By gamut evaluation, both spectral and colorimetric, it is concluded that around 90% of textile colours and around 75% of textile spectra is printable with multichannel printer.

5.2 Conclusion

Thesis has included seven papers, one review based paper (Paper A) with limited evaluation but with the one that has dictated the research direction of the thesis. Two major contribution areas are printer modelling and halftoning, both of which are specific to high-quality multichannel ink-jet printing that are commercially available. Previous research that utilized multichannel printer modelling and/or halftoning are the work by Tzeng (PhD thesis, 1998), on six-colour separation minimizing metamerism, Taplin (MSc thesis, 2001) also worked with CMYKOG configuration with custom ink-set, Gerhardt (PhD thesis, 2007) used custom-ink CMYKRGB printer for its Spectral Vector Error Diffusion, an adaptation of the VED halftoning that works with spectral reflectance input. Although there were many other research in similar areas such as spectral reproduction workflows (Hardeberg, 1999, and recently Urban and Berns, 2011, Morovic et al.,2012), multichannel and spectral printing are starting to get more attention after being last two decades present only in science (Derhak et al., 2015). The ICC has introduced a new framework which will for the first time support spectral data on the input and multi-illuminant common space. However, there is still way to go before multichannel devices could start to communicate in real time.

One of the most challenging part in enabling a spectral reproduction and in particular with multichannel printers, is the trade-off between printer model accuracy and computational time needed to execute an accurate model. The expectation is that this problem could only be abridged by utilization of the physical models or to by specifically modelling light-ink-paper variation. Prevailing modelling ideas today are based on empirical sampling and fast computing (e.g Chen et al., 2004, Li and Luo, 2008, Qiang et al., 2014). On the more physical side of the printing, a single cell Neugebauer, YNSN or CY model has been revising (Hébert and Hersch, 2005, Hersch and Crété, 2005,Rossier et al., 2010). Work by Hersch and Crete (2005) has inspired many more ideas to develop by simple observation that ink spreading (or a dot gain) is a function of superposition conditions. This implies that ink spreading when ink is printed on top of the other ink is very different to the one ink spreading when printed solely on the paper. Assuming proper calibration, this idea works with more or less success across the printing technologies. Unfortunately for the accuracy of this model all superposition conditions must be sampled, printed and measured which limits its use in multichannel printing.To model another physical phenomena and limitation (Paper B), a physical problem of printing the Neugebauer test target for multichannel printing was addressed. Others that addressed this problem call these non-printable or hardly printable (without artefacts) NPs (Tzeng, 1998, Bala, 1999, Chen et al., 2004, Urban, 2009). As highly accurate empirical model require rather large set of training patches to be printed and measured, many started to search for the estimation models or the techniques. Off course, the real need for these training set estimators came with the multichannel printers as no substrate can absorb that much ink. Estimators are usually mathematical techniques such as some form of regression (Bala, 1999, Chen et al., 2004 Urban, 2009). Tzeng (1998) and Taplin (2001) to some extent have used another physical model for colourant mixing such as KM model. This was an important step away from usage of conventional halftone models for halftone prints and that continuous tone model such as KM could be used in combination with a halftone model to help in saving time and resources. Also as a result of using KM model and translation of a reflectance into linear mixing K/S space, the Neugebauer model based on the estimated rather than measured

NPs has performed better. These results are later confirmed by Abebe et al., 2011 who used same approach in estimating NPs for four channel printer. We extended this analysis in following directions: first we showed that it is not only substrate which has a physical limits, it is ink as well (Slavuj et al., 2014). Inks have their saturation point where due to the very high density of the pigments in the area, many patches are some tone of black. It is also shown that simple surface reflection model can count for printing on top of the high absorption NP, whether it is black ink or some other combination. With simple modification in calculation of the NPs, the surface reflection model has doubled the accuracy of the prediction, and much more significant model then also tested DORT2002.

In order to calibrate a model for multichannel printing system (e.g. the Neugebauer model), one could expect an exponential growth in complexity, in computation time and in amount of resources. The Neugebauer linear equations are a simple and elegant solution for modelling a halftone printer. Spectral Neugebauer model does not require great amount of resources for calibration and it is fast to compute. However, in its original form, the SN model is not sufficiently accurate to characterize light-ink-paper interaction and the printer. The Neugebauer idea, although very sound, does not count for many light-ink-substrate interaction phenomena and therefore its accuracy is compromised. One of the solutions for this problem could be found by applying the YN correction to the model. The correction of reflectance curve with YN n-factor increases accuracy of the model by accounting for some of the non-linearities of the light-ink-paper interaction. Improvement in accuracy however is limited because n-factor is an empirical fit (an exponent) which overlooks many underlying physical phenomena. With an assumption that n-factor is a function of both ink type and dot area coverage, a significant improvement to the model accuracy can be made by reducing maximal ink amount used for the channel calibration. What is uncontrollable in the printing process is the dot gain and with the dot gain there is an ink thickness variation of the dots (Paper C). This is important consideration as the SN model assumes equal ink thickness which is almost never the case. Different ink pigmentation and specific ink spreading on the substrate can result in significantly different ink film thickness. Therefore, the optical dot gain that is aimed to model with n-factor is a strong function of the ink thickness (Paper C). The logical solution for the ink thickness variation problem is to use a continuous tone reflectance prediction model such is the Kubelka–Munk (KM) physical model. This model accounts for different ink concentrations and their coverage dependent thicknesses. The proposed model in Paper D is a simple extension of the Murray-Davis (MD) model where the reflectance of the ink dots is estimated with the modified KM model. In general, physical models are less computationally expensive than empirical models and they require less resources (e.g. for the model in Paper D only three calibration patches needed). Channel calibration done with the proposed model (Paper D) yields significantly more accurate SN model then the empirically computed n-factor. In this case, computation of dot gain curves includes both mechanical and optical dot gain.

Multichannel halftoning could be observed as multiple four channel halftoning problem. This is both challenge and opportunity. For example a seven channel printing system has up to 35 four channel combinations. On the other hand, a typical multichannel printer is equipped with CMYKRGB inks where RGB inks are added to enlarge printer gamut. These inks could be observed as lighter versions of CM, CY and MY overprints which greatly simplify the idea of multichannel halftoning. With MC DBS (Paper E), overlaps are simply replaced with some of the RGB inks, reducing significantly computational time and maintaining optimal dot distribution of each channel determined by monochrome DBS. It is

shown that MC DBS is a step forward from channel independent halftoning and that higher image quality can be achieved. When applied after spectral and colorimetric separation, the MC DBS improves overall image quality using the same principle (Paper F). Rather noisy spectral separation with applied MC DBS shows the same image quality like colorimetric separation. It is also shown that when the image quality of a reproduction is evaluated, both separation process and halftoning play their role but is also shown that with the good combination of the separation method and halftoning the maximal image quality can be achieved.

5.3 Perspectives

Potential area of the research for any new model is to explore different printing technologies. The modelling and halftoning work done in the thesis are specific to the multichannel ink-jet technology. This technology has certain specifics, such as close to equal drop volume, very high dot gain, specific chemistry of the inks, dedicated ink for different substrates (e.g. photo black ink for photo paper), and after all, the rather large colour gamut and high resolution. Therefore, it would be beneficial to evaluate whether this findings stands for offset printing or for electrophotographic printing. Potentially, achieving this goal requires an accurate model which consumes optimal resources, and is fast to compute (e.g. to be used in production with offset). One possible direction toward achieving a balance between accuracy and usability is to analyse which inks and what combinations increasing spectral variability of the set. Potentially, ink thickness model is possible to extend to multi-colour printing where it could be used to estimate training data sets so the least measurements should be made for model calibration. Other strategy, as is suggested in Paper C is to optimize cell number and location so the cYNSN model could be effetely but accurately used.

Possibly, multichannel modelling idea could be expanded in with newly developed model, in the similar manner as Tzeng (1999) first converted input reflectance into K/S space where mixing is very close to linear. Later this idea was exploited by many researchers (e.g. Alsam and Hardeberg, 2004) and later by Morovic et al., (2012) who applied YN correction to convert the spectra in 1/n space from which basis vectors could be extracted. The spectral redundancy is rather easily discovered in this manner which could lead to significant simplification of the modelling process.

On the other hand, the same spectral redundancy could be used in ink saving and improvement of image quality (suggested in Paper E). Namely, if expand an ink space (e.g. CMYKRGB) into equivalent NP space (similar to Morovic et al., 2010), the variety of reproduction goals could be chosen (e.g. colour accuracy, texture of image quality, ink saving, etc.). If MC DBS idea is expanded as it was suggested as the potential extension of the process, the decision on the reproduction goal could be decided on a binary level, after separation and halftoning.

The second potential for future research is a further improvement of the accuracy of the spectral printer models. If Neugebauer model is used, the Demichel probability model dependencies on the different halftoning (which was proven in Paper A) must be bypassed. This dependency creates potential compromise between colour accuracy and image quality because its limits the choice of the used halftoning. There, the high image quality dot-of-dot

halftoning cannot be used, as Demichel model assumes channel independency, which is not achieved with this type of halftoning. The alternative methods of computing the probable occurrences of the certain dots are suggested in the literature and are mostly based on pixel counting technique on a camera captured image.

Bibliography

.

Abebe, M., Gerhardt, J., and Hardeberg, J. Y., Kubelka-Munk theory for efficient spectral printer modelling. In Proc. SPIE, vol. 7866, Colour Imaging XVI: Displaying, Processing, Hardcopy, and Applications, 2011.

Agar, A. U., and Allebach, J. P., An iterative cellular YNSN method for colour printer characterization, In Proc. of the Sixth IS&T/SID Colour Imaging Conference, pp. 197-200, 1998.

Agar, A. U., and Allebach, J. P., Model-Based Colour Halftoning Using Direct Binary Search, In IEEE Transactions on Image Processing, Vol.14, No.12, pp. 1945-1959, 2005.

Alsam A., and Hardeberg Y., Optimal colourant design for spectral colour reproduction, Colour Imaging: Processing, Hardcopy, and Applications X, SPIE Proceedings 5667, pp. 38-46, 2005.

Amidror, I., and Hersch, R. D. , Neugebauer and demichel: Dependence and independence in n-screen superpositions for colour printing, In Colour Res. Appl. 25, pp. 267-277, 2000.

Analoui, M. and Allebach, J. P., Model-based halftoning using direct binary search, In Proc. SPIE/IS&T, Vol. 1666, 1992.

Arney, J. S., Arney, C. D., Katsube, M., Engeldrum, P. G., The impact of paper optical properties on hard copy image quality, In Proc. IS&T Non-impact Printing 12: Int. Conf. Digital Print Tech, pp. 166-168, 1996.

Bala, R., Device Characterization, In Digital Colour Imaging Handbook, G Sharma (Ed.), CRC Press, 2003.

Balasubramanian, R., Optimization of the spectral Neugebauer model for printer characterization, In J. Electron. Imaging 8 (2), 156-166, 1999.

Bastani, B., Cressman, B. and Shaw, M. , "Sparse Cellular Neugebauer Model for N-ink Printers", in Proc. IS&T/SID Fourth Colour Imaging Conference: Colour Science, Systems and Applications, 58-60., 1996.

Chen, Y., Berns, R. S. and Taplin, L. A., Six colour printer characterization using an optimized cellular Yule-Nielsen spectral Neugebauer model, In Journal of Imaging Science and Technology, vol. 48, No. 6, Nov. 2004.

BIBLIOGRAPHY

CIE, Commission internationale de l'Eclairage proceedings, Cambridge University Press, 1931.

CIE, Commission internationale de l'Eclairage proceedings, 15:2004 Colorimetry 3rd edition.

Clapper, F. R., and Yule, J. A. C., The Effect of Multiple Internal Reflections on the Densities of Half-tone Prints on Paper, In J. Opt. Soc. Am., vol. 43, no. 7, pp. 600-603, 1953.

Demichel, E., Le procédé, 26:17-21, 26-27, 1924.

Derhak, M., and Rosen, M., Spectral Colorimetry using LabPQR – An Interim Connection Space, J. Imaging Sci. Technol, **50**, pp. 53 – 63, 2006.

Derhak, M. W., Green, P., and Lianza, T. Introducing iccMAX: new frontiers in color management, Color Imaging XX: Displaying, Processing, Hardcopy, and Applications, Proceedings of SPIE/IS&T Electronic Imaging, SPIE, Volume 9395, pp. 9395-20, San Francisco, CA, USA., 2015.

Edström, P., Comparison of the DORT2002 radiative transfer solution method and the Kubelka-Munk model, In Nordic Pulp and Paper Research Journal, Vol 19, no. 3, 2004.

Emmel, P. and Hersch, R. D., Modelling ink spreading for colour prediction, In J. Imaging Sci. Technol. 46(2), 2002.

Floyd, R. and Steinberg, L., An Adaptive Algorithm for Spatial Gray Scale'', in SID Symposium, pp. 36-37, 1975.

Gerhardt, J., Spectral Color Reproduction: Model based and vector error diffusion approaches, PhD Thesis, ENST - GUC, 2007.

Gerhardt, J., and Hardeberg, J. Y., Spectral colour reproduction by vector error diffusion, In Proceedings CGIV, pp. 469-473, 2006.

Green, P.J., Colour Management: Understanding and Using ICC Profiles, Wiley, Feb. 2010.

Green, P. J., and MacDonald, L., Colour Engineering: Achieving Device Independent Colour, Wiley, 2001.

Gooran, S., Dependent Colour Halftoning, Better Quality with Less Ink, In Journal of Imaging Science & Technology, Volume 48, Number 4, pp. 354-362, 2004.

Guild, J., The colorimetric properties of the spectrum, In Philosophical Transactions of the Royal Society of London, Series A, pp. 149-187, 1932.

BIBLIOGRAPHY

Haneishi, H., Suzuki, T. , Shimoyama, N., and Miyake, Y., Color digital halftoning taking colorimetric color reproduction into account, J. Electron. Imaging, vol. 5, no. 1, pp. 97-106, Jan. 1996.

He, Z., Hierarchical Colourant-Based Direct Binary Search Halftoning, IEEE Transactions on Image Processing, Vol. 19, No. 7, July 2010, pp. 1824-1836, 2010.

Hébert M., "Yule-Nielsen effect in halftone prints: graphical analysis method and improvement of the Yule-Nielsen transform", Proc. SPIE 9015, 90150R-1-13, 2014.

Hébert, M., and Hersch, R. D., Review of spectral reflectance models for halftone prints: Principles, Calibration, and prediction accuracy, Colour Res. Appl., vol. 40, no. 4, pp. 383–397, Jun. 2014.

Harrington, S., Color Images Having Multiple Separations With Minimally Overlapping Halftone Dots, U.S. Patent 5493323, 1996.

Hersch, R. D. and Crété F., "Improving the Yule-Nielsen modified Neugebauer model by dot surface coverages depending on the ink superposition conditions," in SPIE 5667, Colour Imaging X: Processing, Hardcopy, and Applications, 4342005, 434-447., 2005.

Herzog, P. G., Knipp, D., Stiebig, H. and Konig, F., Colorimetric characterization of novel multiple-channel sensors for imaging and metrology, J. Electron. Imaging **8**, pp. 342–353 (1999).

Heuberger, K. J. Z., Jing, M. and Persiev, S., Colour Transformations and lookup tables. TAGA/ISCC Proc: 1992, pp. 863-881, 1992.

Hunt, R. W. G., The Reproduction of Colour, 6th Edition, Wiley, 2004.

ICC.1:2004-10. Image technology colour management - architecture, profile format, and data Structure, The International Color Consortium, 2004.

International Colour Consortium, Colour Management, [Online], Available at: www.color.org/icc_white_paper5glossary.pdf, last accessed: 04.10. 2015.

Imai, F. H., Rosen, M. R., and Berns, R. S., Comparative study of metrics for spectral match quality, in Proceedings of European Conference on Colour in Graphics, Imaging and Vision, pp. 492-496, 2002.

ISO 13655:2009 Graphic technology -- Spectral measurement and colorimetric computation for graphic arts images, International organization for standardization, Geneva.

Kawaguchi, T., Tsumura, N., Haneishi, H., Kouzaki, M. and Miyaki, Y., Vector error diffusion method for spectral color reproduction. In IST&T's PICS Conference, pages 394–397, 1999.

BIBLIOGRAPHY

Kubelka, P., and Munk, F., Ein Beitrag zur Optik der Farbanstriche, In Z. Tech. Phys., vol. 11a, pp. 593-601, 1931.

Lee, J. H., and Allebach, J. P., CMYK Halftoning Algorithm Based on Direct Binary Search, In Proceedings IS&T/SID Ninth Colour Imaging Conference, Colour Science and Engineering: Systems, Technologies, Applications, Scottsdale, Arizona, USA, 2001.

Le Moan, S., and Urban,P., A New Connection Space for Low-Dimensional Spectral Color Management, in Measuring, Modeling, and Reproducing Material Appearance, San Francisco, CA, USA, February 2014, vol. 9018, p. 12, IS&T/SPIE.

Lieberman, D. J., and Allebach, J. P., A dual interpretation for direct binary search and its implications for tone reproduction and texture quality, In IEEE Trans. Image Process., vol. 9, no. 11, pp. 1950-1963, Nov. 2000.

Li, C., and Luo, M. R., Further accelerating the inversion of the yule-nielsen modified neugebauer model, in 16th Color Imaging Conference: Color Science and Engineering Systems, Technologies, and Applications, Final Program and Proceedings - IS&T/SID Color Imaging Conference, pp. 84-88, 2008.

Lin, Q., and Allebach, J. P., Color FM screen design using DBS algorithm, Proc. SPIE, Color Imaging: Device-Independent Color, Color Hardcopy, and Graphic Arts III, vol. 3300, pp. 353–361, 1998.

Morovič, J., Morovič, P., and Arnabat, J., HANS: Controlling Ink-Jet Print Attributes Via Neugebauer Primary Area Coverages, In IEEE Transactions on Image Processing, Vol. 21, No. 2, 2012.

Morovic, P., Morovic, J., Arnabat, J., Revisiting Spectral Printing: A Data Driven Approach, 20th Color and Imaging Conference Final Program and Proceedings, IS&T, pp. 335–340, 2012

Murray, A., Monochrome reproduction in photoengraving, J. Franklin Inst., vol. 221, no. 1936, pp. 721-744, 1936.

Namedanian, M., and Gooran, S., High Resolution Analysis of Optical and Physical Dot Gain, Proc. TAGA, San Diego, California, 2010.

Namedanian, M., Gooran, S., and Nyström, D., Investigating the Wavelength Dependency of Dot Gain, In Colour Print, SPIE, Electronic Imaging, San Francisco, California, 2011.

Neugebauer, H. E. J., Die theoretischen Grundlagen des Mehrfarbenbuchdrucks, In SPIE Neugebauer Memorial Seminar on Colour Reproduction, Editor: Sayanagi, K., pp. xv, 203, Tokyo, Japan, 1989.

BIBLIOGRAPHY

Oztan, B., Sharma, G., and Loce, R. P., Quantitative Evaluation of Misregistration Induced Colour Shifts in Colour Halftones, In Proc. of SPIE/IS&T Electronic Imaging Colour Imaging X: Processing, Hardcopy, and Applications, edited by Reiner Eschbach, Gabriel G. Marcu, SPIE, Vol. 5667, 2005.

Palmer, S.E., Vision Science: Photons to Phenomenology, The MIT press, 1999.

Pappas, T., N., Model-Based Halftoning of Colour Images, IEEE TRANSACTIONS ON IMAGE PROCESSING, VOL. 6, NO. 7, pp. 1014-1024, 1997.

Pearson M., n value for general conditions, Proc. TAGA 1980; 32:415-425, 1980.

Rogers, G. L., Neugebauer revisited: random dots in halftone screening, In Colour Research and Application, Vol. 23, pp. 104-113, 1997.

Rolleston, R., and Balasubramanian, R., Accuracy of various types of Neugebauer models. In Proc IS&T SID Col. Imag. Conf., pp. 32-37, 1993.

Rossier, R. and Hersch, R. D., "Ink-dependent n-factors for the Yule-Nielsen modified spectral Neugebauer model", Proc. IS&T 5th conference on colour in Graphics, Imaging and vision, 202-210, 2010.

Ruckdeschel, F. R. and Hauser, O. G., Yule–Nielsen effect on printing: a physical analysis, In Appl. Opt. 17:3376-3383, 1978.

Schanda, J., Colorimetry: Understanding the CIE system, Wiley, 2007.

Shaked, D., Arad, N., Fitzhugh, A., and Sobel, I., Ink Relocation for Color Halftones, Hewlett-Packard Laboratories Technical Report, August 1996. Proceedings version in Proc. of IS&T's Image Processing Image Quality and Image Capture Conf., May 1998.

Shiraiwa, Y., Mizuna, T., Equation to predict colors of halftone prints considering the optical properties of paper, J. Imag. Sci. Tech., 37:385-391, 1993.

Shu, C.H., Li, H. Ancin, and Bhattarcharjya, A., Color stochastic screening with smoothness enhancement, in Proc. IS&T's NIP 13 Int. Conf. Digital Printing Technologies, pp. 522–525, 1997.

Slavuj, R., Coppel, L. G., Olen, M. and Hardeberg, J. Y., Estimating Neugebauer primaries for multi-channel spectral printing modelling, Proc. SPIE 9018. 90180C-1-8, 2014.

Slavuj, R., Nussbaum, P., and Hardeberg, J. Y., Review and analysis of spectral characterization models and halftoning for multi-channel printing, In Proc. IARIGAI, 'Advances in Printing and Media Technology', Vol. XL, pp. 265-275, Chemnitz, Germany, 2013.

BIBLIOGRAPHY

Specification ICC.1:2010-12 (Profile version 4.3.0.0), [Online], Available at: http://colour.org/specification/ICC1v43_2010-12.pdf, last accessed: 04.10.2015.

Taplin, L. A., Spectral Modelling of a Six-Colour Inkjet Printer, Msc Thesis , RIT, 2001.

Tzeng, D., and Berns, R. S., Spectral-Based Ink Selection for Multiple-Ink Printing I. Colourant Estimation of Original Objects, The Sixth Colour Imaging Conference: Colour Science, Systems and Applications, pp. 106-111, 1998.

Tzeng, D., Spectral-based color separation algorithm development for multi-ink color reproduction, Ph.D. thesis (Rochester Institute of Technology, 1999).

Yule, J. A. C., The penetration of light into paper and its effect on halftone reproductions. In TAGA, Proc. 3, pp. 65-76, 1951.

Urban, P., Berns, R. S., Paramer Mismatch-based Spectral Gamut Mapping, In IEEE Transactions on Image Processing, Vol.20, Issue 6, pp. 1599-1610, 2011.

Urban, P., and Rosen, M., Spectral-based Image Reproduction Workflow, From Capture to Print, Presentation, Rochester Institute of Technology, USA, 2008.

Urban, P., Ink limitation for Spectral or Constant Colour Printing, 11th AIC congress, Sydney, Australia, 2009.

Urban, P., Spectral Image Reproduction Workflow: From Pixel to Print, ROND, Spectral Printing – Opportunities, Challenges and Outlook, MIUN, Sweden, 2013.

Viggiano, J.A.S., The GRL dot gain model, TAGA Proceedings 35, 423-439, 1983.

Zitinski, P. J., Nystrom, D., Gooran, S., Multi-channel printing by Orthogonal and Non-Orthogonal Halftoning', In Proceedings of 12th International AIC Congress, pp. 597-604, Newcastle, UK, 2012.

Zuffi, S., Schettini, R. and Mauri, G., Spectral-based printer modelling and characterization, In Journal of Electronic Imaging 14(2), 2005.

Wang, M., and Parker, K. J., Properties of jointly-blue noise masks and applications to color halftoning, J. Imaging Sci. Technol., vol. 44, no. 4, pp. 360–370, Jul./Aug. 2000.

Wright, W. D., A re-determination of the trichromatic coefficients of the spectral colours. In Transactions of the Optical Society 30 (4), pp. 141-164, 1928.

Wyble, D. R., and Berns, R. S., A Critical Review of Spectral Models Applied to Binary Colour Printing, 1999.

Wyszecki, G., Evaluation of metameric colors, Journal of the Optical Society of America 48, pp. 451-454, 1958.

BIBLIOGRAPHY

Wyszecki, G., and Stiles, W. S., Color Science: Concepts and Methods, Quantitative Data and Formulae, 2nd Edition, Wiley, 2000.

Part II

Included Papers

Chapter 6

Paper A

Review and analysis of spectral characterization models and halftoning for multichannel printing

Radovan Slavuj, Peter Nussbaum, Jon Yngve Hardeberg

Published in

Proceedings of

IARIGAI

(Advances in Printing and Media Technology)

Vol. XL,

Pages 265-275

Chemnitz, Germany, 2013

Chapter 6

Review and analysis of spectral characterization models and halftoning for multichannel printing

Radovan Slavuj *, Peter Nussbaum*, Jon Yngve Hardeberg*
* The Norwegian Colour and Visual Computing Laboratory
Gjøvik University College, P.O. Box 191, N-2802, Gjøvik, Norway
radovan.slavuj@hig.no, peter.nussbaum@hig.no, jon.hardeberg@hig.no

1. Introduction

There has been a long tendency to accurately communicate colour from outside world to a print. Every object has the ability to selectively absorb and reflect certain wavelengths of the incoming light. As the Human Visual System (HVS) is performing its function through three-chromatic nature of its sensors, we build our system and devices that perform its colour information acquisition and reproduction based on this fact. Most of the imaging devices we use today are still three to four colour (channel) processes. Reducing the dimensionality of the incoming light to three, we have established trichromatic colour management paradigm. The problem has always been that this reduced trichromatic information could be resolved of many of the spectral metamers, and this could occur not only when we change the illumination but also when we change the observer. Spectral information is therefore, the true and full information about an object's ability to selectively attune the light. Spectral printer models, takes this physical information of its primaries and with linear addition, they derive the spectral output. The models rely heavily to assumptions made to the physical behaviour of the ink, paper and light which is less than obvious and easy to model. With this difficulty to model the physical behaviour come the advantages of using spectral system: reduced metamerism, higher accuracy, convenience in incorporation of the other physical phenomena (gloss, textured surface), possibility to convey true appearance of the scene, etc. Although spectral imaging has been used in many industries for many decades (e.g. medicine, security), the attention in graphic arts is received around two decades ago. However, even till today, there has not been a real application of the spectral reproduction system. The reason is that with advantages come the shortcomings: complexity and computational intensity. The current ICC architecture is still not able to incorporate such system due to its shortcomings (ICC White Paper, 2010). Therefore, spectral reproduction or spectral printing is jet to see the light on the greater scale. It is however, one of the most researched areas in printing industry for the last two decades, as the computational power increases and the number of the researches are working around it (Taplin, 2001, Urban and Rosen, 2008, Tzeng and Berns, 1998, Gerhardt and Hardeberg, 2006). Introduction of the multichannel printing has occurred within the conventional printing where the standard CMYK printing processes were enriched by two more channels where the gamut of the conventional printing was simply not enough to satisfy the demanding needs. These ink configurations are almost a standard in today ink jet printing, as it is the technology that provides a high flexibility needed to incorporate such

system. Spectral printing has the interest in using these multichannel processes in the sense of better sampling of the input spectra and producing the spectrally matched output. The logic behind this is that more colours will mean more degrees of freedom in reproduction of the right colour. Classical example of this is that there is only one CMYK four colour combination, but multiple one exists if we have a seven channel system. Same holds for three and two colour combination. Printer models convert the input to the output by modelling the behaviour of the printing system and its colorants. Physical or spectral models are relying on the physical information of the primary colours and make their approximation based on the assumption linear mixing of the colorants on the substrate.

The aim of this work is to provide a comprehensive review of the spectral characterization models used for multichannel printing and to evaluate how two major types of halftoning influence parameters of the models (specifically dot gain). Moreover, we have evaluated if the modelling process is halftone independent. The main contribution is going toward discovering controllable and the most suitable halftoning algorithm for multichannel printing.

2. Spectral printer models

First spectral – colour printer model was introduced for single colour print on substrate (Murray, 1936):

$$R_\lambda = a_i R_{\lambda,\mathrm{i}} + (1 - a_i) R_{\lambda,\mathrm{i}} \qquad (1)$$

This is Murray-Davies (MD) model for single colour on the paper. It assumes that the reflectance R_λ of the certain area is the product of the relative coverage of ink a_i, paper $(1 - a_i)$ and reflectance of the ink$R_{\lambda,\mathrm{i}}$at full coverage. There are two types of dot coverage: theoretical and effective dot coverage. The former is the digital information sent to the printer and latter is the real dot on the paper. During printing process, ink penetrates to the substrate and phenomenon of dot gain occurs. It is called physical or mechanical dot gain as it is caused by printing system (contact or non-contact) and is resulting in physical spreading of the ink as it deviates from the desired shape. In order to calculate effective dot area one must invert the MD model:

$$a_{eff} = \frac{R_{min,meas} - R_{min,p}}{R_{min,i} - R_{min,p}} \qquad (2)$$

where subscript $\boldsymbol{p}$ is the reflectance of the substrate (paper), $\boldsymbol{i}$ is the reflectance of the primary ink and $\boldsymbol{R_{min}}$ is here to denote that the calculation is not performed with whole reflectance curve. Rather, it takes minimum value of the reflectance as it is the one that will be most affected with the dot gain. The estimated factor $\boldsymbol{a_{eff}}$ is the scaling factor for the input reflectance that translates the reflectance of primary ink after dot gain. If we are interested in how our dot gain is influenced by the change in spectra, we can rewrite the equation to a matrix calculation using least squared minimization:

$$a_{eff} = R_{m,p}\, R_{i,p}^T \left(R_{i,p}\ R_{i,p}^T\right)^{-1} \qquad (3)$$

Here, $R_{m,p} = R_{meas} - R_p$, $R_{i,p} = R_i - R_p$, where R_{meas}, R_p *and* $R_i$and are row vectors with spectral data. Other type of dot gain that MD model doesn't account for is optical dot gain. This phenomenon occurs due to the light scattering within the substrate. This implies that substrate near the dot does not have same reflectance value as pure substrate. It is actually a combination of the light that has passed to the ink filter, scattered inside the substrate and left out from unprinted area. Although this phenomenon is not necessarily unfavourable (it increases the colour gamut), it adds complexity into modelling.

2.1 Neugebauer model (NG)

Neugebauer extended MD model for multi-colour output by linear summation of the product of tone area coverage of each colourant and its reflectance (Neugebauer, 1989):

$R_{\lambda=} \sum_i a_i \, R_{\lambda,\mathrm{i,max}}$ (4)

The model performs interpolation using so called Neugebauer primaries (NP) as a nodes in n dimensional space. For three colour case there are 8 NP's: substrate, cyan, magenta, yellow, red, green, blue and black (assumed when all three primaries are mixed together). Beside linearity that MD assumes, there is an assumption of randomness and independence of dot distribution where fractional dot coverage is represented by Demichelis equations (Demichelis, 1924):

$a_w = (1 - a_c)(1 - a_m)(1 - a_y)$ (5)
$a_c = a_c(1 - a_m)(1 - a_y)$
$a_m = (1 - a_c)a_m(1 - a_y)$
$a_m = (1 - a_c)(1 - a_m)a_y$
$a_r = (1 - a_c)a_m a_y$
$a_g = (1 - a_m)a_c a_y$
$a_b = (1 - a_y)a_c a_m$
$a_k = a_c a_m a_y$

This theoretical fractional coverage could be replaced with effective dot coverage calculated with inversed MD model. The condition of randomness that NG model assumes can be satisfied by using rotated screens or stochastic patterns, where for dot-on-dot printers has to be modified (Bala, 2003).

The NP's are only measurements that are required as an input for this model, where physical dot gain can be estimated for each printing primary and can serve as the input for Demichelis equations for better accuracy. However, the classical NG model does not account for optical dot gain and as that cannot provide a good estimate of printer output.

2.2 Yule-Nielsen n factor

The analysis of the measured and estimated reflectance showed that optical dot gain adds to the non-linearity of the ink-paper interaction (Yule, 1951). Yule-Nielsen n factor is empirically determined number to which the base reflectance is raised to give a better estimate:

$$R_\lambda = \left[a_i R_{\lambda,\mathrm{i}}^{\frac{1}{n}} + (1 - a_i) R_{\lambda,\mathrm{p}}^{\frac{1}{n}} \right]^n \qquad (6)$$

This factor is determined through mathematical optimization, although it could be derived with simple iteration process. Exponent *1/n* is transforming the reflectance space into one that is considered linear and then scaled back to the reflectance space by raising to the power on n. There has been attempts to assign a physical meaning to the n factor (Ruckdeschel, 1978, Pearson, 1980), but most of the authors came up with one conclusion: n=1 corresponds to the MD model, where for n=2 it is believed that represents highly scattered substrate. However, with ink-jet printing, the effect of the dot gain is significantly higher than with other printing technology.

There is a potential caveat in the process of determining and assigning n factor. Namely, the n factor could be used to model both optical and physical dot gain, which is not the ideal situation as we are relying on a single number. Much better option will be to apply the n factor to the already corrected reflectance for the physical dot gain. When we measure the single colour ramp to provide an estimate of the physical dot gain, the measuring instrument, being the area measuring device will effectively record the optical dot gain as well. The best scenario would be to separate physical and optical dot gain, which is not trivial process (Namedanian and Gooran, 2010) and not feasible to perform every time when new characterization model is needed. Potentially, determination of the n factor could be done as a function of the wavelength. This implies that the reflectance of the area is actually dependent on the dot gain, or that ink penetration will cause the reflectance attenuation. Although this approach provides better modelling of the n factor, it is not proven that the optical dot gain is wavelength dependent (Namedanian et al., 2008). This brings back the fact that the n factor does not represent a physical phenomenon.

2.3 Cellular NG

The main aim of the cellular model is to increase precision of interpolation by increasing number of the sampling points and this would lead to a more accurate printer model at the end (Heuberger et al., 1992, Rolleston and Balasubramanian, 1993). More sampling points will lead to the division of the printer gamut into cells, where sampled points serve as the nodes for lower and upper boundaries of the cell. There are significant non-linearity introduced by paper ink interaction and those will reflect on interpolation precision in the process. This is in fact the main problem of the classical NG model where the cellular extension is much less prone to this.

If the dot gain has been accounted for, the sampling of the printer colour space for cellular model will than include the effective dot coverage. The search for the desired point is then performed equivalently to the inversed MD model with the exception of the end points which are in this case lower and upper boundary of the searched cell:

$$a_{eff} = \frac{R_{\lambda,i} - R_{\lambda,L}}{R_{\lambda,L} - R_{\lambda,U}} \qquad (7)$$

Here, $R_{\lambda,i}$ denote the reflectance of the ink, $R_{\lambda,L}$ denotes node on the lower boundary of the cell, and $R_{\lambda,U}$ is the upper boundary node.

The problem with this model is that it requires high number of training (measurement) patches. This number is the function of number of levels in the sampling along single colourant (3 for 0, 50%, 100% coverage), raised to the power of number of the colorants (channels). If we have 5 level sampling combined with 7 channel printing system we would end up measuring around 75.000 patches. Although this will provide highly accurate model it is simply not feasible bearing in mind that each change of the paper or a colourant would require new model. It is showed that by converting to the cellular model we can get improvements over classical YNSN model but to the extent of 25% in RMS spectral precision (Taplin, 2001). There have been attempts to reduce number of patches (Chen et al., 2004) and measurement intensity by estimation of some nodes. There is also an assumption that some part of the space should be sampled with higher frequency than other. To determine what area is that, one must analyse spectral or colour error gradation throughout the printer space. There is also an issue of the cells search for interpolation process. As the printing relies on the metamerism to produce colour match, there are multiple cells that can map to the same colour. To obtain the "right one", one must set a condition for optimization process that is based on the particular requirement of the model usage. This constraint can be spectral difference or metamerism minimization as well as the colour difference under specified illuminant.

2.4 NG based models: improvements and extensions

There have been many attempts and improvements to the Neugebauer model and its extensions: YNSN and cellular. With assumption that ink spreading is not the same on paper and superimposed on another ink (Emmel and Hersch, 2002) the proposition is made to use calibration curves for each two and three colour overprint. This helps the model to perform better but requires additional measurement especially when it is applied to multichannel system. In fact, each two or more colour NP would have its own calibration curve and this is what makes this model similar to the cellular approach. Multiple attempts were also made to estimate the parameters for the NG model such are dot gain, n factor and primaries (Abebe et al., 2011, Agar and Allebach, 1998, Balasubramanian, 1999, Zuffi et al., 2005). Especially the physically non realizable primaries were addressed (where more than four colours need to be printed on an area) and although not printable, these NP's are very useful for sampling of the space for interpolation.

2.5 Continuous tone model: Kubelka- Munk model (KM)

Many types of colouration systems have used this model for prediction of the colour mixture. It is also widely used for various purposes in graphic arts where primarily halftone systems are usage. It is assumed that most of the scattering comes from the paper and therefore the single constant KM (Kubelka and Munk, 1931) theory was considered to be very useful for halftone printing. It bases its approximation by considering ratio of scattering and absorption coefficients of the mixture:

$$(K/S)_\lambda = \frac{(1-R_\lambda)^2}{2R_\lambda} \quad (8)$$

Where R_λ is the spectral reflectance of the mixture, K is the absorption coefficient and S stands for scattering coefficient. To use this model for halftone printers, K/S factor is calculated for each ink at maximum coverage and for the paper:

$$(K/S)_{\lambda,i} = (K/S)_{\lambda,i,max} - (K/S)_{\lambda,p} \quad (9)$$

For multichannel case, the previous equation can be expanded:

$$(K/S)_{\lambda,mix} = (K/S)_{\lambda,p} + \sum_i c_i (K/S)_{\lambda,i} \quad (10)$$

Where c is the weighting on the unit K/S and is based on the concentration of the ink. In the K/S space, the additivity of the mixture is assumed and it is the space where the reflectance is behaving in linear manner. This fact was used by Chen for the model inversion where he used K/S space instead of the ink space where this linearity does not stand. Also, inversion of the model can be done analytically and it is straightforward process:

$$R_\lambda = 1 + \left(\frac{K}{S}\right)_{\lambda,mix} - \sqrt{\left(\frac{K}{S}\right)^2_{\lambda,mix} + 2\left(\frac{K}{S}\right)_{\lambda,mix}} \quad (11)$$

There is also the cellular version of the KM model that performs the same operation like cellular NG model and also requires intermediate steps for measurements. The interest in using KM model is particularly strong in estimation of the physically non-realizable primaries that are needed for good space sampling and later interpolation. Also, estimation of the primaries can be used to reduce number patches needed for cellular NG model.

3. Halftoning for multichannel printing

Halftoning is the method of conveying the continuous tone information with binary devices. It performs the simulation and grey tone variation by either modulating the size (amplitude) or frequency of placement of binary dots. As the technology moves forward, the resolution that can be achieved with printers are increased in last two decades as it's the ability of the printers to simulate continuous tone image. Especially this is the case with ink – jet printers which are inherently FM type of printers, but resolution went so high that they have the ability to simulate the AM halftoning efficiently. Also, there are the ink-jet printers that employ multi-level halftoning, meaning that they can address more than one dot at the place.

The attributes of a halftoning are usually evaluated through the image quality measures such are: sharpness, number of grey levels, tone gradation, stability, etc. We are interested here in how different algorithms influence the precision of the spectral printer models and their parameters. As there are a division between AM and FM halftoning methods, we will evaluate one from each option with spectral Neugebauer model applied on seven channel printer. We are interested in how different influences the dot gain, ink-spreading, ink-

limitations, and the final colour of the NP's. As ink-jet printers cannot vary the size of the dot, they effectively simulate AM halftoning by striking multiple dots to form a larger one. In such configuration, we can evaluate is the ink spreading the same when we print isolated dot on the paper or it varies when it is printed over another dot (same or different ink).

Spectral printer modelling has the interest in exploiting the possibility of different halftoning patterns as those can produce significantly different colour with the same input. This difference can go up to ΔE of 26 and can be exploited by releasing the restrictions imposed by ink-system (Morovič et al., 2012). Namely, if printer space is observed as NP's space, produced with different halftone patterns, the great variability in selecting so called "halftone metamers" opens up. Classic AM patterns are rosette, stochastic halftoning produces random distribution, iterative processes such as IMCDP (Iterative Method Controlling Dot Placement) (Gooran, 2004), DBS (Dynamic Binary Search) (Analoui and J. P. Allebach, 1992) produce same colour like previous two but less ink usage, due to dependent dot placement. They are taking into account previous separation and tend, through iteration process, to maximize the distance between adjacent dots. These algorithms are particularly interested for multichannel printing where ink-overlaps do not allow that for whatever reason we print more than four colours per area.

4. Method

The goal of the experiment is to evaluate how different are the halftoning types for determination of the input parameters for spectral modelling of multichannel printer. For this work, we used HP Z3200 ink-jet printer which is a twelve channel printer with CMYKRGB as independent channels. Primary purpose of the RGB channels is to increase the gamut where CMYK system shows shortcomings. For the purpose of spectral printing, these channels are treated as independent from CMYK. To perform spectral printing and modelling, one needs to establish full control over printer channels and bypass colour management. We have done it through the Onyx Production House RIP by sending seven channels TIFF file previously made with Matlab where RGB channels are treated as spot colours (Figure 1). Halftoning algorithms are selected from the RIP. For modelling we used YNSN model which requires the test target made out of 128 patches that represent each possible combination of the seven channel system (Figure 2). As we printed full-tone patches, the light channels were effectively excluded.

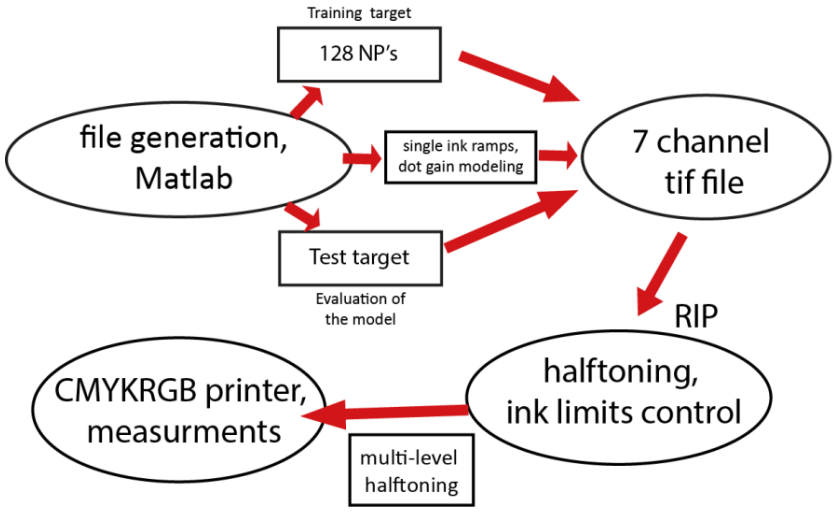

Figure 1. Spectral printing framework

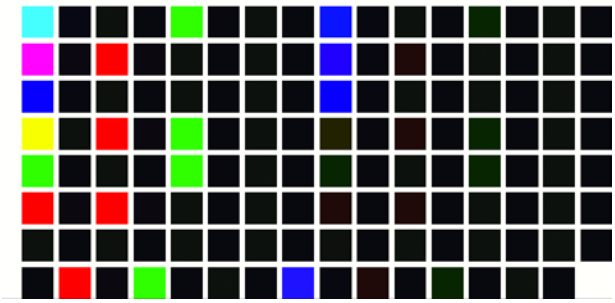

Figure 2. 128 Neugebauer primaries

To model the dot gain (for each type of halftoning), we output single colour ramps with given halftoning as well as two colour overprints in order to evaluate ink spreading both ink on paper and ink on ink (AM). We compute dot gain curves with spectral form of inversed MD model (Figure 3).

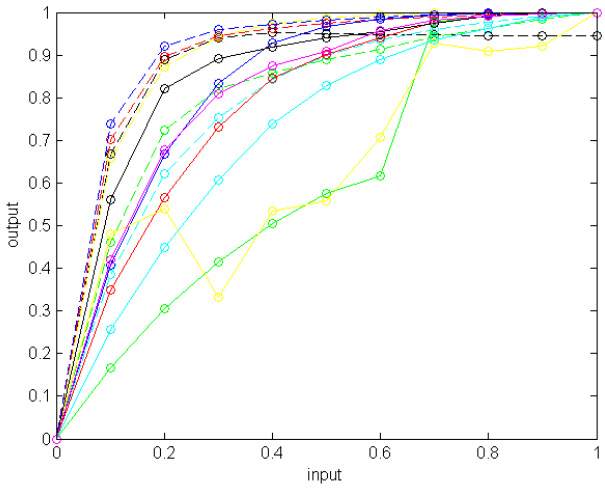

Figure 3. Effective dot gain for each channel where full line is AM and dashed FM halftoning

After obtaining dot gain curves, we have corrected the image of the NP's for each channel using Matlab. Compensated image in resolution 1200 x 1000 is sent to the printer and for this experiment we used HP Heavyweight Coated paper. As this printer employs multi-level haftoning, the amount of ink outputted to the paper is controlled with ink limits. With this, we are able to prevent ink bleeding and yet to have full-tones NP's. To emphasize the difference in the halftoning, we employed YNSN model and select n factor of 2 globally (on each channel) for both type of halftoning which would otherwise be both halftone and channel specific. As the inputs we used effective dot coverage curves and target comprised of NP's. The accuracy of the YNSN model is performed with test set comprising samples from entire printer gamut. The space was sampled using three levels for each colourant (0, 50%, and 100%) and the combination thereof. All together this target contained 3^7 or 6561 digital values that were compensated for dot gain prior printing the patches. We have selected a subset of this chart and for evaluation of the model and halftoning. This is to evaluate if we can used an AM halftoning based model to simulate the output made with FM or in other words, is the model halftone specific. All measurements were performed by following ISO 13655 methodology, with X-rite I1 instrument with UV cut filter mounted. As we are focused mainly on modelling of the colour properties of the printer, we have excluded the paper induced change caused by OBA's.

5. Results and discussion

We have evaluated the performance of the YNSN model on the 7 channel ink jet printer by using fixed n factor of 2 and the input image was corrected for the physical dot gain (Table 1). Sampling the colour space with NP's occurs in much higher frequency in the dark region and CIE ΔE_{00} was used as a colorimetric error metric since it more accurately estimates perceptual colour differences in this region than ΔE_{ab}.

By analysis of the maximum colour difference, which occurs in saturated magenta, red and yellow region we could sample that area more frequently which would imply using the cellular NG model. This way we should improve interpolation process in the area where small changes are more perceptible.

Table1. The performance of the YNSN model applied to the 7 channel printer using different halftoning

NG forward Printer model (AM)	sRMS (mean)	ΔE^*_{ab} (mean)	ΔE^*_{ab} (std)	ΔE^*_{ab} (max)	ΔE^*_{00} $(mean)$	ΔE^*_{00} (std)	ΔE^*_{00} (max)
YNSN(test AM)	0.031	6.43	3.22	15.19	4.88	2.78	12.18
YNSN(test FM)	0.034	9.88	5.57	27.13	7.55	4.31	21.61
NG forward Printer model (FM)							
YNSN(test FM)	0.038	7.82	4.1	21.15	5.23	3.16	18.43
YNSN(test AM)	0.040	12.43	7.43	30.8	9.89	5.94	26.55

Different halftoning will produce significantly different dot overlaps and therefore different colour per patch and different NP's. It is true that we can compensate for this with different calibration curves, but in order to account for the difference in halftoning one must have ink-spreading curves (Figure 4) for each ink over other inks (assuming that printing order is in CMYKRGB). This would require usage of the IS-YNSN (Emmel and Hersch, 2002) model to account fully for the difference in halftone patterns.

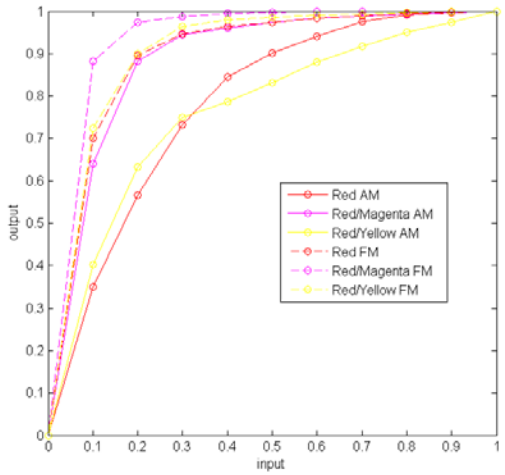

Figure 4. Ink spreading curves for Red channel superimposed to Magenta and Yellow for both AM and FM halftoning

Furthermore, it is known that AM is more prone to the optical dot gain than FM due to isolated dot placement. This would require halftone specific determination of the YN n factor. Physical limitation of the ink per area challenges the whole concept as the trial and error test must be performed to find right amount of ink for a particular substrate. Currently we have no explanation for irregular curves with AM halftoned green and yellow ramps on Figure 3 as it may come from different factors like calculation process, measurement error or due to specific chemistry of the yellow and green ink.

6. Conclusions and Further work

We have evaluated would it be possible and what are the factors that determine could the modelling of the multichannel printer be halftoning independent. As the halftone algorithms are developing apart from colour management, there has not been the one that is recommended to use for spectral reproduction workflow. They all have advantages and disadvantages. However, the fact is that different patterns produces different colour, and each one of them can be observed as a NP. According to this, we can obtain much higher subset of the primaries and their interaction which in return can increase spectral precision of the both forward and inverse model.

Each halftoning produces different type and amount of overlaps with other dots. In order to make modelling process halftone independent, one must use ink-spreading curves for each superimposing condition and specific optical dot gain modelling in addition to effective dot coverage curves for a dot on the substrate.

Precision of the modelling further might depend on the precision of measuring instrument in dark region as it is the area that is oversampled with NP's. Effectively this could result in much better sampled primaries and subsequent interpolation. As the over 70 % of NP's are located in the dark region, it makes sense to estimate those using continuous tone mixing models like KM. These are referred as physically not realizable (not printable) colours. With estimation we could expand the printer space and have more accurate interpolation, especially in the area around dark end of the lightness axis where HVS is most sensitive.

Other improvements would be to investigate how dependent FM halftoning options work with spectral printing. They take into account previous separation for the dot placement and in that manner the less ink is outputted to the area.

All parameters that are included are specific to the model. Starting from paper selection, ink, halftoning, ink limit, printing order, measurement geometry, dot gain (both physical and optical) and ink spreading, all of this should be fixed and modeled accordingly.

Acknowledgments

This work was supported by the Marie Curie Initial Training Networks (ITN) CP7.0 N-290154 funding. Special thanks to all CP 7.0 members for sharing knowledge and providing excellent working environment

Chapter 6

REFERENCES

Abebe, M., Gerhardt, J., and Hardeberg, J. Y. (2011), Kubelka-Munk theory for efficient spectral printer modelling. Proc. SPIE 7866, Colour Imaging XVI: Displaying, Processing, Hardcopy, and Applications.

Agar, A. U. and Allebach, J. P. (1998), An iterative cellular YNSN method for colour printer characterization, Proc. of the Sixth IS&T/SID Colour Imaging Conference, 197–200, (1998).

Analoui, M. and Allebach, J. P. (1992), Model-based halftoning using direct binary search, Proc. SPIE/IS&T, 1666, 96.

Bala, R. (2003), Device Characterization, in Digital Colour Imaging Handbook, G Sharma (Ed.), CRC Press.

Balasubramanian, R. (1999), Optimization of the spectral Neugebauer model for printer characterization, J. Electron. Imaging 8 (2), 156–166, (1999).

Chen,Y., Berns, R. S. and Taplin, L. A. (2004) , Six colour printer characterization using an optimized cellular Yule-Nielsen spectral Neugebauer model, Journal of Imaging Science and Technology, vol. 48, No. 6, Nov. 2004.

Demichel, M. E. (1924), Procédé; 26:17-21, 26-27.

Emmel, P. and Hersch, R. D. (2002), Modelling ink spreading for colour prediction, J. Imaging Sci. Technol. 46(2), (2002).

Gerhardt, J. and Hardeberg, J. Y. (2006), Spectral colour reproduction by vector error diffusion. In Proceedings CGIV 2006, pages 469–473, 2006.

Gooran, S. (2004), Dependent Colour Halftoning, Better Quality with Less Ink, Journal of Imaging Science & Technology, Volume 48, Number 4, pp. 354-362, July/August 2004.

Heuberger, K. J. Z., Jing, M. and Persiev, S. (1992), Colour Transformations and lookup tables. TAGA/ISCC Proc: 1992, pp. 863-881.

ISO 13655:2009 Graphic technology -- Spectral measurement and colorimetric computation for graphic arts images

Kubelka, P. and Munk, F. (1931), Ein Beitrag zur Optik der Farbanstriche, Z. Tech Phys.**12**, pp.593-601

Morovič, J., Morovič, P. and Arnabat, J. (2012), HANS: Controlling Ink-Jet Print Attributes Via Neugebauer Primary Area Coverages, IEEE Transactions On Image Processing, Vol. 21, No. 2, FEBRUARY 2012

Namedanian, M. and Gooran,S. (2010), High Resolution Analysis of Optical and Physical Dot Gain, Proc. TAGA (Technical Association of the Graphic Arts), March 2010, San Diego, California.

Namedanian, M., Gooran, S., and Nyström, D. (2011), Investigating the Wavelength Dependency of Dot Gain in Colour Print, SPIE, Electronic Imaging, January 2011, San Francisco, California.

Neugebauer, H. E. J. (1989), Die theoretischen Grundlagen des Mehrfarbenbuchdrucks. In Neugebauer Memorial Seminar on Colour Reproduction: 14-15 December 1989, Tokyo, Japan (Sayanagi, K., ed.), pp. xv, 203, SPIE

Murray, A. (1936), Monochrome reproduction in photoengraving, J Franklin Inst., **221**, pp.721-744

Pearson M. (1980), n value for general conditions. TAGA Proc 1980; 32:415– 425.

Rolleston, R.and Balasubramanian, R. (1993), Accuracy of various types of Neugebauer models. Proc IS&T SID Col. Imag. Conf. pp. 32-37 (1993)

Ruckdeschel, F.R. and Hauser, O.G. (1978), Yule–Nielsen effect on printing: a physical analysis. Appl Opt 1978; 17:3376 –3383.

Taplin, L. A. (2001), Spectral Modelling of a Six-Colour Inkjet Printer, Msc Thesis , RIT 2001.

Tzeng, D., and Berns, R. S. (1998), Spectral-Based Ink Selection for Multiple-Ink Printing I. Colourant Estimation of Original Objects, The Sixth Colour Imaging Conference: Colour Science, Systems and Applications, pp. 106 -111, 1998

Yule, J. A. C. (1951), The penetration of light into paper and its effect on halftone reproductions. TAGA, Proc. **3**, pp.65-76

Urban, P., and Rosen, M. (2008), Spectral-based Image Reproduction Workflow, From Capture to Print, Presentation, Rochester Institute of Technology, USA, 2008

Zuffi, S., Schettini, R. and Mauri, G. (2005), Spectral-based printer modelling and characterization, Journal of Electronic Imaging 14(2), 023008 (Apr–Jun 2005).

http://colour.org/specification/ICC1v43_2010-12.pdf - Specification ICC.1:2010-12 (Profile version 4.3.0.0)

Chapter 7

Paper B

Measuring or Estimating Neugebauer Primaries for Multichannel Printer Modelling

Radovan Slavuj, Ludovic G. Coppel, Melissa Olen and Jon Yngve Hardeberg

Published in

Proceedings of

SPIE Electronic Imaging

(Measuring, Modelling, and Reproducing Material Appearance)

Vol. 9018,

Pages 90180C

San Francisco, USA, 2014.

Chapter 7

Estimating Neugebauer Primaries for Multichannel Printer Modelling

Radovan Slavuj[a], Ludovic G. Coppel[a], Melissa Olen[b], Jon Yngve Hardeberg[a]

[a]The Norwegian Colour and Visual Computing Laboratory, Gjøvik University College, Norway;

[b]University of West England, Bristol, UK

ABSTRACT

Multichannel printer modelling has been an active area of research in the field of spectral printing. The most commonly used models for characterization of such systems are the Spectral Neugebauer (SN) and its extensions. This work addresses issues that can arise during calibration and testing of the SN model when modelling a 7-colourant printer. Since most substrates are limited in their capacity to take in large amount of ink, it is not always possible to print all colourant combinations necessary to determine the Neugebauer primaries (NP). A common solution is to estimate the non-printable Neugebauer primaries from the single colourant primaries using the Kubelka-Munk (KM) optical model. In this work we test whether a better estimate can be obtained using general radiative transfer theory, which better represents the angular variation of the reflectance from highly absorbing media, and takes surface scattering into account. For this purpose we use the DORT2002 model. We conclude DORT2002 does not offer significant improvements over KM in the estimation of the NPs, but a significant improvement is obtained when using a simple surface scattering model. When the estimated primaries are used as inputs to the SN model instead of measured ones, it is found the SN model performs the same or better in terms of colour difference and spectral error. If the mixed measured and estimated primaries are used as inputs to the SN model, it performs better than using either measured or estimated.

1. INTRODUCTION

The idea of spectral printing is to match input spectra, or at least to reduce colour differences under different illuminations. Multichannel systems provide an enlarged set of possible colourant combinations and can therefore produce better spectral matches. Today's multichannel inkjet printers are usually equipped with 7 independent channels (e.g. CMYKRGB), and provide both larger colour and spectral gamut. The direct benefit for spectral printing is measured in number of printable reflectances.

However, additional colourants increase the complexity of spectral printer models, such as the widely used Spectral Neugebauer (SN) model and its extensions. Calibration of these models requires a set of Neugebauer's Primaries (NP) that represents all colourant combinations. For a seven channel printing system, the number of patches required to calibrate the SN model is 127. At least half of these patches are overprints of four and more

colourants, where each colourant is sent to the printer with 100% theoretical coverage. This means that many patches have 300% coverage or more. On a majority of substrates, these NP's are not printable without significant artifacts. Mixing wet inks on top of each other can, for instance, lead to bleeding. Due to these physical limitations, it is generally not possible to print five or more solid primaries in one location. Controlling ink limits is therefore the primary concern for a seven colour printing system. The majority of the colourants employed in inkjet printing systems reach their maximum effective coverage on a substrate around 70% nominal coverage. After calibration of each channel, four colours can be printed with maximum effective coverage on the majority of substrates. For seven channel systems, the maximum coverage that needs to be printed is around 490% of the effective coverage (or 700% theoretical). This fact implies that there is very limited number of substrates that are capable of absorbing that much ink and subsequently to be used for calibration of the SN model. There have been attempts to deal with this limitation, primarily with estimation of the non-printable NPs. Balasubmarian estimated the NPs using weighted linear regression[1], which requires a training set for calibration. This approach was used later by Chen, et.al.[2] to reduce the number of patches needed for calibration of the Cellular YNSN model. Tzeng[3] used the Kubelka-Munk[4] (KM) model to estimate NPs assuming translucent inks printed on highly scattering substrates. Chen, et.al.[5] used instead the single constant KM model to estimate the NPs in a Yule-Nielsen modified Spectral Neugebauer model[6] (YNSN). A similar approach was adopted by Abebe et.al.[7] who used single constant KM to estimate primaries for a CMYK printer. More recently, Urban[8] introduced a simple multi-linear interpolation that performs on an extended printer space and account for non-printable primaries. With this modification of the inverse YNSN, he also reported that it performs better than before the correction has been applied. KM is a simplification of general transfer theory and is known to be less accurate for media with strong light absorption. Therefore, more recent radiative transfer models taking into account the directionality of light and the measurement geometry can potentially give better estimates for the NPs than KM.

The present work aims at finding an alternative tool for estimation of primaries. Therefore, the main goal is to evaluate whether general radiative transfer can improve the NPs estimation and subsequently the performance of the SN model. We use the DORT2002 software[9,10] that solves the radiative transfer problem in turbid media using the discrete ordinate method and propose a simple surface scattering model on top of the bulk scattering model. We then compare the performance of the SN model with estimated or measured NPs, for three different substrates that differ in how much ink they can take in without significant artefacts. To control the extent of these possible artefacts we apply different maximal ink limits and report also a limited effect of ink limits on the measured spectral reflectance.

2. METHOD

On a paper with high ink absorbency (we chose the Somerset Velvet paper that can take in a large amount of ink) we first tested whether there is any significance to printing full coverage of each colour with varied ink limitations. Here, the same source file was printed with 700%, 490%, or 240% total achievable coverage. To conclude on this, spectral curves of printing primary, secondary, and dark colours are compared for each ink limitation. We then compared the performance of the KM and DORT2002 models in predicting the multi-

colourant NPs from measured single-colourant NPs. As many of the NPs are dark, dense colours, surface reflection significantly affected the measured reflectance factor. To account for this we introduced a simple surface reflection model on top of both KM and DORT2002. Finally, we tested the spectral Neugebauer model with measured or estimated primaries for all substrates.

2.1 Experimental setup

Test prints were run on a Canon iPF8000 multi-channel inkjet printer. This printer comprises 12 ink channels, seven of which were used here. In addition to the standard cyan, magenta, yellow, and black ink colourants, red, green and blue were also used. In order to selectively control the ink colourant combinations to obtain the final printed colour, a direct dialogue must be established between input data and the printer output. The Caldera RIP was employed to address this requirement. The training chart, designed for calibration, was created in Matlab (Mathworks Inc.) and sent to printer in the form of a 7-channel tiff file where each channel has a 100% theoretical coverage. For the test of the SN model we created a set of primary, secondary and tertiary ramps (473 patches altogether) that had 10% increase in theoretical coverage and samples whole printer gamut. All prints are measured with a GretagMacbeth i1 spectrophotometer.

Three inkjet papers were chosen from a range of media that are typically used for graphic and fine art printing: Somerset Enhanced Velvet (255g/m^2) is a 100% cotton, matte, artist grade inkjet paper. Boasting a high whiteness despite low amount of optical brightening agents, it is an archival paper with a felted, low textured surface. Canson Infinity Baryta Photographic (310g/m^2) is a semi-gloss paper designed after traditional dark room photographic paper. It is ideally suited for the printing of photographic reproductions. HP Matte Litho-realistic Paper (270g/m^2) is a fine art paper with a smooth surface reminiscent of traditional lithographic papers. It is an ideal paper for graphic arts printing and similar applications where detail and sharp edges are essential.

The two matte papers were printed using matte black ink, and the semi-gloss paper printed with photo black ink. The variations in total ink limits, as described below, were printed with only this one variable while the initial printer characterization was maintained. Each training chart was first printed with a total ink limit of 700%. This total of 700 comprises 100% of each of the seven ink colourant where the individual 100% is the result of the per channel ink restriction established during the linearization.

The second sets of NPs were printed with the ink limit determined by Caldera's *Easy Media* workflow. This workflow prompts the user to print a custom dynamic ink limit chart, which it generates for each calibration process (printer/paper combination) based upon the linearization curves. This post-linearization method is based on ink densities from the linearization curves, not input densities. Here the total ink limit that can thus be printed, by this definition, is the total of each ink post linearization. This means that if each ink channel were theoretically restricted to 70%, the maximum ink limit possible would be 490%.

With reference to input density parameters for setting up the total ink limit, as was applied in the case of the 700% prints, a custom ink limit chart was used. The design for this is based on the simplified dynamic chart, yet extended for printing with seven channels with a total possible ink limit of 700%. The simplified dynamic target was designed for only

four colour printing with CMYK, and uses different colour sequences to alter the point at which each colour is introduced. This colour order was reproduced in the custom design for the first 4 colours, and then extended to add an additional range from 410% to 700% ink coverage. The description of the ink limits applied and the chart used for particular substrates is given in Table 1.

Table 1. Ink limitation applied on a substrate and the chart that has been used for a given ink limit

Print Sample Number	Paper Type	Ink Limit Applied	Ink limit Method
1	Somerset Velvet Enh.	700%	None
2	Somerset Velvet Enh.	400%	Custom Chart
3	Somerset Velvet Enh.	240%	Caldera Chart
4	HP Litho---realistic	700%	None
5	HP Litho---realistic	290%	Custom Chart
6	HP Litho---realistic	190%	Caldera Chart
7	Canson Infinity Baryta	700%	None
8	Canson Infinity Baryta	270%	Custom Chart
9	Canson Infinity Baryta	200%	Caldera Chart

2.2. NPs estimation model

The single-constant KM model relates the reflectance of an opaque medium to the ratio of the absorption coefficient K/S. K/S is determined spectrally for each colourant from the measurement of the spectral reflectance factor. A simple additional rule is then applied to estimate the K/S of colourant mixtures,

$$K/S_{\text{mix}} = \Sigma\, K/S \qquad (1)$$

DORT2002 requires both the scattering and absorption to be specified. In order to use it as a single-constant model, the scattering coefficient was arbitrarily set to 1 (meaning $K/S = K$) and the absorption coefficient was estimated by minimizing the square of the error between simulated and measured reflectance. The optimization was performed with the lsqnonlin tool in Matlab. In addition, the asymmetry factor, g, must be specified. This factor defines the angular distribution at single scattering events according to the Henyey-Greenstein phase function. The asymmetry factor was set to 0.7 as this value has been shown to better represent paper materials. Different values were also tested without significant impact on the results. The simulations with DORT2002 were performed with the 45/0 geometry, i.e. the same as for the measurement with the spectrophotometer. The same additional rule was then applied as with the KM model and the forward DORT2002 can then compute the reflectance factor of colourant mixtures.

In order to account for surface reflection we introduced a simple surface reflection model within the estimation process. For each paper substrate, the minimum measured reflectance was assumed to be the surface contribution to the reflectance factor. This minimum was obtained for one of the black patches for which the bulk reflectance was negligible. The

surface component was then subtracted from the measurement of the single-colourant patches prior to K/S estimation and added back to the estimated reflectance factors of colourant mixtures.

3. RESULTS AND DISCUSSION

The Somerset Velvet Enhanced paper demonstrated a capacity to accept higher ink levels, with no pooling of the ink due to the papers high absorbency. However there are some instances of ink spreading across the paper fibers around the edges, and some appearance of small, stipple like blotching as the ink absorbed either into the raised fibers of the paper or the valleys in between. The measurements of these samples still maintain accuracy, especially with several readings averaged to compensate for the slight variance that may be caused by the measuring instruments position on the sample. These effects are almost entirely eliminated in the print sample at 400%, but can be seen at a close viewing distance. This is also the case in the print sample at 240%, but again the effects are further reduced.

When printing with the HP Litho, pooling of the ink also took place when the 700% ink limit was applied, but as it dried the majority of the excess ink was absorbed back into the paper. The effect of this is seen in a blotchy appearance of the ink surface. In some patches not all the ink could be absorbed and it dried on the surface of the paper as opposed to in the coating. There are also sections where in some patches the inks have spread along the paper fibers resulting in fuzzy edges. Where 290% ink limits were applied, which was determined by the custom ink limit chart, there are also some instances of blotchy colour and fuzzy edges. This is most likely due to the patch size in the print samples being considerably larger that the size of the patch in the ink limit chart. This result is likely due to an uneven inkjet coating layer, so when a small area of the paper has a thinner coating layer the ink may have flowed into a valley in the paper surface causing this neighboring area to become over inked. These artefacts are eliminated in the print sample where the lowest ink limit is applied.

The Canson Baryta's ink limits are lower than the HP Litho and Somerset Velvet, which is due to the coating acting as a barrier and preventing ink absorption into the underlying paper. The result of high volumes of ink, as when printed at 700% ink, generated a lake effect on the surface of the paper with severe pooling. This leads to colour reading errors as the density of ink varies over each patch depending on how the drips dried. This effect was eliminated when the lower ink limits were applied. The one visible difference between the two samples with lower ink limits was the higher volume of 270% did increase the bronzing effect in the print.

We continued analysis with the evaluation of spectra as a function of the ink limitation and ink amount. Figure 2 shows the spectral reflectance of the primary inks, secondary and dark colours (four and more colour overprints) printed on the three different substrates and with three different ink limitation setups. Only the Somerset Velvet paper (first column) can accommodate all ink limit settings without any significant bleeding and other artefacts.

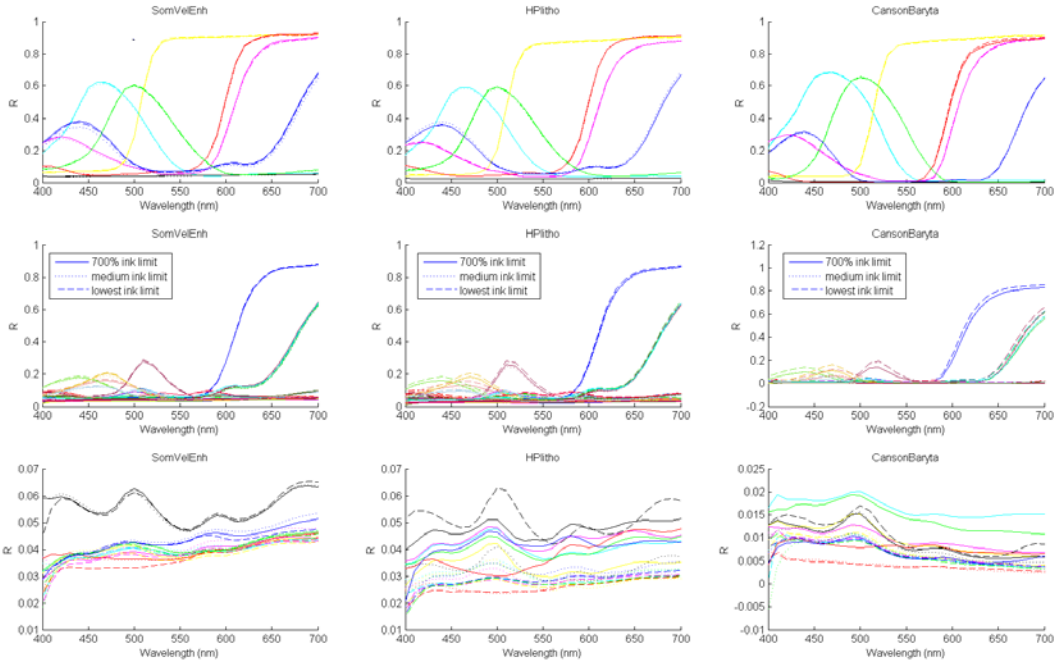

Figure 2. Spectral reflectance curves of printed primary, secondary and dark colours with variable ink limits.

From Figure 2, it can be seen that the reflectance factor does not significantly depend on the ink amount. The explanation for this is that once an ink mixture reaches its maximum density, it cannot go any further. However, this finding is significant for ink and time saving of many authors that have dealt with same problem when creating the training patches for SN model or its cellular extension[2,8,11]. The small reflectance change exhibited in columns 2 and 3 of are the result of artefacts that occur during printing with high amounts of ink, rather than a result of the ink limitation setting. The performance of the KM and DOORT2002 models in estimating the Neugebauer primaries of colourant mixtures are shown in Figure 3. We report the accuracy as colour difference (ΔE^*_{00} under D50 illuminant) as the spectral RMS is very small and not a good representation due to the many dark samples (Table 2).

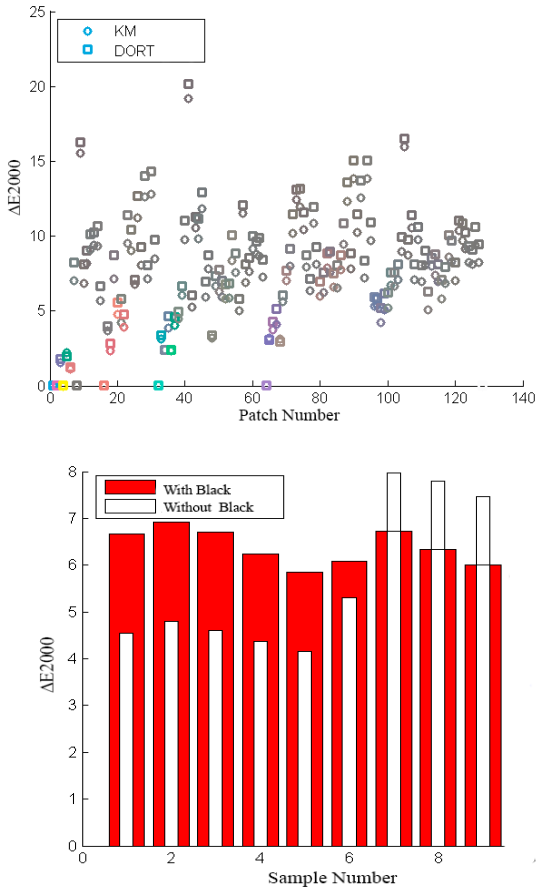

Figure 3. Left: Colour difference between predicted and measured spectral reflectance, reported as ΔE2000, for all 128 patches, using both DORT2002 (squares) and KM model (circles). Right: Mean value for each substrate and ink limitation setting for all samples (red) and for all samples without black ink (white).

These initial results show that the prediction for both KM and DOORT2002 model is generally not satisfactory. DOORT2002 performs slightly better in estimating secondaries and tertiaries, but fails to keep the advantage in dark samples. These dark samples primarily come from a combination with black ink, but it could be also the result of mixing complementary colours. As these dark samples produce high errors in estimation, we have also included analysis without black ink in order to demonstrate this. These results could be seen on the bar plot (white bars). The only exception to this claim is the samples from 7-9, which is the photo paper that uses Photo Black ink that contains different properties. Next we introduced a simple surface reflection model to the estimation process. As mentioned, both KM and DOORT2002 make no assumption on the structure of the surface or any surface phenomena. As many of these occur within the process of printing NPs, we expect that we can improve estimation error with such correction (Figure 4).

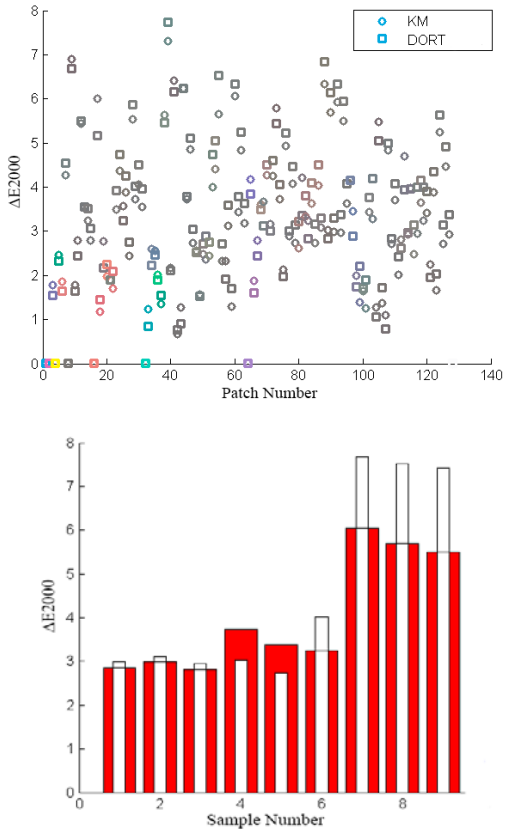

Figure 4. Estimation error for Somerset Velvet paper using both KM and DOORT2002 model with surface reflection model (right) and the mean estimation error for each substrate and ink limit setting (left).

Applying the simple surface reflection model doubles the mean accuracy for the first and second substrates but does not improve it for the third substrate (Photo Paper). Also, here we have included analysis without black ink. This proves that the surface phenomena occurs much more for the dark and dense mixture of all colour combinations, rather than just with black ink. Further on, we evaluated the extent to which this surface reflection model will help individually to KM and DOORT2002 model.

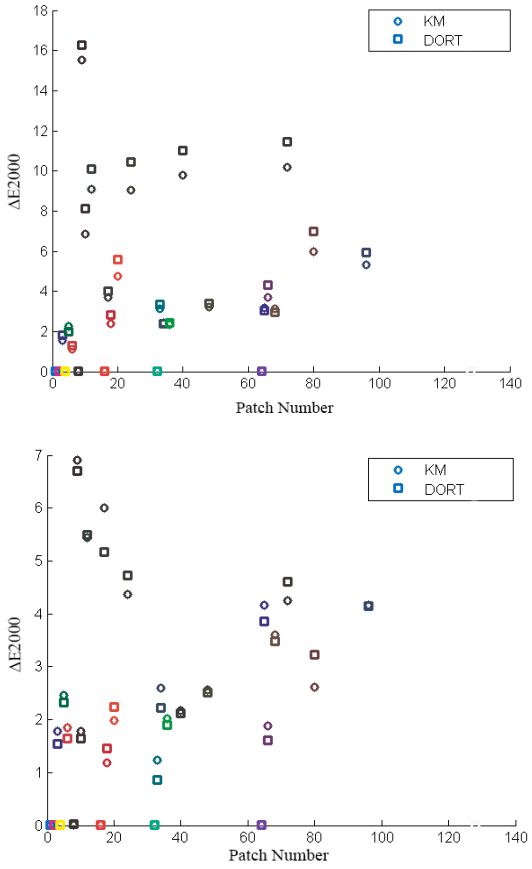

Figure 5. Comparison of performance of the KM and DORT2002 without and with surface reflection model for Somerset Velvet paper

As seen in Figure 5, the surface reflectance model has significant improvements in performance overall, but even more so with DOORT2002. From the graph on the left, it can be seen that DOORT2002 is equal or worse than KM, where on the right graph, with introduction of the surface reflection, DOORT2002 is better or equal to the KM model for 80% of sample patches. The summarization of the findings in the estimation process is shown in Table 2. The weakness of the surface model used here is that it assumes that the surface contribution is equal for all patches. This assumption does not hold when gloss varies with the number of ink and ink combinations.

Table 2. Estimation error for KM and DOORT2002 model with and without surface reflection model

Somerset Velvet	Mean(RMS)	Max(RMS)	Mean(ΔE^*_{00})	Max(ΔE^*_{00})
KM no surf refl.	0.017	0.032	6.67	17.1
KM with surf refl.	0.007	0.021	2.85	8.03
DOORT no surf refl.	0.019	0.036	7.51	18.1
DOORT with surf refl.	0.007	0.025	2.94	8.23

We then performed the SN model using only measured, only estimated and a combination of both. The difference here is that we based the decision of whether to use estimated or measured based not only on non-printable criteria, but also on estimation error. The measured NP's are mostly primaries, secondaries and tertiaries and all others that are below a mean ΔE^*_{00}value of 3 in the estimation process. We performed this process for the Somerset Velvet substrate with 700% theoretical coverage that showed no significant artefacts during printing. The results are shown in Table 3.

Table 3. Performance of the SN model with different combination of the inputs: measured, estimated and mixed NP's

SN forward Printer model	Mean(RMS)	Mean(ΔE^*_{00})	Std (ΔE^*_{00})	Max(ΔE^*_{00})
SN Measured Primaries	0.031	4.88	2.78	12.18
SN Estimated Primaries (KM)	0.033	4.72	1.53	14.02
SN Estimated Primaries (DOORT2002)	0.028	4.39	1.78	15.13
SN Mixed Primaries	0.022	4.03	1.47	12.93

Although the estimation accuracy seems insufficient, it corresponds better to the non-linearity in assumed linear space by SN equations. Once the SN model has been calibrated with effective dot coverage prior to the printing, it is assumed that it is transformed to a linear mixing space. However, with printing inks this is not the case. This explains why the maximum error is increasing while mean and standard deviation are slightly improved. The best scenario is to use mixed measured and estimated primaries. First of all, printing the training chart is simply not a feasible process due to the difficulty in reproducing some of the NP's. Secondly, it improves the SN overall performance in both spectral and colour domain.

When more than four colours are printed in a particular area, there will be a certain colour cast of the seemingly neutral colour (black in this case). This is the reason for a high colour difference in those areas as most of the colour difference formulas (especially used

ΔE2000 is sensitive in dark region). Therefore, the estimation process could be further optimized based on the colour that is printed on top of the others (mostly RGB in CMYKRGB configuration).

4. CONCLUSIONS

In this work we have evaluated printing of the Neugebauer primaries on different substrates and the influence of ink limitation. Only a handful of substrates are capable of accommodating the high ink amount needed for multichannel printer characterization. However we have found that printing with the maximum ink amount is not necessary as there is no difference in spectra of the NPs when printed with different ink limits. The only noticeable fact in the evaluation of the effect of the ink limits is that the large ink amount can lead to artefacts that influence the performance of the SN model. We have found that using DOORT2002 or KM model does not make a significant difference for the estimation of the primaries. The general conclusion of this estimation process is that more information should be included to describe physical process in ink mixing of the highly dense samples. Introduction of the surface scattering model significantly improves estimation with either KM or DOORT2002.

Our research has shown that the SN model performs the best when used with a mixture of measured and estimated NPs. This is due to the fact that it was too difficult to print without significant artefacts on most substrates and therefore the estimated NPs are necessary for use in these instances.

REFERENCES

[1] Balasubramanian, R. (1999), Optimization of the spectral Neugebauer model for printer characterization, J. Electron. Imaging 8 (2), 156–166, (1999).

[2] Chen,Y., Berns, R. S. and Taplin, L. A. (2004) , Six colour printer characterization using an optimized cellular Yule-Nielsen spectral Neugebauer model, Journal of Imaging Science and Technology, vol. 48, No. 6, Nov. 2004.

[3] Tzeng, D., and Berns, R. S. (1998), Spectral-Based Ink Selection for Multiple-Ink Printing I. Colourant Estimation of Original Objects, The Sixth Colour Imaging Conference: Colour Science, Systems and Applications, pp. 106 -111, 1998

[4] Kubelka, P. and Munk, F. (1931), Ein Beitrag zur Optik der Farbanstriche, Z. Tech Phys.12, pp.593-601.

[5] Chen,Y., Berns, R. S. and Taplin, L. A. Extending Printing Colour Gamut by Optimizing the Spectral Reflectance of Inks, Twelfth Colour Imaging Conference: Colour Science and Engineering Systems, Technologies, and Applications Scottsdale, AZ; November 2004; p. 163-169

[6] Yule, J. A. C. (1951), The penetration of light into paper and its effect on halftone reproductions. TAGA, Proc. 3, pp.65-76

[7] Abebe, M., Gerhardt, J., and Hardeberg, J. Y. (2011), Kubelka-Munk theory for efficient spectral printer modelling. Proc. SPIE 7866, Colour Imaging XVI: Displaying, Processing, Hardcopy, and Applications.

[8] Urban, P. (2009), Ink limitation for Spectral or Constant Colour Printing, 11th AIC congress, Sydney, Australia

[9] Edström, P. (2004), Numerical Performance of the DORT2002 Radiative Transfer Solution Method, submitted to Appl. Numer. Math.

[10] Edström, P. (2004), Comparison of the DORT2002 radiative transfer solution method and the Kubelka-Munk model, Nordic Pulp and Paper Research Journal Vol 19. no. 3/2004

[11] Taplin, L. A. (2001), Spectral Modelling of a Six-Colour Inkjet Printer, Msc Thesis , Rochester Institute of Technology, 2001.

Chapter 8

Paper C

Effect of ink spreading and ink amount on the accuracy of the Yule-Nielsen modified spectral Neugebauer model

Radovan Slavuj, Ludovic G. Coppel, Jon Yngve Hardeberg,

Published in

Proceedings of

SPIE Electronic Imaging

(Colour Imaging XX: Displaying, Processing, Hardcopy, and Applications)

Vol. 9395,

Pages 93950E

San Francisco, USA, 2015.

Chapter 8

Effect of ink spreading and ink amount on the accuracy of the Yule-Nielsen modified spectral Neugebauer model

Radovan Slavuj, Ludovic G. Coppel, Jon Yngve Hardeberg

The Norwegian Colour and Visual Computing Laboratory, Gjøvik University College, Norway

ABSTRACT

To control printers so that the mixture of inks results in specific colour under defined visual environment requires a spectral reflectance model that estimates reflectance spectra from nominal dot coverage. The topic of this paper is to investigate the dependence of the Yule-Nielsen modified spectral Neugebauer (YNSN) model accuracy on ink amount. It is shown that the performance of the YNSN model strongly depends on the maximum ink amount applied. In a cellular implementation, this limitation mainly occurs for high coverage prints, which impacts on the optimal cell design. Effective coverages derived from both Murray-Davis (MD) and YNSN show large ink spreading. As ink-jet printing is a non-impact printing process, the ink volume deposited per unit area (pixel) is constant, leading to the hypothesis that isolated ink dots have lower thickness that the full-tone ink film. Measured spectral reflectance curves show similar trend, which supports the hypothesis. The reduced accuracy of YNSN can thus be explained with the fact that patches with lower effective coverage have a mean ink thickness very different from that of the full-tone patch. The effect will be stronger for small dot coverage and large dot gain and could partially explain why the Yule-Nielsen *n*-factor is different for different inks. The performance of the YNSN model could be improved with integration of ink thickness variation.

Chapter 8

1. INTRODUCTION

Spectral reflectance models allow predicting reflectance spectra from nominal dot coverage. As printing in general produces a non-linear output to its input signal, the inverse printer models are often not analytically invertible and optimization routines are required to obtain ink amounts that would in return produce a given reflectance. Spectral reflectance models allow predicting reflectance spectra from nominal ink surface coverage. The inverse model, most often based on optimization techniques, allows then determining the different ink coverages that produces the closest spectrum as a specific spectrum, or a specific colour under a defined illuminant, given that this colour is reproducible, i.e. within the printer and substrate gamut. The well-known Yule-Nielsen modified spectral Neugebauer (YNSN) model is one of the most accurate predictive models for the spectral reflectance of printed halftone colours and can also account for different mechanical dot gain depending on ink superposition conditions[1]. The accuracy of the model is further enhanced by dividing the coverage space in different subdomains in which the YNSN is applied, leading to the so-called cellular Yule-Nielsen modified spectral Neugebauer model (cYNSN).

$$R = (\sum_{k=1}^{N} a_k R_k^{1/n})^n \quad (1)$$

where N is the number of all possible ink combinations, or number of Neugebauer primaries (NP), a_k is the effective coverage of NP k, and R_k is the reflectance of the k^{th} NP. For a bi-level (dot or no dot), four colour printer, $N=2^4=16$ while a_k is different for each NP. The Yule-Nielsen (YN) transform introduces a non-linear relationship between the reflectance of a halftone and the reflectance of the substrate and solid ink. However, this model is empirical and it is valid only for one combination of substrate, ink set, halftoning and viewing condition. This is why the n-factor, originally design to account for optical dot gain, accounts for many other factors[2,3]. In addition, the n-factor is often significantly different for different inks[4]. Printing substrates have usually a certain ink limit beyond which the print suffers artifacts such as cockling, bleeding or gloss non-uniformity. As YNSN requires 100% coverage from each ink channel to determine the NPs, this becomes a prominent problem for multichannel printing[5]. To tackle this problem optimal ink limit for the substrate must be set. Ink spreading makes printed dots larger, a phenomenon known as mechanical or physical dot gain while light scattering within substrate optically increase size of the dots (optical dot gain). As a consequence, the relationship between nominal and effective dot coverage is non-linear and effective dot coverage reaches rapidly 100% already at relatively low nominal coverage. Therefore, an ink clipping or channel ink limitation could be applied even for single ink NP.

We show in this work that although the effective coverage does not vary much beyond a given nominal coverage, the spectral reflectance of full-tone patch is yet significantly affected beyond this limit. It should be emphasized that the coverages obtained by optimization with YNSN are effective coverages, that is, for a specific ink, the partial area covered by dots with ink reflectance of the 100% coverage that produces closest spectrum to the measured spectrum. Hence the calculated effective coverages are dependent on the

reflectance of the dots. We notice however that for non-impact printing technology like ink-jet, the volume of ink deposited on the substrate does not depend on the substrate and that larger dots must have smaller thicknesses. We further demonstrate that the dot thickness dependency on coverage introduces a non-linearity that the YN *n*-factor empirically attempts to take into account. The findings lead to a better understanding of the relationship between nominal dot area coverage and measured spectrum. Also, an improved model in which dependence of ink thickness on dot area is proposed.

2. METHOD

To study the influence of the maximum nominal ink coverage on the accuracy of the cYNSN model, single ink patches with 29 nominal coverages ranging from 0 to 1 are printed for all seven independent channels (CMYKRGB) of a multichannel printer. The printer used is a Hewlett-Packard Z3200 ink-jet printer and the substrate is a 9100 semi-matt EFI Offset Proof Paper, chosen for its very low content of fluorescing whitening agents. The patches are pre-halftoned in Matlab at 1200dpi and binary, seven channel Tiff files are sent to the printer through Caldera RIP. The ink limit is set optimal for the substrate and is kept constant so that ink amounts are solely determined by coverage. The spectral reflectance factor of the patches is measured with a X-Rite i1 spectrophotometer with no UV cut-off filter and 45/0 measuring geometry.

Using Eq.(1) with n=1 and N=2, i.e. the Murray-Davis (MD) model, the effective coverage of the patches is determined to get the minimal *rms* between predicted and measured spectral reflectance factor. Two measured NPs are used in this calculation, the unprinted paper white and the maximum nominal coverage patch, one for each ink. From obtained spectral reflectance of the patches, the one closest to the 50% effective dot coverage is chosen as the node of a two-level cellular model. The cYNSN is then calibrated for different maximum nominal coverage $a_{\max}$. The n-factor is then optimized for minimal *rms* in the range of nominal coverage between 0% and $a_{\max.}$ The maximum colour difference between predicted and measured patch is then estimated with ΔE_{00} (D50/2°) and reported as a function of $a_{\max.}$ This describes the accuracy of the cYNSN as the maximum colour difference for different choices of maximum nominal coverage. The simpler YNSN model is tested in the same manner. The reflectance factor of the patches at the different $a_{\max}$ levels is then analyzed and related to the accuracy of the models. The purpose is to discuss the effect of absorption coefficients for pigment based ink-jet inks, indicating a decrease of the dot thickness at lower coverages as compared to full-tone patches.

3. RESULTS AND ANALYSIS

The effective dot coverage calculated with the MD model versus nominal coverage for all seven inks is shown in Figure 1. The results indicate large dot gain, especially with black colour (K) achieving around 90% effective dot coverage at 20% nominal coverage input. Also from Figure 1, it can be seen that no significant change in effective dot coverage occurs after 40% K or 70% M.

Figure 2 shows the maximum ΔE_{00} colour difference as a measure of the YNSN performance in the range from 0% to $a_{\max}$. The results are shown for all seven single ink

channel predictions at five different levels of selected maximum nominal coverages: 100, 95, 90, 85 and 50%.

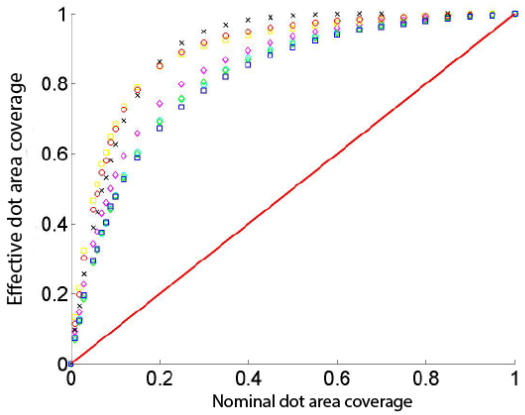

Figure 1. Predicted effective coverage determined with the Murray-Davis model versus nominal coverage for the 7 inks represented with their colours and dot shapes. The straight red line shows a one-to-one relationship. The estimated dot gain reaches 50% effective coverage at around 10% nominal coverage.

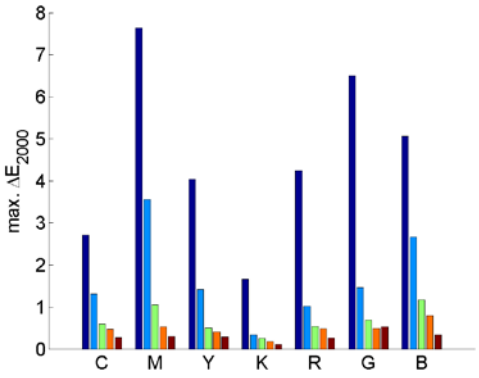

Figure 2. Maximum colour difference between YNSN predicted and measured spectra expressed as ΔE_{00} for different maximum nominal coverages a_{max} (blue 100%, cyan 95%, green 90%, orange 85% and red 50%). a_{max} = 0.5 corresponds to the node of the lower coverages cell in the cYNSN model. The cellular model performs very well in that range. The performance of the YNSN model is strongly dependent on the choice of maximum nominal ink coverage.

The performance of the YNSN is strongly dependent on the choice on maximum nominal coverage or in other words on last calibration point (patch). Using 50% as maximum corresponds to the lower coverage cell of the two-cell cYNSN model. Colour accuracy of that cell is satisfying with a maximum ΔE_{00} for all channels being less than one. The single cell (or classical) YNSN performs fairly well until 90% of maximum nominal coverage where $\Delta E_{00} < 2$, while for 85% is $\Delta E_{00} < 1$. However, using a 100% as maximum point results in large colour differences where e.g. magenta is larger than 7 in ΔE_{00} units. Figure 3 shows the performance of the cYNSN model in the higher coverage cell (50 to 100 % coverage).

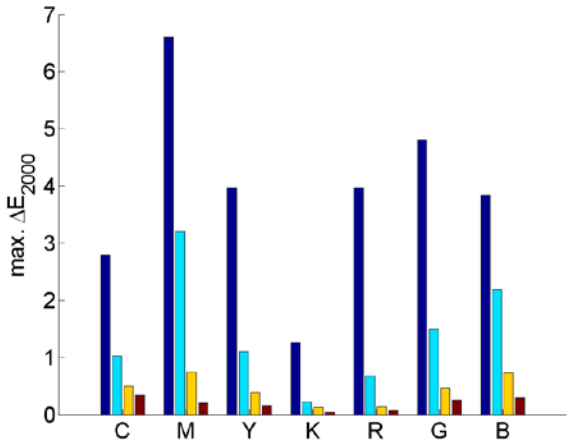

Figure 3: Maximum colour difference between predicted and measured spectra of the high coverage cell in cYNSN expressed as ΔE2000 for different maximum nominal coverages (blue 100%, cyan 95%, yellow 90% and red 85%). The performance of the cellular model is strongly dependent on the choice of maximum nominal ink coverage and is especially low for magenta when using 100% maximum coverage.

As compared to the lower coverage cell in Figure 2, the model performs badly when using 100% as maximum nominal coverage. As for the YNSN model, the performance becomes acceptable when maximum ink coverage is restrained in-between 85% and 90%. Apart from the magenta ink, the maximum ΔE_{00} is also less than 3 when selecting 95% maximum coverage calibration point.

The increase of the performance of the YNSN model when limiting the maximum ink thickness is in fact expected since this corresponds to performing cellular implementation with a cell defined from 0 to maximum coverage but less than 100%. From the results in Figure 2, it can be concluded that a cellular implementation of the YNSN model would perform better when using 85% coverage as intermediate level instead of 50%. Namely, the YNSN would still perform well in low coverage cell while higher coverage cell would certainly perform better than in Figure 3 when limited to coverages between 85% and 100%.

Figure 4 shows the spectral reflectance factor of magenta for different effective coverages. Magenta is selected for further analysis for its highest max. ΔE_{00} error. It can be observed that the reflectance factor drops rapidly to almost zero in the middle wavelength band (corresponds to green region of the electromagnetic spectrum) while it decreases more gradually in the lower wavelength band (blue region). It is evident from the graph that a combination of the 0% and 85% curves is more likely to accurately predict the 50% curve then a combination of the 0% and 100% curves. Visually, magenta ink becomes more reddish with increasing coverage. It is virtually impossible to predict the 50% curve region from 500nm to 600nm as a combination of two nearly flat reflectance curves, no matter how large YN *n*-factor is. On the other hand, similar curves were presented by Yang[8], not for increasing coverage, but for addition of more ink on full-tone patch. In a multilevel (multi-pass) printing mode, where multiple dots can be addressed at given location, similar curves could be expected for different ink levels. In our bi-level printing mode, where the pixels are either dots or no dots, the measured spectral reflectance suggest that the ink thickness depends on the MD predicted effective coverages and thus on nominal coverage. This supports our initial observation on that mechanical dot gain must result in thinner dots since volume of ink deposited by the ink-jet printer is constant and does not depend on the substrate of on ink spreading. Because of the significant ink spreading leading to mechanical dot gain, the ink dots become larger and thinner. This effect is related to the relative and not the absolute dot gain since the dot thickness is proportional to the dot area for constant volume.

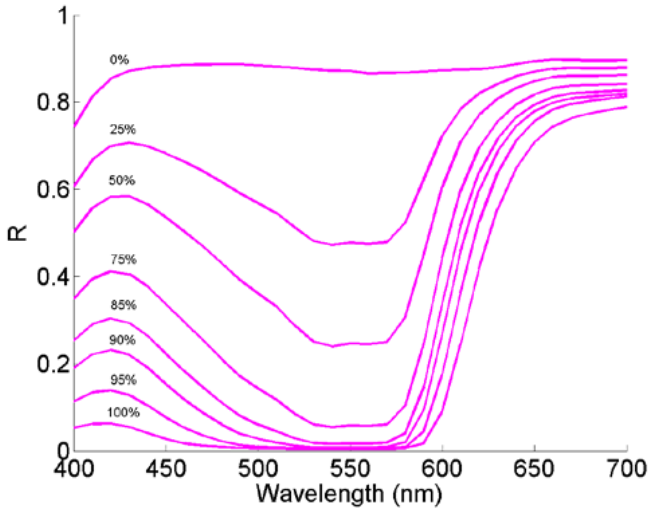

Figure 4: Spectral reflectance factor of the magenta patches at different effective coverages (indicated in the figure). The reflectance factor drops almost to zero at 550 nm already at 85% coverage, while it decreases only gradually in the blue region of the electromagnetic spectrum. Constructing the 50% curve as a combination or the 0% and 100% is not feasible, no matter how large n is, and the performance of the YNSN model is poor if 100% is used as maximum coverage.

Therefore the effect is expected to be the largest at the lower nominal coverages. It is important to remind that the coverages in Figure 4 are the predicted coverages obtained with the MD model and not physical coverages. This rather drastic change of the spectral reflectance properties is due to that the inks are not ideal, in a sense that they are absorbing light in their transparent windows (like blue and red for magenta). This is characteristic for the magenta ink but applies to the other inks as well. Since the Yule-Nielsen *n*-factor is compensating the non-linearity of spectral reflectance, different ink spectral characteristic partially explains why *n*-factor depends on the ink and not only on the substrate.

4. DISCUSSION AND CONCLUSIONS

The results show that the performance of the YNSN model is strongly dependent on the choice of maximum ink coverage, while the model performs very satisfactory when the maximum ink coverage is restrained to around 85-90%, which is almost equivalent to using 100% maximum ink coverage with less ink amount. This implies two things. First, since the ink amount has a significant impact on the performance of the YNSN model it should be reported and discussed when evaluating the model accuracy on a sample set. Second, when using maximum ink coverage and ink amount in our case, a cellular implementation with two cells will perform better with a cell boundary at 85% than at 50%. These results indicate that a cell division based on perceptual spacing of interpolation cells as suggested by Bastani et.al.[7] is not always the optimal choice.

The effective dot coverages derived from both the Murray-Davis and optimized YNSN models show very large dot gain leading to the hypothesis that ink dots have a smaller thickness than full-tone ink film since the ink volume on each pixel is constant. The measured spectral reflectance curves show similar trends to those of ink film with increasing thickness, which supports the hypothesis. The lesser accuracy of the YNSN model when using maximum ink thickness can then be explained with the fact that the patches with lower coverage have a mean ink thickness very different from that of the full ink full-tone patch. This observation implies also that the Yule-Nielsen n-factor is accounting for varying ink thickness that results in non-linear relationships between the spectral reflectance at different ink coverage. This can partially explains why the n-factor is often determined as being different for different inks on the same substrate.

The effect of significant ink spreading on the dot spectral reflectance will be related to the relative and not the absolute dot gain since the dot thickness is proportional to the dot area for constant volume. This means that the effect will be largest when the dots are small and the dot gain large. The analysis presented in this paper suggests that the performance of the YNSN model could be improved by incorporating the change of ink thickness related to the mechanical dot gain in the optimization of the effective coverage and *n*. This can be easily implemented by modifying the spectral reflectance of the ink according to the ink thickness determined as a fraction of full-tone ink thickness that is directly related to the relative dot gain. This requires on the other hand, to predict scattering and absorption coefficient of the inks in order to relate spectral reflectance to ink thickness, in a way similar to that proposed by Yang[6]. This is the subject of ongoing research and evaluation of the enhanced YNSN

model and will be presented in future. Also, other type of substrates/ink combinations will be exercised.

Acknowledgements
This work was supported by the Marie Curie Initial Training Networks (ITN) CP7.0 N-290154 funding. Special thanks to Peter Nussbaum who helped with the work and to Caldera who provided with the RIP.

REFERENCES

[1] Hersch, R. D. and Crété F., "Improving the Yule-Nielsen modified Neugebauer model by dot surface coverages depending on the ink superposition conditions," in SPIE 5667, Colour Imaging X: Processing, Hardcopy, and Applications, 4342005, 434-447., (2005)

[2] Wyble D. R. and Berns R. S., "A critical review of spectral models applied to binary colour printing", Col. Res. Appl. 25(1), 4-19., (2000)

[3] Hébert M., "Yule-Nielsen effect in halftone prints: graphical analysis method and improvement of the Yule-Nielsen transform", Proc. SPIE 9015, 90150R-1-13, (2014)

[4] Rossier, R. and Hersch, R. D., "Ink-dependent n-factors for the Yule-Nielsen modified spectral Neugebauer model", Proc. IS&T 5th conference on colour in Graphics, Imaging and vision, 202-210, (2010)

[5] Slavuj, R., Coppel, L. G., Olen, M. and Hardeberg, J.Y., "Estimating Neugebauer primaries for multi-channel spectral printing modelling", Proc. SPIE 9018. 90180C-1-8, (2014)

[6] Yang, L., "Characterization of inks and ink application for ink-jet printing: model and simulation", J. Opt. Soc. Am. A 20(7), 1149-1154. , (2003)

[7] Bastani, B., Cressman, B. and Shaw, M. , "Sparse Cellular Neugebauer Model for N-ink Printers", in Proc. IS&T/SID Fourth Colour Imaging Conference: Colour Science, Systems and Applications, 58-60., (1996)

Chapter 9

Paper D

Modelling coverage dependent ink thickness in ink-jet printing

Ludovic Gustafsson Coppel, Radovan Slavuj and Jon-Yngve Hardeberg

Submitted to Applied Optics

Chapter 9

Modelling coverage dependent ink thickness in ink-jet printing

Ludovic Gustafsson Coppel, Radovan Slavuj and Jon-Yngve Hardeberg

The Norwegian Colour and Visual Computing Laboratory, Gjøvik University College.

ABSTRACT

We propose a simple extension of the Murray-Davis halftone reflectance model that accounts for the change of ink dot reflectance due to ink spreading. Significant improvement of the prediction accuracy is obtained for a range of paper substrates and printer combinations compared to the classical Yule-Nielsen and Clapper-Yule models. The results show that ink dot thickness dependency is the main factor limiting the validity of the Murray-Davis model and that optical dot gain can be neglected when the model is calibrated for one specific printer, ink and substrate combination. The proposed model provides a better understanding of the reflectance from halftone prints that contributes to the development of physical models for simpler and faster printer calibration to different substrates.

Chapter 9

1. INTRODUCION

The spectral reflectance from halftone prints is the result of the interaction of light with the printed paper. The ink dots deposition over a substrate results in a very complex structure with dot size, shapes and overlaps that depend on the printing process, substrate and inks. The final physical structure is unknown and difficult to model from process parameters, therefore simpler models, calibrated for specific ink sets, printing process, and substrate combination, have been developed. Classical spectral reflectance predictions models are the Murray-Davis [1], the Yule-Nielsen [2], and the Clapper-Yule [3] models, which can be extended to multicolour halftones with the Neugebauer model [4, 5]. These models are regression based [6] and infer apparent surface coverages from the measurement of the spectral reflectance of a limited number of samples (calibration patches). They also all describe the reflectance of a halftone as a combination of the reflectance of the unprinted surface and the reflectance of a fulltone print [7]. Several extensions have been proposed over the years, including a probabilistic treatment of the optical dot gain [8], ink superposition dependent apparent surface coverage [9], surface roughness [10] or fluorescence [11].

The cellular implementation of the classical models, first proposed by Heugebauer et al. [12] in 1992, may provide the best improvement in terms of spectral reflectance prediction, to the cost of an increased number of calibration patches, but it does not provide a better understanding of the reflectance of halftone prints. In all these model extensions, the transmittance of the ink dots is equal to that of the fulltone ink film and does not depend on the dot enlargement due to ink spreading. On the other hand, Emmel and Hersch [13] observed that in inkjet printing, the amount of ink deposited is constant and not dependent of the substrate and of the ink spreading. They proposed a model for ink spreading based on a set of empirical rules describing the ink spreading of ink drops as a function of neighboring dots [14]. Emmel and Hersch used then the Kubelka-Munk theory to compute the transmittance of the dots with different shapes. In this paper, we propose a simpler model that is an extension of the original Murray-Davis (MD) model in which we account for the change of reflectance of the ink dots with ink spreading. In a previous paper [15], we observed that the Yule-Nielsen (YN) model fails to predict the reflectance of halftone patches as a combination of the reflectance from the paper and fulltone patch. We argued that the spectral reflectance of the ink dots at lower nominal coverages must be significantly different to that of the fulltone patch and that this change of ink reflectance cannot be attributed solely to optical dot gain. In contrast to the Emmel and Hersch model, our model is only based on measured spectral reflectance factors. We assume ink dots of constant thickness on top of the substrate but adjust the dot thickness according to the apparent surface coverage. Our model yields much larger dot gain than the MD model and considers halftones, already at moderate nominal coverages, as ink films whose thickness is smaller than the thickness of a fulltone print. We test the model on different substrate and printer combinations, and show that the reflectance of single colorant halftones can be predicted very accurately even when neglecting optical dot gain. The rest of the paper is organized as follows. In Section 2, we describe the classical spectral reflectance prediction models and derive our proposed extension and its parameter estimation method. We compare the prediction of our model to the results obtained with the classical models in Section 3. We discuss the results in Section 4 and underline the impact of ink spreading on the ink reflectance and its implications on the relationship between nominal coverage and

reflectance factor, before concluding and pointing out directions for further research in Section 5.

2. METHOD

2.1 Print samples and measurements

In order to test our model and compare it to the YN and Clapper-Yule (CY) models, we print single ink patches with 29 nominal coverages ranging from 0 to 1 using seven (CMYKRGB) different inks. A range of different paper substrates are used together with a Hewlett Packard Z3200 multichannel printer (HP printer). In addition, an Canon image-PROGRAF iPF6450 (Canon printer) is used with a matte photo paper. The different printer/substrate combinations used are listed in Table 1. In order to maximize the control of the printer, the patches are halftoned with Matlab (The Mathworks, Inc.) using the Iterative Method Controlling the Dot Placement (IMCDP) developed by Gooran [15]. For the HP printer, a 1200 dpi CMYKRGB tiff file is generated and sent to a Caldera (Caldera, Strasbourg, France) Raster Image Processor (RIP) with all colour management features off. For the Canon printer, seven individual bmp files (one for each ink channel) are generated and sent directly to the printer through a custom-made printer driver developed by Voxvil (Voxvil AB, Örnsköldsvik, Sweden). The spectral reflectance factor of the samples printed with the HP printer are measured with a i1Pro spectrophotometer (x-rite, Inc.) with UV-excitation included. One sample is also measured with a similar spectrophotometer equipped with a UV cut-off filter in order to assess the impact of fluorescence on the model accuracy. For the samples printed with the Canon printer, a Spectro LFP spectrophotometer (BARBIERI electronic, Bressanone/Brixen, Italy) is used instead. We report all color difference with ΔE2000 computed from the measured and predicted $L*a*b*$ values under a D50 illuminant and for a 2◦ observer.

Table 1. List of paper substrates used with the two printers.

Printer	Paper
HP	HP Premium Gloss Photo Paper
HP	Mondi colour copy,100 g/m^2
HP	9100 semi-matt EFI Offset Proof Paper
HP	HP Premium Instant-dry Satin Photo Paper
HP	HP Heavyweight Coated Paper
Canon	Canon Matte Photo Paper MP-101

2.2 Spectral reflectance prediction model

The simplest way to predict the reflectance of a halftone print is to calculate the weighted average of all areas of the prints. For a one-colourant print this is described with the Murray-Davis (MD) formula [1],

$$R_{\mathbf{MD}}(\lambda) = a^{\mathrm{app}} R_{\mathrm{i}}(\lambda) + (1 - a^{\mathrm{app}}) R_{\mathrm{s}}(\lambda)\,, \tag{1}$$

where a^{app} is the apparent ink coverage, $R_{\mathrm{i}}(\lambda)$ is the reflectance factor of full tone ink, and $R_{\mathrm{s}}(\lambda)$ is the reflectance factor of the bare substrate. Equation (1) does not generally predict well the spectral reflectance factor of halftones. Due to the lateral light propagation within the substrate, part of the light incident on the substrate at the proximity of an ink dot is absorbed by the ink after being reflected from the substrate. This shadowing effect, known as optical dot gain or Yule-Nielsen effect makes the ink dot appear larger than their physical size. Yule and Nielsen [2] proposed an empirical model to account for the nonlinear relationship between the reflectance factor and the apparent coverage. The YN model expresses the spectral reflectance raised to the power $1/n$ as a linear combination of the spectral reflectance of the Neugebauer primaries (NP) raised to the power $1/n$ as

$$R_{\mathbf{YN}}(\lambda) = \left[a^{\mathrm{app}} R_{\mathrm{i}}(\lambda)^{1/n} + (1 - a^{\mathrm{app}}) R_{\mathrm{s}}(\lambda)^{1/n}\right]^{n}, \tag{2}$$

where n is the so-called Yule-Nielsen factor. The n factor is determined by minimizing the color difference (ΔE_{2000}) between the reflectance factor obtained with Eq. (2) and the measured reflectance factor R(λ). Another classical spectral reflectance prediction model is the CY model [3], which considers the multiple internal reflections occurring at the air-print and air- substrate surface boundaries. For a single colorant patch, the CY equation can be written as [16]

$$R_{\mathbf{CY}}(\lambda) = K r_{\mathrm{s}} + \frac{(1-r_{\mathrm{s}})(1-r_{\mathrm{i}}) R_S^*(\lambda)(1-a^{\mathrm{app}}+a^{\mathrm{app}} t(\lambda))^2}{1-R_S^*(\lambda) r_{\mathrm{i}} - (1-a^{\mathrm{app}}+a^{\mathrm{app}} t(\lambda)^2)}, \tag{3}$$

where rs is the surface reflectance at the air-paper interface, ri is the inner reflectance at the same boundary, t(λ) is the transmittance of the ink dots, Ks(λ) is the amount of surface reflection that reaches the detector, and $R_s^*(\lambda)$ is the intrinsic reflectance of the substrate (without surface reflection correction). For a 45/0 measurement geometry and for a refractive index of the ink and substrate equal to 1.5, $r_s = 0.05$ and $r_i = 0.6$, assuming that the light reflected from the substrate is Lambertian [17]. $R_s^*(\lambda)$ and t(λ) are obtained by inverting Eq. (3) with $a^{app} = 0$ and $a^{app} = 1$, respectively.

We introduce here a new model of the form

$$R_{\mathbf{NEW}}(\lambda) = a^{\mathrm{app}} R_{\mathrm{i}}(\lambda, a^{\mathrm{app}}) + (1 - a^{\mathrm{app}}) R_{\mathrm{s}}(\lambda), \tag{4}$$

where the ink reflectance $R_{\mathrm{i}}(\lambda, a^{\mathrm{app}})$ does not only depend on wavelength but also on the apparent coverage a^{app}. This model can be seen as an extension of the MD formula in which we account for variation in the ink dot reflectance with apparent coverage. This extensions differs from earlier extensions such as the one from Arney et al. [18] in which both R_{i} and R_{s} varying with coverage due to optical dot gain. Instead, $R_{\mathrm{i}}(\lambda, a^{\mathrm{app}})$ is here assumed to vary due to ink thickness variations and optical dot gain is neglected, leaving $R_{\mathrm{s}}(\lambda)$ unaffected. Our assumption relies on the fact that in inkjet printing, the volume of ink deposited on the substrate is independent of the substrate. Assuming further a constant thickness of the dried ink's dots, we can easily relate the apparent dot thickness d^{app} to the apparent a^{app} and nominal coverage a^{nom} as

$$d^{\mathrm{app}} = \frac{a^{\mathrm{app}}}{a^{\mathrm{nom}}} d_{\max} \ , \tag{5}$$

where $d_{\max}$ is the thickness at maximum nominal coverage. Neglecting scattering in inks, the intrinsic transmittance $T_{\mathrm{i}}^{*}(\lambda)$ of the ink dots reads

$$T_{\mathrm{i}}^{*}(\lambda) = e^{-K(\lambda)d^{app}} \tag{6}$$

where $K(\lambda)$ is the absorption coefficient. We obtain then the reflectance of the ink dot on top of the substrate with

$$R_i' = [T_i^{*}(\lambda)]^2 \, R_s^{*}(\lambda) \tag{7}$$

where $R_s^{*}(\lambda)$ is the intrinsic substrate reflectance obtained by inverting Eq. (3). We finally apply the Saunderson's correction [19] to account for the reflection at the air-ink boundary in the same manner as in the CY model [Eq. (3)]. This yields the reflectance factor of the ink dot as function of the dot thickness

$$R_{\mathrm{i}}'(\lambda, a^{app}) = K_s(\lambda) + \frac{(1-r_s)(1-r_i)R_i'}{1-r_i R_i'(\lambda)}. \tag{8}$$

In order to calibrate the model, we need to determine the absorption coefficient K and the surface parameter Ks of the inks. The maximum ink thickness $d_{\max}$ is unknown but Eq. (6) can be rewritten as function of $K(\lambda)\, d_{\max}$, and $d^{\mathrm{app}}/\, d_{\max}$, which can be obtained from Eq. (5). Hence we only need to determine $K(\lambda)d_{\max}$. The surface reflection parameter $K\mathrm{s}(\lambda)$ is assumed to be the same for the substrate and the ink, but dependent on the substrate. Glossy substrates are expected to reflect less light towards the detector than matte substrate and $K\mathrm{s}(\lambda)$ is here first estimated as the reflectance of the fulltone black patch, which is assumed to absorb all light transmitted by the top surface. Since different inks may yield different gloss levels we rewrite $K\mathrm{s}(\lambda)$ as

$$K_s(\lambda) = \alpha_i K_s^{K}(\lambda) \tag{9}$$

where $K_s^{K}$is the measured reflectance factor of the full tone black ink, and α_{i} is a coefficient for each of the six other inks. αi and $K(\lambda)\, d_{\max}$ are determined by minimizing the color error between the predicted Ri $(\lambda, 1)$, obtained from Eqs. (5- 8) with $a^{\mathrm{app}} = 1$, and the measured reflectance of the full coverage patches at different ink film thickness. For all the printer/ink/substrate combinations in this study, we use all patches with nominal coverage larger than 0.2 for the estimation of $K(\lambda)\, d_{\max}$. This means that we assume, based on the total dot gain curves, that all patches with nominal coverage larger than 0.2 are fulltone with different ink film thickness and not halftones looking as fulltone because of the optical dot gain. Once $K(\lambda)\, d_{\max}$ and $K\mathrm{s}(\lambda)$ are determined, we can estimate the apparent coverages at lower nominal coverages by minimizing the color error between predicted [Eq. (4)] and measured halftone patch reflectance factor.

In this model, optical dot gain is neglected. However, a transformation similar to the Yule-Nielsen model can be applied on Eq. (4). Another approach, which then considers

complete lateral diffusion of the light within the substrate, is to modify the CY model [Eq. (3)] to account for the change of the ink dot transmittance due to ink spreading. This is easily done by applying T_i^*, obtained from Eq. (6) instead of the coverage independent transmittance t in Eq. (3). This model is referred to as R_{CY}^{NEW}.

3. RESULTS AND ANALYSIS

The estimated αi coefficients of the inks on the different substrates are given in Table 2. The parameter estimation calculations showed that only the red and blue inks have a significantly different surface reflection than the other inks therefore αi is reported only for those two inks. Also the red and blue inks appeared to have very similar optimum αi irrespective of the substrate. For the other inks (CMYKG), αi was set to 1. A special case is the copy paper substrate on which black could not be printed with full coverage without severe bleeding. For this substrate, we use $K_S(\lambda) = r_S$, assuming a wavelength independent Lambertian reflection from the matte surface.

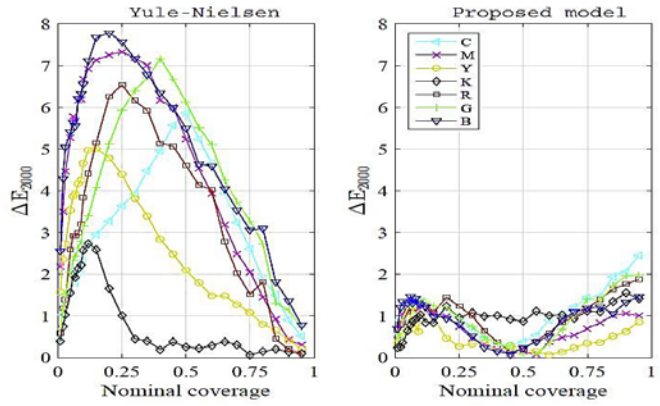

Figure 1. Color difference between predicted and measured spectral reflectance of the halftone patches printed with the HP printer on the Photo paper with the Yule-Nielsen model (left) and the proposed R_{CY}^{NEW} model (right). The n factor is optimized for each coverage and each ink for the YN model.

Figure 1 shows the color difference between predicted and measured spectral reflectance versus nominal coverage of the single colorant halftone patches, for the YN model and the proposed *MD*NEW model (HP printer and Photo Paper). The Yule- Nielsen model yields unacceptably large errors with up to 6- 8 ΔE_{2000} for the chromatic inks. The proposed model on the other hand leads to significantly lower errors, with almost all patches below 1.5 ΔE_{2000}. Similar results are obtained for all tested printer and substrate combinations, except for the Copy paper, as summarized in Table 2. This Copy paper substrate is the only one that is not optimized for the printer it is used with and leads to significant bleeding, ink penetration and uneven patches, especially for the black ink that was finally not printed and thus not included in the evaluation. For the Canon printer, used only with one substrate, the proposed model performs even better with a maximum ΔE_{2000} of 1.2, compared to a

maximum ΔE_{2000} of 5.5 when using the YN model (Fig. 2). As shown in Table 2, the CY model performs even worse than the YN model. However, when modelling coverage dependent ink thickness, CYNEW performs as well as the proposed MDNEW model even though the proposed model performs slightly better.

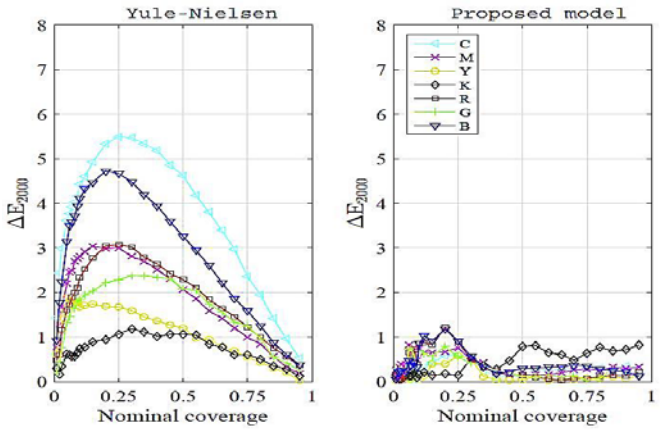

Fig. 2. Color difference between predicted and measured spectral reflectance of the halftone patches printed with the Canon printer on the MP100 paper with the Yule-Nielsen model (left) and the proposed RNEW MD model (right). The n factor is optimized for each coverage and each ink for the YN model.

Table 2. Surface reflection coefficient αi for red and blue inks, mean and maximum color difference between predicted and measured spectral reflectance of the halftone patches (all 7 single colorant ramps except for the Copy case, which is without black) for the different printer and paper combinations, as obtained with the Yule-Nielsen model, the Clapper-Yule model, and the proposed models.

Printer/Paper	$\alpha_{R/B}$	Mean ΔE_{2000}				Max ΔE_{2000}			
		YN	CY	CY^{NEW}	MD^{NEW}	YN	CY	CY^{NEW}	MD^{NEW}
HP/Photo	0.5	3.3	4.8	1.1	0.9	7.8	17.7	4.6	2.6
HP/Copy	-	2.1	2.6	2.2	2.2	5.5	8.0	8.8	6.5
HP/Proof	0.3	2.6	4.4	0.7	0.6	8.1	15.7	2.4	1.6
HP/Satin	0.7	2.8	4.8	0.7	0.6	8.1	17.5	2.8	2.7
HP/HeavyWeight	0.5	3.7	4.3	0.8	0.9	9.9	15.0	3.9	3.5
HP/HW no UV	0.6	3.8	4.4	0.7	0.7	10.0	15.0	3.6	3.1
Canon/MP-100	0.7	2.0	2.5	0.4	0.3	5.5	8.2	1.2	1.2

Figure 3 shows the measured and predicted spectral reflectance factor for three nominal coverages and the spectral reflectance factor of the unprinted paper and fulltone patches, for magenta inks. For the HP printer and Photo Paper, the spectral reflectance factor of magenta drops rapidly to almost zero in the middle wavelength band as the nominal coverage increases, while it decreases more gradually in the lower wavelength band (blue region). Visually, magenta patches become more reddish with increasing nominal coverage. As already reported by Slavuj et al. [14], the YN model fails to predict the reflectance of the halftone patches from the reflectance of the paper and of the fulltone patch. From Fig. 3 (left), it is evident that the halftone reflectance region in the range from 500 nm to 600 nm cannot be predicted as a combination of two nearly flat reflectance curves, no matter how large the YN n factor is. On the other hand, the proposed model yields much better spectral prediction, although it is just the weighted average of the ink dots' and of the paper's reflectance. However, the reflectance of the ink dots is no longer equal to that of the fulltone patch and is instead determined by the extent of ink spreading (or mechanical dot gain). Figure 4 shows the estimated spectral reflectance factor of the magenta ink dots printed with the HP printer in the Photo Paper at 27 nominal coverages. The estimated reflectance of the ink dots changes drastically with nominal ink coverage. In our proposed model, large mechanical dot gain leads to thinner ink dots with significantly higher reflectance than the reflectance of the fulltone patch. When we then take the weighted average of the ink dots' and paper's reflectance, we obtain a good prediction of the halftone patch's reflectance, as shown in Fig. 3 for magenta on Photo Paper. At 0.2 nominal coverage, the apparent coverage is 1 meaning that all dots merge into an ink film whose thickness is according to our model proportional to the nominal coverage.

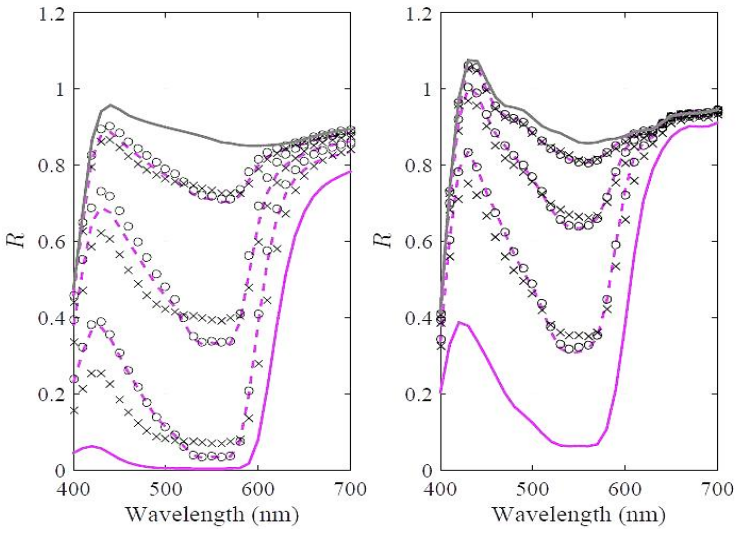

Figure 3. Measured (lines) of the paper and 100% coverage patch (solid) and predicted spectral reflectance factor of magenta patches at 0.01, 0.05 and 0.2 nominal coverage with

the Yule- Nielsen model (crosses) and with the proposed model (circles). HP printer on the Photo paper (left) and Canon printer on the MP-100 paper (right).

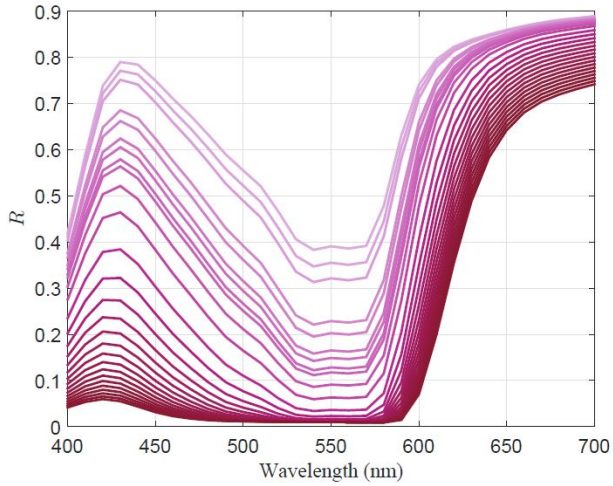

Figure 4. Estimated spectral reflectance factors of the ink dots for the magenta patches printed with HP on Photo Paper at 27 nominal coverages. At lower nominal coverages, the reflectance of the ink dots is much larger than that of the fulltone ink patch, because the dots are much thinner than the fulltone ink film.

This predicted spectral reflectance factor fits very well the measured one (Fig. 5). Similar curves are obtained for the other printer/ink/substrate combinations.

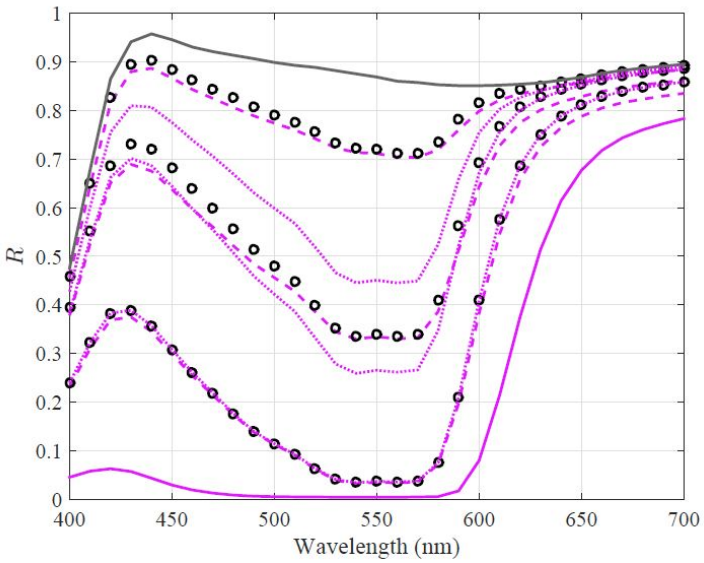

Figure 5. Measured and predicted spectral reflectance factor of the magenta patches as in Figure 4, with the corresponding estimated ink dot reflectances at 0.01, 0.05 and 0.2 nominal coverage (dotted lines). The predicted spectra is the weighted average of the paper (grey line) and ink dot (dashed) spectra. At 0.2 nominal coverage, the estimated apparent coverage is 1 and the reflectance of the patch is that of the ink dots (or ink film).

Figure 6 shows the estimated apparent absorption coefficient of the cyan ink inks for the different printer/substrate combinations, as obtained with the MDNEW model. Figure 7 shows the apparent absorption of the green ink. For all inks, the apparent absorption coefficient depends not only on the printer (i.e. the actual inks used) but also on the substrate.

Figure 8 compares the estimated apparent dot gain, reported as the difference between apparent coverage and nominal coverage, obtained with the YN model and the proposed model for the Photo Paper. Figure 9 compares the cyan dot gain for the different printer/substrate combinations. It is clear that the proposed model leads to much larger apparent dot gain.

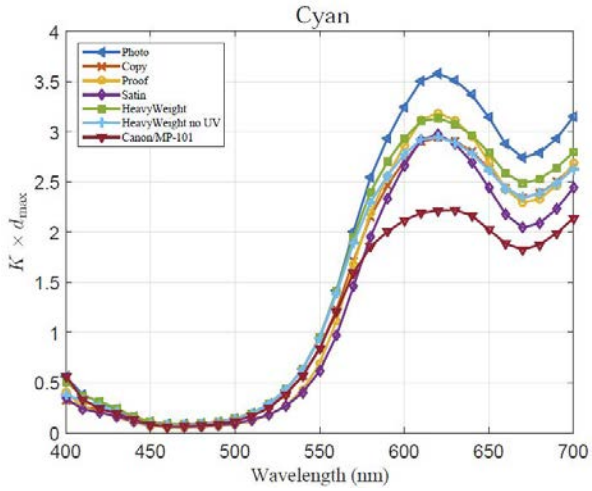

Fig. 6. Estimated absorption coefficients of the cyan ink for the different printer/substrate combinations.

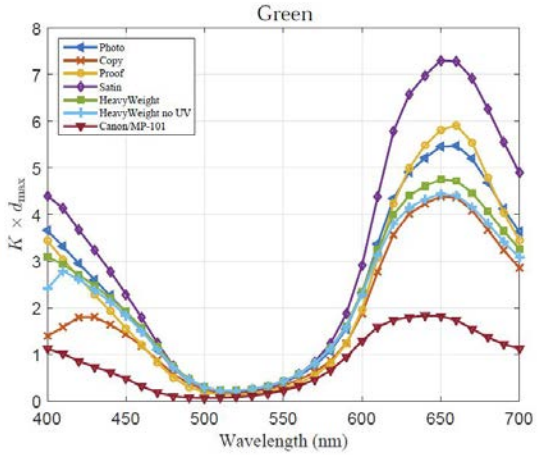

Fig. 7. Estimated absorption coefficients of the green ink for the different printer/substrate combinations.

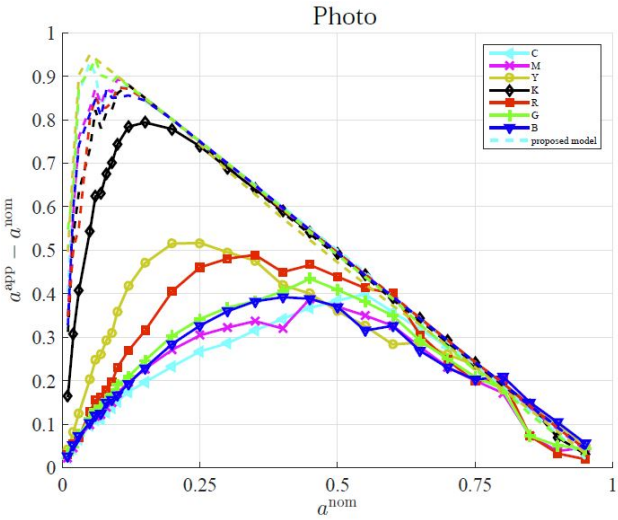

Figure 8. Apparent dot gain estimated on the Photo Paper. Solid lines stand for the Yule-Nielsen model and dashed lines for the proposed model with coverage dependent ink thickness.

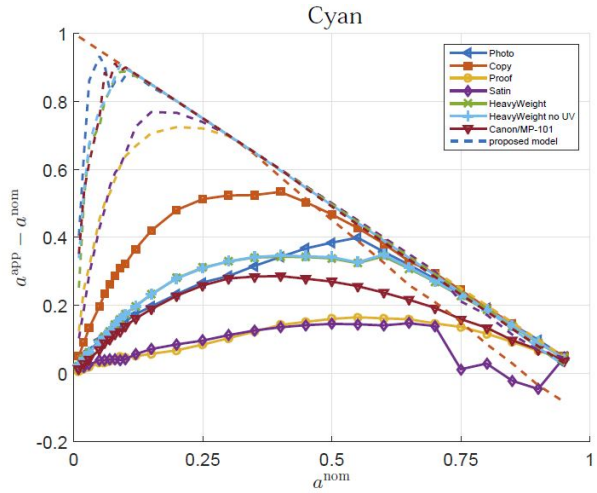

Figure 9. Apparent dot gain estimated for Cyan for all printer/substrate combinations. Solid lines stand for the Yule- Nielsen model and dashed lines for the proposed model with coverage dependent ink thickness.

4. DISCUSSION

The proposed model is a simple extension of the Murray-Davis (MD) model where the reflectance of the inks dots is estimated from their thickness. The thickness of the dots is directly related to the difference between apparent coverage and nominal coverage, since a dot that gets twice as large needs to be half as high in order to keep ink volume constant. At a given nominal coverage, complete ink spreading occurs and the halftone is modelled as an ink film whose thickness is proportional to the nominal coverage. This model leads to a drastic increase of the prediction accuracy, when compared to the Yule-Nielsen (YN) and the Clapper-Yule (CY) models. The accuracy improvement is the largest for light- and mid-tones (Fig. 2), where the estimated apparent dot gain with the YN and the proposed model differ the most (Fig. 9). The YN model performs nevertheless better than the proposed model for the Copy paper substrate. This substrate leads however to a strong ink penetration, which deviates far from our assumption of ink dots spreading on top of the substrate. The difference in (total) apparent dot gain can partly be explained by the fact that our model neglects optical dot gain. On the other hand, the YN model assumes constant ink thickness and in case the ink film is thinner, the apparent coverage needs to be reduced in order to compensate for erroneously large absorption by the ink dots. As shown in Fig. (3), the shape of the reflectance spectrum of halftone patches can be very different to that of the bare paper and fulltone patch. As exemplified in Fig. (4), the effect of ink thickness reduction on the shape of the spectra is much more important the effect of optical dot gain modelled by the YN non-linear transform. The good accuracy obtained with our model suggests therefore that the main factor is a dependency of ink dot thickness on nominal coverage, rather than optical dot gain. This can also explain why the YN n values as well as the light diffusion probability in probabilistic models can be unexpectedly large [20]. We also applied a YN transform on top of our model in Eq. (4). Increasing n leads as expected to

smaller apparent coverages, but has not a significant impact on the color prediction accuracy. The same applies to our modified CY model in which total diffuseness within the substrate leads to smaller apparent coverages with comparable color accuracy. These results indicate that our model cannot separate the contribution of optical dot gain from that of mechanical dot gain. Thus, estimating the optical dot gain would require another method [21]. On the other hand, very good prediction accuracy is obtained when neglected optical dot gain, even though the estimated apparent surface coverages are most likely overestimated with our method. The proposed model is calibrated by estimating the absorption coefficient and the dot gain curves (Fig. 9). The model requires at least two patches at different nominal coverages that can be considered as ink films (maximum ink spreading). In the present study, we assume that the dot gain is maximum from 0.2 nominal ink coverage. The results in Fig. 9 show that the estimated dot gain is already at maximum for lower nominal coverage for some ink/substrate combinations, but also that some other ink/substrate combinations seems to show less dot gain. This implies that different optimum ranges of nominal coverages may be needed for estimating the coefficients of different inks when printed on different substrates. The apparent absorption coefficients are dependent not only on the printer (i.e. the actual inks used) but also on the substrate. This can be explained by different extent of ink penetration into the substrate as discussed for instance by Yang [22, 23] while our model assumes ink dots and films on top of the substrate. The complex interaction between ink and substrate is however beyond the scope of this article and our model relies therefore on estimating these coefficients for each ink/substrate combination. Moreover, substrate dependent absorption coefficient should not be estimated from the reflectance of fulltones with different thicknesses obtained by printing multiple fulltone on top of each other.

5. CONCLUSIONS AND FURTHER WORK

We propose a simple extension of the Murray-Davis model for halftone reflectance in which we account for the change of the reflectance of the ink dots due to ink spreading and neglect optical dot gain. The model yields a significant improvement of the prediction accuracy compared to the classical Yule-Nielsen and Clapper-Yule models for several paper substrates and printer combinations. Our analysis show that a reduction of ink dot thickness and optical dot gain have comparable effect on the spectral reflectance therefore these two factors cannot be separated using the model. However, dot thickness reduction due to ink spreading is the major factor and since it can compensate for optical dot gain the latter can be neglected when the model is calibrated for one specific printer, ink and substrate combination. On the contrary, models neglecting dot thickness variation cannot predict accurately the reflectance of halftones as a combination of the reflectance of the bare paper and fulltone reflectances.

Extension to multicolour halftones will require estimating the reflectance of the overlap of ink dots of varying thickness as these cannot be measured from their fulltone counterparts (the Neugebauer primaries) due to different ink thickness. This could be done by modelling the reflectance of ink mixture [24] with the respective ink thicknesses.

Acknowledgements

This work was supported by the Marie Curie Initial Training Networks (ITN) CP7.0 N-290154 funding. We thank Paula Zitinski Elias at Linköping University, Sweden, for the

samples and measurements of the paper printed with the Canon printer, and Caldera for providing us with the RIP software.

REFERENCES

[1] A. Murray, "Monochrome reproduction in photoengraving," J. Franklin Inst., vol. 221, no. 1936, pp. 721–744, 1936.

[2] J. A. C. Yule and W. J. Nielsen, "The penetration of light into paper and its effect on halftone reproduction," in Proc. TAGA 3, 1951, pp. 65–67.

[3] F. R. Clapper and J. A. C. Yule, "The Effect of Multiple Internal Reflections on the Densities of Half-tone Prints on Paper *," J. Opt. Soc. Am., vol. 43, no. 7, pp. 600–603, 1953.

[4] H. E. J. Neugebauer, "Die Theoretischen Grundlagen des Mehrfarbenbuchdrucks," Zeirschrift für wissenschaftliche Photogr., vol. 36, no. 4, pp. 73–79, 1937.

[5] D. Wyble and A. Kraushaar, "The theoretical basis of multicolour letterpress printing, Hans E. J. Neugebauer," Colour Res. Appl., vol. 30, no. 5, pp. 322–331, 2005.

[6] D. R. Wyble and R. S. Berns, "A Critical Review of Spectral Models Applied to Binary Colour Printing," 1999.

[7] M. Hébert and R. D. Hersch, "Review of spectral reflectance models for halftone prints: Principles, Calibration, and prediction accuracy," Colour Res. Appl., vol. 40, no. 4, pp. 383–397, Jun. 2014.

[8] L. Yang, "Probabilistic spectral model of colour halftone incorporating substrate fluorescence and interface reflections," J. Opt. Soc. Am. A, vol. 27, no. 10, pp. 2115–2112, 2010.

[9] R. D. Hersch and F. Crété, "Improving the Yule-Nielsen modified spectral Neugebauer model by dot surface coverages depending on the ink superposition conditions," in IS&T/SPIE Electronic Imaging Symposium, Vol. 5667, 2005, vol. 5667, pp. 434–445.

[10] M. Hébert and R. D. Hersch, "Extending the Clapper-Yule model to rough printing supports," JOSA A, vol. 22, no. 9, pp. 1952–1967, 2005.

[11] R. D. Hersch, "Spectral Neugebauer-based colour halftone prediction model accounting for paper fluorescence.," Appl. Opt., vol. 53, no. 24, pp. 5380–90, Aug. 2014.

[12] K. Heuberger, Z. M. Jing, and S. Persiev, "Color transformations and lookup tables," in "Proceedings of the 18th conference of the Technical Association of the Graphics Arts" (TAGA, 1992), pp. 863–881.

[13] P. Emmel and R. D. Hersch, "A Unified Model for Colour Prediction of Halftoned Prints," J. Imaging Sci. Tech., vol. 44, no. 4, pp. 351–360, 2000.

[14] P. Emmel and R. D. Hersch, "Modeling ink spreading for color prediction," J. Imaging Sci. Tech. **46**, 237–246 (2002).

[15] R. Slavuj, L. G. Coppel, and J. Y. Hardeberg, "Effect of ink spreading and ink amount on the accuracy of the Yule-Nielsen modified spectral Neugebauer model," in Proc. I&T/SPIE Electronic Imaging, 2015, vol. 9395, p. 93950E–93950E–6.

[16] R. D. Hersch, M. Brichon, T. Bugnon, P. Amrhyn, F. Crété, S. Mourad, H. Janser, Y. Jiang, and M. Riepenhoff, "Deducing ink thickness variations by a spectral prediction model," Colour Res. Appl., vol. 34, no. 6, pp. 432–442, Dec. 2009.

[17] M. Hébert, R. D. Hersch, and P. Emmel, "Fundamentals of Optics and Radiometry for Colour Reproduction," in Handbook of Digital Imaging, M. Kriss, Ed. Chichester, UK: John Wiley & Sons, Ltd, 2015.

[18] J. S. Arney, P. G. Engeldrum, and H. Zeng, "An expanded Murray-Davies model of tone reproduction in halftone imaging," J. imaging Sci. Technol., vol. 39, no. 6, pp. 502–508, 1995.

[19] J. L. Saunderson, "Calculation of the color of pigmented plastics," J. Opt. Soc. Am. 32, 727–729 (1942).

[20] L. G. Coppel, "Dot gain analysis from probabilistic spectral modelling of colour halftone," in "Advanced in Printing and Media Technology, vol 41," , M. Lovreˇcek and N. Enlund, eds. (IARIGAI, 2014), pp. 13–18.

[21] M. Namedanian, L. G. Coppel, M. Neuman, S. Gooran, P. Edström, and P. Kolseth, "Analysis of Optical and Physical Dot Gain by Microscale Image Histogram and Modulation Transfer Functions," J. Imaging Sci. Tech. 57, 20501–20504 (2013).

[22] L. Yang, S. Gooran, and B. Kruse, "Simulation of Optical Dot Gain in Multichromatic Tone Reproduction," J. Imaging Sci. Tech. 45, 198–204 (2001).

[23] L. Yang, "Ink-paper interaction - a study in ink-jet color reproduction," Ph.D. thesis, Linköping Universisty, Sweden (2003).

[24] R. Slavuj, L. G. Coppel, M. Olen, and J. Y. Hardeberg, "Estimating neugebauer primaries for multi-channel spectral printing modeling," Proc. SPIE 9018, 90180C (2014).

Chapter 10

Paper E

Multichannel DBS halftoning for improved texture quality

Radovan Slavuj, Marius Pedersen

Published in

Proceedings of

SPIE Electronic Imaging

(Colour Imaging XX: Displaying, Processing, Hardcopy, and Applications)

Vol. 9395,

Pages 93950I

San Francisco, USA, 2015.

Chapter 10

Multichannel DBS halftoning for improved texture quality

Radovan Slavuj, Marius Pedersen

The Norwegian Colour and Visual Computing Laboratory, Gjøvik University College, Norway

ABSTRACT

The paper aims to develop a method for multichannel halftoning based on the Direct Binary Search (DBS) algorithm. We integrate specifics and benefits of multichannel printing into the halftoning method in order to further improve texture quality of DBS and to create halftoning that would suit for multichannel printing. Originally, multichannel printing is developed for an extended colour gamut, at the same time additional channels can help to improve individual and combined texture of colour halftoning. It does so in a similar manner to the introduction of the light colours (diluted inks) in printing. Namely, if one observes Red, Green and Blue inks as the light version of the M+Y, C+Y, C+M combinations, the visibility of the unwanted halftoning textures can be reduced. Analogy can be extent to any number of ink combinations, or Neugebauer Primaries (NPs) as the alternative building blocks. The extended variability of printing spatially distributed NPs could provide many practical solution and improvements in colour accuracy, image quality, and could enable spectral printing. This could be done by selection of NPs per dot area location based on the constraint of the desired reproduction. Replacement with brighter NP at the location could induce a colour difference where a tradeoff between image quality and colour accuracy is created. With multichannel enabled DBS haftoning, we are able to reduce visibility of the textures, to provide better rendering of transitions, especially in mid and dark tones.

Chapter 10

1. INTRODUCTION

There have been limited halftoning algorithms that are specific to multichannel printing. The question raised is: what could be a goal of multichannel halftoning? One idea is that multichannel halftoning should accommodate up to 7 channels per area by defining different angles for additional colourants [1]. However, majority of printing substrates and mixing of more than four inks leads to the level of saturation above which the outcome is not predictable. The substrates get saturated at 300% ink limit and the same stands for inks. Mixing more than this amount of ink does not lead to any change [2] and only artifacts, such as ink bleeding, are expected. This fact needs to be integrated into optimization of the multichannel printer models where in theory one should be able to have mixture of any possible ink combinations. Many authors appreciate this fact [3, 4] and one common solution is to have either estimation of the non-printable ink combinations or to restrict combination to four inks. More probable goal of multichannel halftoning then becomes a spatial distribution of various ink combinations of up to four colours. To enable better spectral reproduction, all possible channel combinations should be possible to print even though some combinations would not normally be printed, (e.g. RGBK).

On the other hand multichannel halftoning could utilize extra channels (e.g. secondary and complementary colours) in replacement of two or three colour overprints in order to reduce visibility of the texture. On this assumption we define two goals: to create method of halftoning based on DBS that works in multichannel environment and to improve quality of colour DBS by controlling texture quality and visibility of the pattern. DBS halftoning is selected for its state of the art quality of the textures.

In essence, the method proposed in this work could be utilized in a reproduction framework where goals and decisions are not primarily based on colour accuracy. Rather, it should be a tradeoff between colour accuracy and image quality. The paper starts with a background of halftoning and its differences with colour management paradigm. In Section 2 we introduce proposed method of multichannel DBS halftoning. With multiple channels we try reduce visibility of the texture, one of the main concerns of any haftoning. It should be noted here that we are not attempting to improve texture quality by modifying spatial distribution of dots, but through post-processing that aims to reduce brightness of the textures. Therefore, in Section 3, we present both objective and subjective evaluation of the texture quality. In Section 4 we conclude that by using multiple channels it is possible to improve texture quality on the expense of colour difference and we introduce further work.

1.1 Background

The human eye cannot differentiate between individual points with resolution of 60 L\cm = 150 LPI (0,167mm dot size) [5]. It integrates over the surface and if the dots are fine enough, the eye would not be able to differentiate the halftone image from continuous tone. Therefore, halftoning is used to render continuous-tone images with output devices that are capable of printing only two or a small number of different gray levels. Halftoning algorithms perform by generating a high spatial frequency pattern of that is not well

resolved by the human observer at normal viewing distances. To simulate transitions from light to mid-tone one can vary the size of binary dot or the frequency of dot placement at particular place. The former correspond to AM (Amplitude Modulated) raster and latter to FM (frequency modulated). The FM screening is also called stochastic screening due to random distribution of the dots. There is also a possibility to combine AM and FM halfoning to hybrid approach. In this case, part of the image with dark and light areas would be halftoned using AM raster, while mid-tone would be covered with FM halftones. To produce a good colour halftone one has to place coloured dots so that the following specifications are optimally met [6]:

- The dot placement pattern is visually unnoticeable.
- The local average colour is the desired colour.
- The colours used reduce the notice-ability of the pattern.

The behavior of the printer almost always deviates from what is assumed. The dot placement is not ideal, which leads to unwanted dot overlaps. Addition to that is a physical (mechanical) dot gain which is a function of printing technology and the type of haltoning (AM vs FM) [7]. Dot gain is random individual dot increase in size and comes as a result of interaction between colourant and surface. By having small isolated dots, FM halftone structure is more prone to dot-gain and is not the same for all colourants. Once the dot overlaps occur, the additive law does not stand in all cases. This is mostly due to the level of ink saturation for a substrate. Colour halftoning algorithms that do not account for dot enlargements suffer from incorrect colour reproduction. A common solution is to apply a tone correction LUT directly on the continuous tone image to pre-compensate for dot gain. Another solution is to use a model (or an ICC profile) to compensate for this before the final ink amounts are determined. Additinaly, dot gain is dependable whether the dot is printed directly on the paper or superimposed with other colour dot [8].

All unwanted overlaps (or any overlaps for that matter) will yield a darker tone on the place of overlap. Necessarily, this would reduce the gradation in dark areas which is particularly important for some application areas like fine art printing[9]. Gray Component Replacement (GCR) is another strategy used in printing that further reduced variability in dark region. Multichannel printing (e.g. CMYKRGB) can achieve “rich blacks” by various combinations of three or four inks. Therefore, to achieve gradation and variability in dark region, an approach similar to one used with light colours can be applied. The most noticeable result of using light cyan and light magenta inks is the removal of a distinct and harsh halftoning dot appearance that appears in prints that use diluted solutions of cyan and magenta on top of the CMYK ink configuration. Usually, when printing a dark colour the printer will saturate the area with ink dots, but will use fewer ink dots to create the effect of a light colour. However, the individual cyan and magenta ink dots will stand out in a sparse pattern due to their darker colour against a white background; the result is undesirable when it is noticed. By using light cyan or magenta, the printer can saturate areas that would typically use halftoning with these inks to remove the look of sparse magenta and cyan dots. Therefore, the higher the contrast of the ink dots with the subst

the greater is the chance of the colour pattern detection. This is one of the reasons why Yellow is somewhat disregarded in both AM and FM halftoning.

In general, there are two common situations that drive the need for extra colours (addition to CMYK). The first is when high density saturated colour is needed to be reproduced, such as rich reds, orange and clear green, deep blues and purples. Another situation is when the tonal range (gradation) needs to be extended, which leads to use of light colours. These are essentially very different driving motives to use extra channels from the one that "spectral printing"has. Major goals of the spectral printing are spectral and colour accuracy, multi-illuminant reproduction and avoidance of metamerism [10]. By having extended number of inks, it is more likely that spectral reflectance could be reproduced more accurately. To characterize the printer and to predict its output, a forward printer model is used (e.g. Neugebauer model). To estimate ink combinations and amounts that would reproduce desired colour an inverse printer model is used. In multichannel printing, based on the ink amount predicted by inverse printer model, there can multiple ink combinations that could map to the same colour. The combination that minimizes an error metric is usually chosen. As printer models are calibrated for a given halftoning, the predicted ink combination will give targeted colour only when printed with that halftoning. This means that they are calibrated for a dot gain and specific dot overlap. As this overlap is hard to control, especially in generic FM (stochastic) devices, such are ink-jet printers, the reproduction is dependent on the ability of the printing system to properly address the dots. Also, the majority of halftoning algorithms are channel independent, which will necessarily produce unwanted visible low frequency patterns that reduce image quality. The reason for this is that halftoning algorithms are developed independently from colour management which leaves the final result of the reproduction to be a black box. It could be concluded here that colour management is concerned only to reproduce targeted colour, without any concern on image quality, texture visibility, dot arrangements, etc. These concerns are primarily addressed when designing halftoning algorithm.

1.1.1 DBS Halftoning

The Direct Binary Search (DBS) halftoning has been for many years the algorithm that gives the best textures and image quality. It started with monochrome version [11], and have since then been upgraded with several colour versions [12, 13, 14, 15]. It is one of the model based algorithms where a Human Visual System (HVS) model and printer model are taken into account when performing optimization. Optimization yields best possible dot distribution on the area. The input original image is pre-halftoned where the initial halftone is generated. A series of iterations are done, and with every iteration and through the HVS filter, the haltone is compared with the original (Figure 1). The changes on the halftone image are done through toggling (turning pixel location on or off) and swapping pixels within defined block. By comparison the error metric is calculated and algorithm converges when this metric reaches a minimum.

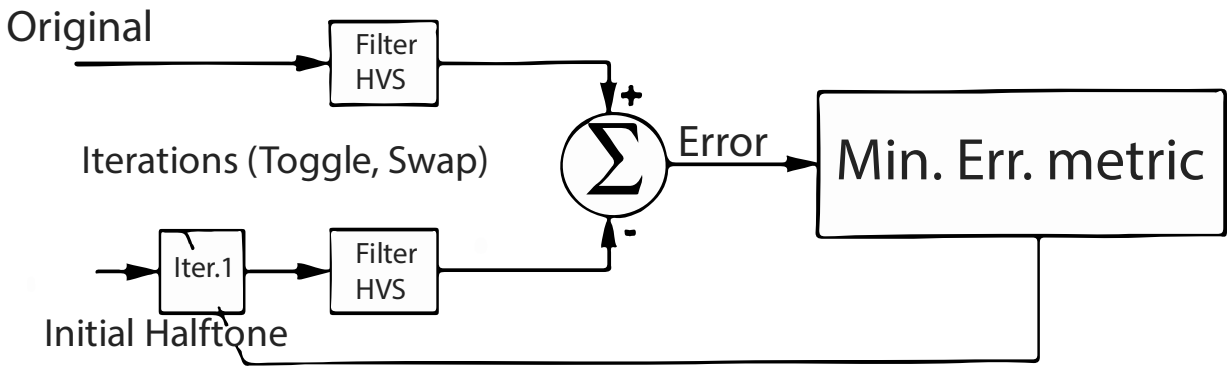

Figure 1. Direct Binary Search halftoning algorithm framework

In the colour version the texture is dependent on the colourants, both individual and combined. To control the quality of each colourant texture separately along with the total dot distribution, Li and Allebach [12] developed the colour based (CB) DBS halftoning. They have regarded that yellow ink, as being of low contrast to the paper, should be discarded in optimization of the halftone. The relevant channels are cyan and magenta and these should be distributed as uniform and possible and their overlaps are controlled with maximization of dot-off-dot halftoning. First, the dot overlapping and positions of magenta and cyan dots are decided by a monochrome DBS halftoning algorithm. Then, dot colouring is accomplished by a swap-only DBS heuristic constrained on the predetermined dot positions in the first step.

The extension of this approach is introduced by He [15] . The yellow channel, which was disregarded by Li and Alebach[12], was taken into account as, when combined with other channels (cyan and magenta), it introduces high density textures that becomes visible. The author calls his method hierarchical DBS where each channel and their overlaps are sequentially halftoned based on their texture visibility. Such arrangement for four colour printing systems is as follows: K (black), B (blue as combination of cyan and magenta), R and G (red and green as combination of magenta and yellow and cyan and yellow), then Magenta and Cyan (threated equally and halftoned together), and finally yellow.

In order to increase the gamut and save ink, a model is developed that has Neugebauer Primaries (NPs) as the output instead of individual dots and uses modified version of Error Diffusion (ED) to place NPs [16]. This way, it is possible to use extended set of metamers to satisfy reproduction goals with optimal ink input.

2. PROPOSED METHOD

To describe a method first we introduce concept of printing Neugabauer primaries and then we describe how the dot positioning is done and how colouration step is performed. Then we describe evaluation method intruding used image quality metrics and test images that are to be used in subjective and objective evaluation process.

2.1. Fundamentals

The most commonly used multichannel printer model is Yule-Nielsen Spectral Neugebauer (YNSN) [17]. It defines a new space with Neugebauer Primaries (NPs) as building blocks instead of primary inks (Figure 2). They represent prints of all primary colourants in the system and each possible combination thereof.

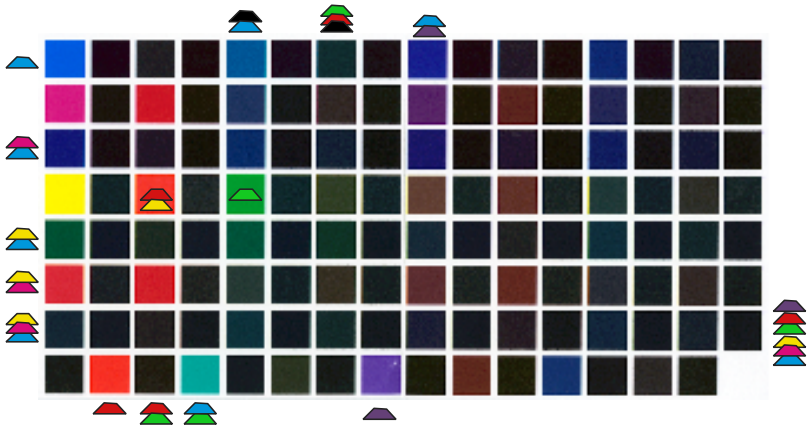

Figure 2. Neugebauer Primaries calibration patches, the target and example layers (primary inks combination) used to create patch next to it.

To simplify explanation, we define a single printing location (a dot area) as a NP. A similar approach to printer modelling and halftoning can be found in Morovič, et. al. [16]. The idea is that a dot location is a NP and the halftoning defines their spatial distribution. For halftoning algorithm, we use DBS heuristic to determine dot locations. We use this algorithm because it provides optimal spatial distribution of inks (NPs in our case), and it uses dot-of-dot strategy to reduce pattern visibility when used with multiple colourants. The most important feature of colour DBS is to reduce visibility of colour overlaps by avoiding high density points [12, 14] .To further improve texture quality and visibility we select form the set of NPs, the one which is closest to colour but with higher brightness. Usually this would lead to usage of secondary or complementary colour combination. Therefore, a selection of the NP occurs on dot level, so the benefit of reducing texture visibility could be visible even at low dot area coverages. Replacement becomes even more desirable when there is a three colour overprint to prevent ink bleeding and to provide

greater tonal gradation in dark and mid-tones. Therefore, the primaries overlap (CMY) and their replacement with secondaries (RGB) is essentially selection of the different NPs. It has to emphasize here that there is two types of NPs, the dot location NP (e.g. dot-on-dot) and spatial NP (% of area covered with the NP). Printing dot-on-dot would additionally increase dot gain of colourants[8] so the resolution is somewhat sacrificed. However, we expecting that most of the multichannel systems where this would be utilized are high resolution ink jet printers. Also, the already high dot gain of ink-jet printers would lead to problematic high coverage areas (e.g. over 300%), but it is proven that the same colour is achieved with much less ink and reduced coverage patches [2].

2.2 Multichannel halftoning workflow

A colour reproduction can have different goals, the most prominent ones being colour accuracy and image quality. Colour accuracy means low colour difference, which is developed for a large colour patches. Image quality is primarily determined by spatial distribution of pixels. The colour accurate image could be then observed as the one with minimal colour difference of pixels between original and reproduction. Metameric colour reproduction workflow aims to have a colour match under one reference illuminant (e.g. D50), where a spectral reproduction workflow aims to reproduce exact reflectance per input image pixel. The quality of the printed image (assuming halftone printing) is improved by reducing visibility of halftoning pattern, either artifacts (e.g. worms) or channel overlapping phenomena[18]. The colour accuracy is designed for relatively large colour patches matching while majority of halftoning artefacts are primarily visible in the luminance channel [19]. The multichannel printing workflow that is enabled to meet all of these needs is shown on Figure 3.

Each of the *n* input channels is hafltoned with monochrome DBS. The colouration is based on selection of the NPs. The "right NP" depends on the constraints of the desired reproduction. Therefore, multichannel halftoning is specific for a desired goal, although it might be the case where these goals co-exist. The advantage of this approach is that all the decisions are made in one step where separation and halftoning have already been performed.

2.3 Experiment

In this work, we are aim to quantify the cost of the NP change on dot location by expressing the colour difference and through image quality metrics. In short, we would like to identify and quantify tradeoff between image quality and colour accuracy. A multichannel printer (e.g. CMYKRGB configuration) is already equipped with what would be secondary colours

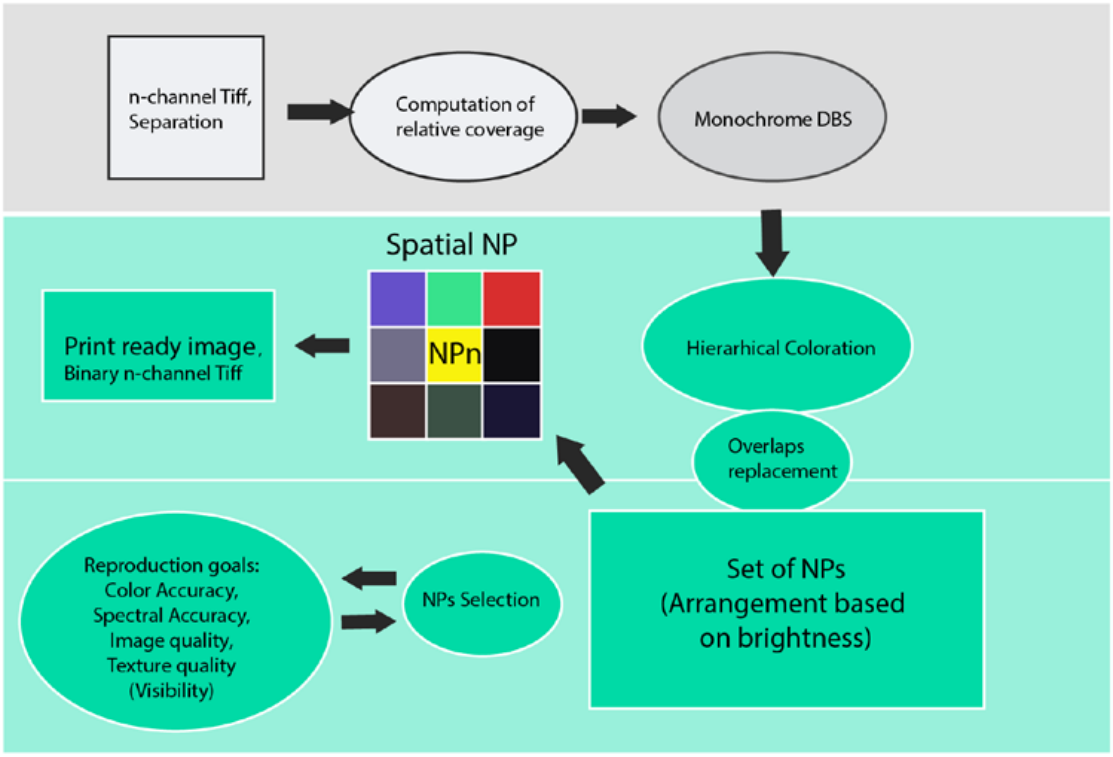

Figure 3. Multichannel halftoning framework. The overall dot positioning is performed with monochrome DBS. By combining individually halftoned channels, the overlaps are identified. Colouration of the monochrome pattern is based on identification and positioning of NPs. The hierarchical colouration is based on brightness or visibility of a NP, where the darkest or the most visible one is placed first. Every subsequent NP placement is constrained with previous NPs locations. For every different reproduction goal the colouring step (the selection of NPs) is different.

in conventional CMYK configuration. Regarding dot positioning, this advantage can result in textures that are less visible (e.g. selecting blue colour instead of combination of the cyan and magenta). Subsequently, this is extendable to any of the NPs (e.g. instead of using magenta yellow and cyan, red and cyan could be used) that would reduce density or visibility of the texture. The number of inks used to create an NP is limited to four channels (for practical reasons), although it is possible to extend to whatever number is needed for a particular application. Also we try to minimize dot - on - dot (or NP over NP) printing and to have both individual and combined texture uniformity. Overlaps are not desirable as they increase visibility of the halftone pattern. We could reduce this problem by replacing NP on dot location with less visible one and with this to increase the chance of dot-off-dot halftone.

Colouration and identification of overlaps is done by masking in Matlab, where the decisions are done on binary level. It has to be noted here that in the colouration stage we do not aim to have optimal individual and combined textures like is the case in [12,14] .Rather we make sure that more visible textures (e.g. of overlaps) are optimally distributed. The image is saved as the binary n-channel tiff (seven channels in our case), where each channel has its own coordinates for dot locations. The HP Z3200 12 ink (7 independent channels - CMYKRGB) printer is controlled via Caldera RIP and their n-channel printing option. The printer is run in custom seven channel mode, where each channel has been compensated for dot gain. No colour management has been involved at this stage. The paper used for printing all images is an EFI 9100 proofing semi-matte paper. To measure samples and express the colour difference, we used i1 spectrophotometer, which combined measurement uncertainties are 3.4 in DE2000 units. For all image quality metrics computation we have used scanned images from an Epson Expression 10000XL for which we have built custom ICC profile using printed Kodak Q61 IT 8.7/2 Target. Scanned images with profile are converted to CIELab space where they are compared with original digital file also converted CIELab space with same profile. The framework[20,21] is shown on Figure 4.

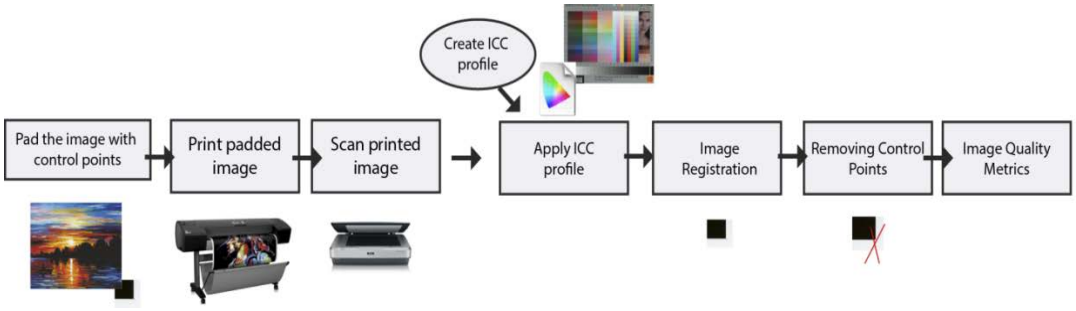

Figure 4. Image quality evaluation framework

Detailed explanation of scanning resolution and uncertainties in evaluation of the halftones could be found in Pedersen[18].To provide a figure of merit for reduction of texture visibility, we use the Noise Quality Measure (NQM) metric, which correspond to perceptual noise [22]. The NQM is applied in luminance channel only as most of the changes are evident there. Therefore, the metric is computed on the Y channel in CIE XYZ space, and both original image and scanned print are filtered with HVS model to account for the viewing conditions. The assumed viewing distance is set to 50 cm.

Also, to evaluate graininess of the uniform patch, we compute standard deviation of ΔE_{00} for every pixel. Graininess is aperiodic fluctuations of density at a spatial frequency greater than 0.4 cycles per millimeter in all directions[23]. In other words, graininess of uniform colour patches is expressed as standard deviation of measurement of optical density. As this approach is not readily applicable in colour reproduction, we measure graininess as the standard deviation of the differences in colour as measured by ΔE_{00} as in Ortiz Segovia, et.al.[24]. Note here that we do not aim to have a comprehensive image quality evaluation, but a restricted number of metrics that are mostly suitable to quantify visibility of the textures that halftoning method produces. To test texture visibility we print and scan uniform patches, transition ramps and paintings reproductions. All comparison is made against channel independent CMYK DBS. For representational purpose, all images are converted to sRGB space. Therefore all images represented in this paper are scans of the prints instead of the simulations.

3. RESULTS AND DISCUSSION

Evaluation is as follows: first we visually demonstrate change from primary inks overprint to secondary inks through printed ramps, then show how this change result on the example of painting reproduction and then we compute image quality metrics as the objective measure of this change. We also divide evaluation on two and three colour overprint replacement.

3.1 Two colour overprint replacement

First we evaluate the texture visibility and colour difference for a change from two primaries overprint to secondary colour (C+M vs B, C+Y vs G, M+Y vs R). We have printed ramps with various dot area coverages to evaluate how colour differences vary in three different regions: highlights, mid-tones and dark tones (Figure 5 and Table 1).

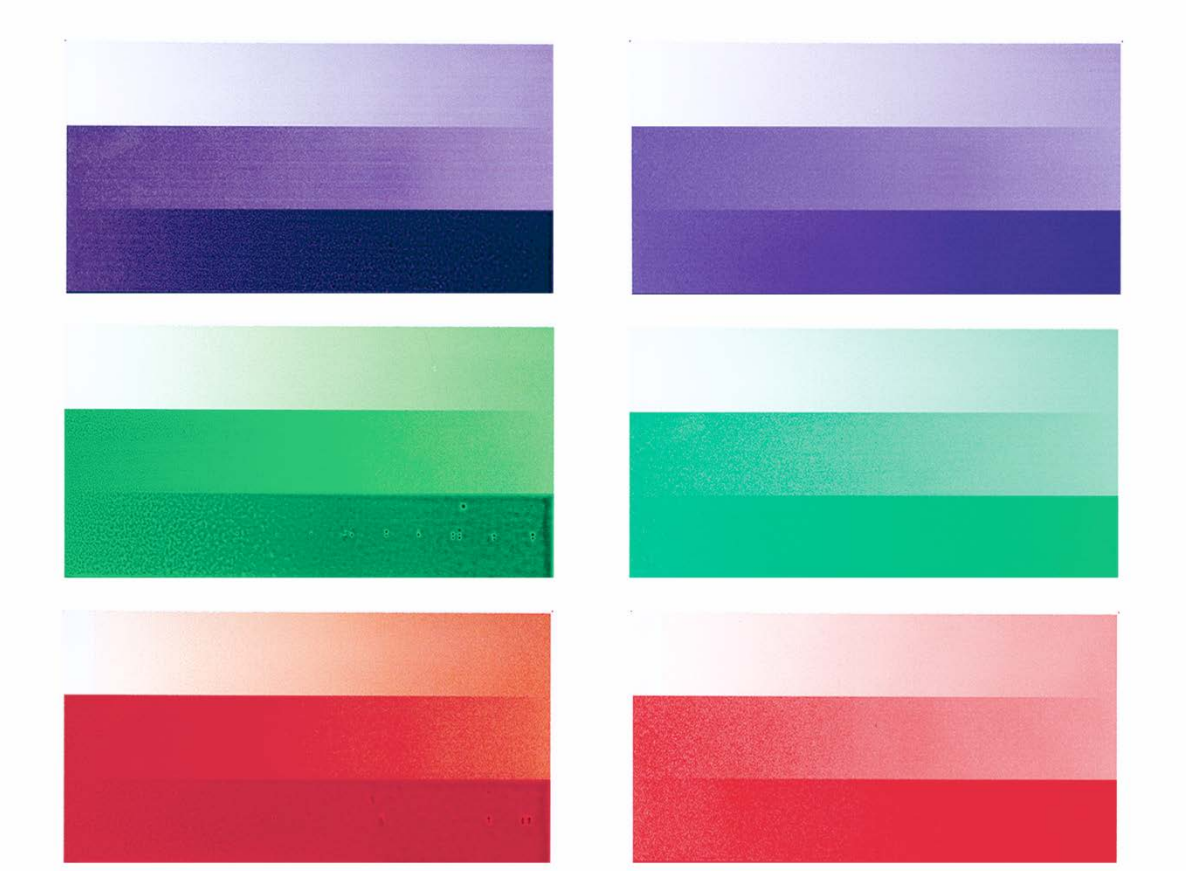

Figure 5. Ramps of two primaries combination and its secondary equivalent. It is readily noticeable that these colours are different in both hue and lightness. The ramps on the left are used with CMYK DBS while on right are used in multichannel DBS. Printing artefacts on the left block of ramps (CMYK DBS) are the result of ink bleeding but do have not significant influence on results

Figure 6. Painting reproduction – "Fisherman", where previous step of primary overlaps is replaced with secondaries (Left – original, Middle - CMYK DBS, Right - Multichannel DBS). Greater detail variation can be obtained using multichannel DBS method.

To emphasize the performance of these two halftonings in a more realistic case, we have reproduced input RGB image of a painting using both CMYK channel independent DBS and multichannel DBS (Figure 6). This image has significant amount of colours located on or at near proximity to the gamut boundary of a CMYK printing system. Therefore it is expected that multichannel DBS outperform the four colour version. Image in the middle on Figure 6, shows another problem of channel independent halftoning, where multiple overlaps occur in the small area, the dot gain. The dot gain itself is increased with mixture of colorants and over - usage of ink lead to ink bleeding at some areas. However, with the multichannel DBS, which is channel dependent halftoning (right image on Figure 6), it is rather obvious that significantly more details could be obtained in dark tones of the image.

As mentioned, the figure of merit for multichannel DBS performance is expressed through two image quality metrics: NQM and Graininess of uniform patches. On the Figure 7, the NQM score is presented for all three ramps and the evaluated painting reproduction.

The spider plot on Figure 7 shows that improvements in noise (texture) visibility could be achieved with the change from primaries overlap to secondaries.

In order to calculate the cost and benefit of the overlap replacement we also compute colour difference (Table 1) expressed in ΔE_{00} applied in three different regions: highlights, mid and dark tones of the ramps on the Figure 5. The method of replacement on ramps is all or nothing, and so it with the test images. However it could not be claimed that the colour difference presented in Table 1 is the colour difference in these regions of any image.

The colour difference depends on average colour of the area, which may involve different percentage of overlaps. Table 1 shows a significant cost in terms of colour difference with the change of the secondary NP. It must be noted here that the colour difference obtained here is between two reproductions, not original and reproduction.

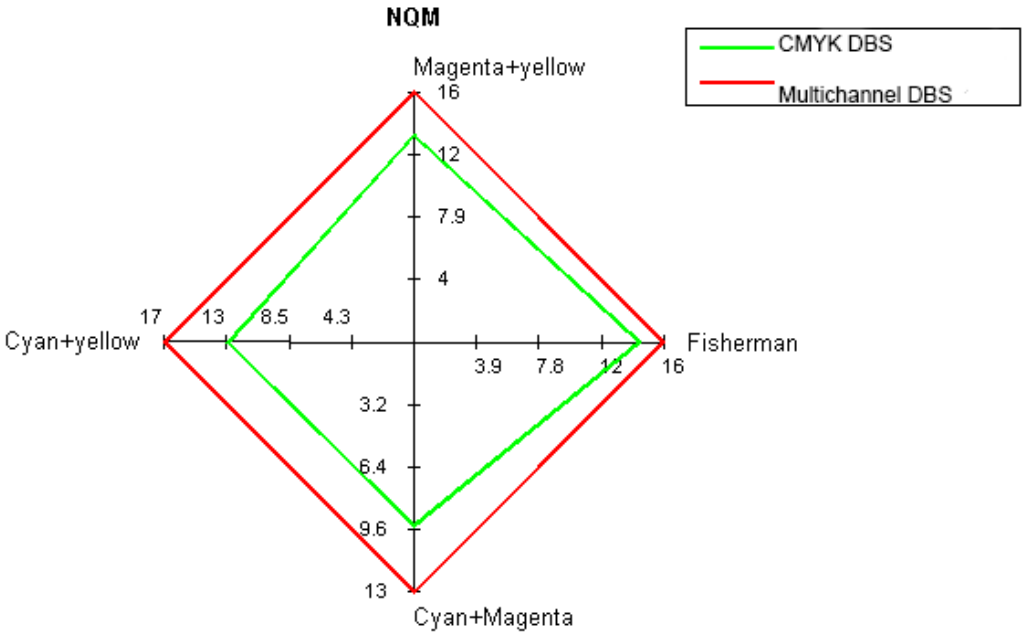

Figure 7. Performance of the multichannel DBS against CMYK DBS in NQM score for ramps on Figure 5 and painting reproduction on Figure 6. A higher score indicates higher quality.

Table 1. ΔE_{00} Colour difference between CMYK DBS and Multichannel DBS for different regions of the two colour overlap replacement.

	Highlights	Mid-tones	Dark - tones
C+M vs Blue	**3.64**	**7.94**	**10.4**
C+Y vs Green	**7.02**	**14.73**	**19.9**
M+Y vs Red	**8.16**	**15.63**	**8.94**

Therefore, no claim is made for the reproduction colour difference for which it is expected to be even better when using multichannel DBS instead of CMYK DBS.

In order to evaluate graininess, we use uniform colour patches and calculate standard deviation of ΔE_{00} from pixel to pixel (Figure 8). Therefore we select uniform patches from 10 then 20, 40, 60, 80 and 100% dot area coverage and take the mean score for each colour. As it is the case with colour difference in Table 1 where difference varies with increased dot area coverage, and as expected, the graininess is highest for low coverage patches (Figure 9).

Therefore standard deviation for CMYK DBS patches is 2.58 while for the multichannel DBS is 1.71 in ΔE_{00} units which resembles less grainy textures of the multichannel DBS.

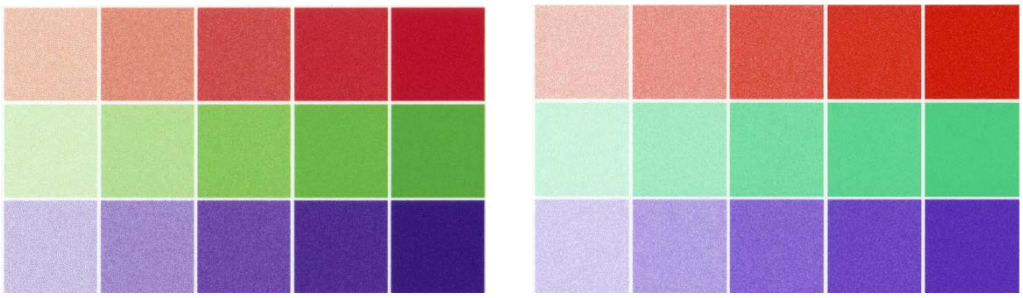

Figure 8. Evaluation of graininess of the uniform colour patch. Here again there is comparison between two primary overprint vs secondary colour.

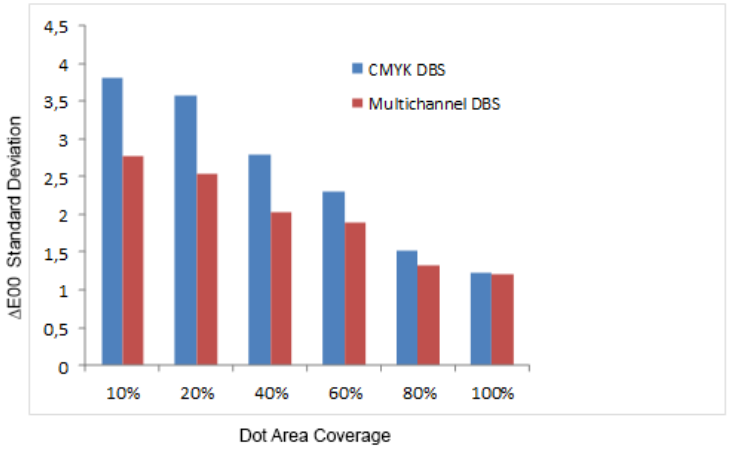

Figure 9. Graininess evaluation of the CMYK DBS and multichannel DBS expressed for different coverage uniform patches in terms of standard deviation of the ΔE_{00} colour difference.

3.2 Three colour overprint replacement

Next we evaluate three colour overprint that should produce neutrals C+M+Y against B+Y, R+C, G+M. Here we also expect to have reduction of texture visibility. The method is the same as the one used in previous step. Again we start with printed ramps, visual example and conclude with colour difference and image quality metrics as a figure of merit.

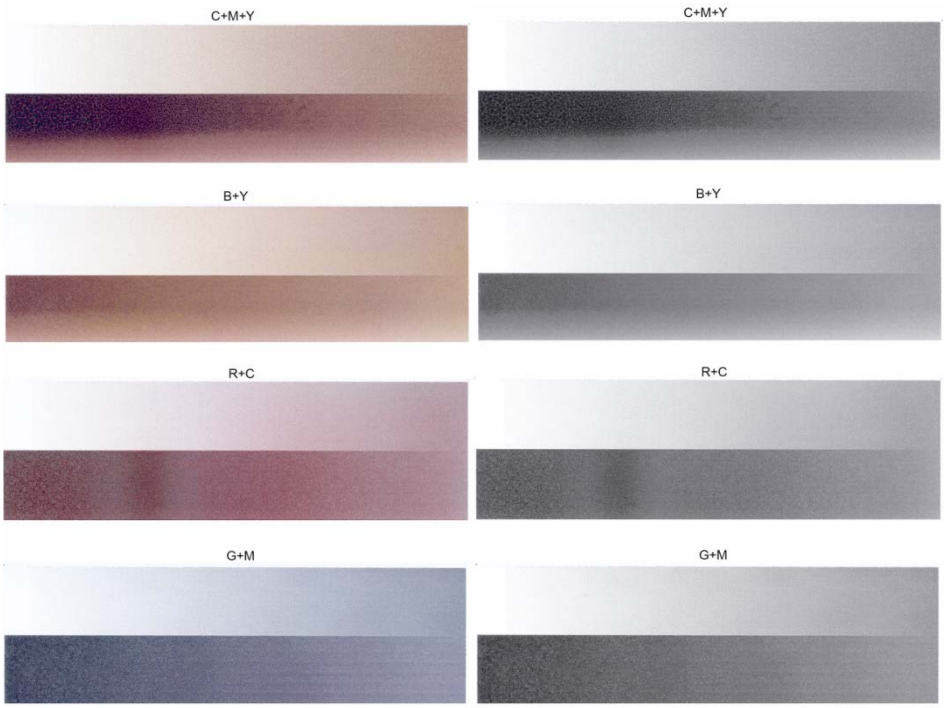

Figure 10. Ramps of near neutrals that are replacement to CMY combination. The CMY combination is CMYK DBS way of achieving neutrals while multichannel DBS can achieve this with different combinations (BY, RC,GM). On the right side, the grayscale of the colour ramps is presented to emphasize lightness difference that is gaining using multichannel DBS

In the Table 2, colour difference measured with instrument, between CMY and BY, RC and GM ramps is presented. Quantifying average colour difference and standard deviation we aim to quantify the cost of the three colour replacement. It is evident visually and from the table that BY combination is closest to CMY by colour but with significant reduction in brightness. This is true for all regions, highlights, mid-tones and dark tones which standard deviation of the ΔE_{00} colour difference indicates (Table 2).

Although RC and GM combination provide reasonable alternative to the CMY, the colour difference is high which could be visually perceived on Figure 10 and Figure 11.

Table 2. ΔE_{00} Colour Difference of the three colour dot overlaps replacement on Figure 10.

CMY vs	Mean	Standard deviation
BY	**5.8**	**4.2**
RC	**9.5**	**7.6**
GM	**14.9**	**7.1**

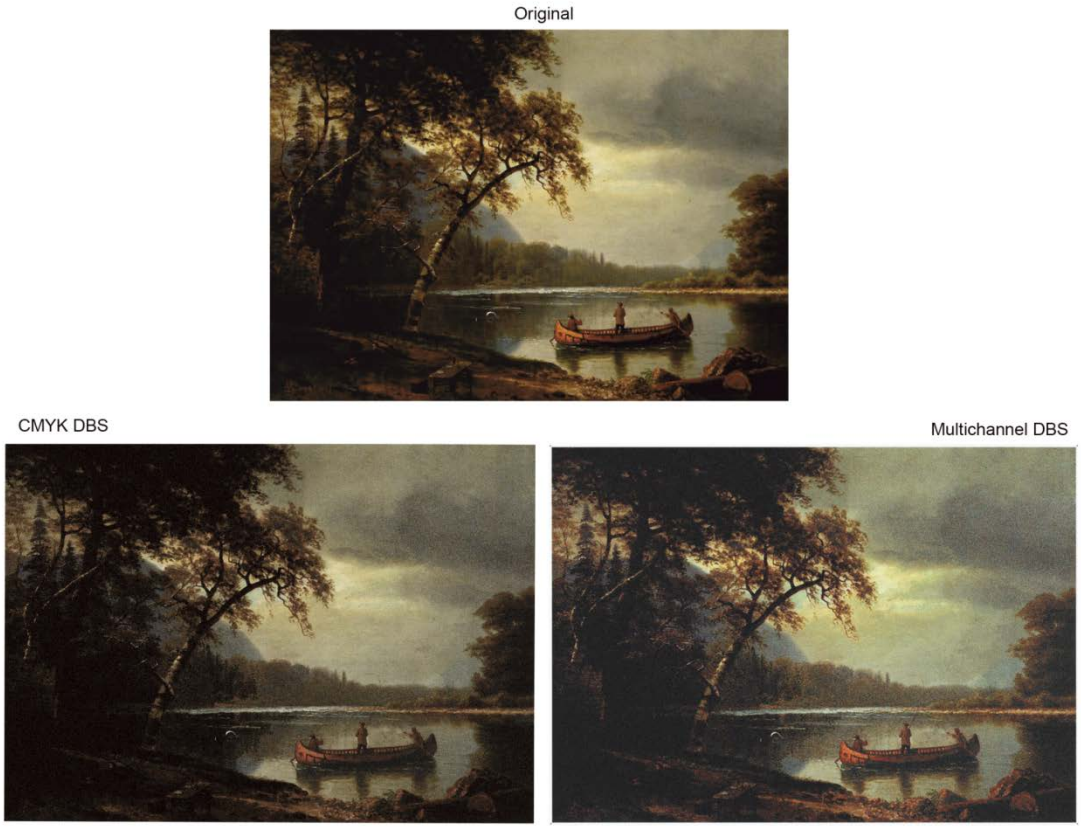

Figure 11. Reproduction of the painting using the three colour replacement defined on Figure 10. Top – Original, Bottom Left – CMYK DBS, Bottom Right – Multichannel DBS.

With multichannel DBS there is an improvement in details reproduction although to expense of colour accuracy. It could be seen on paintings reproduction that the close to neutral colours are much less bright, but there a significant colour shift, especially with GM combination (see Figure 10).

It is evident (in Table 2 and visually) that best reproduction would be when replacement of CMY dot combination is made with BY or to some extent with RC. However this would depend on the viewing environment and reproduction goals.

Once the number of overlaps exceeds three, the number of metamers increases but is also rapidly approaching the level of saturation where adding more colour dots would not make any change in brightness. In other words, it cannot get more black than this. However, multiple options for four channel overprint would additionally increase variability in dark region and would increase the gamut in this region [25].

4. CONCLUSIONS AND FUTURE WORK

In this work we have developed a framework for multichannel FM halftoning. The underlying halftoning algorithm is Direct Binary Search (DBS) whose spatial distribution of dots is proven to be the paramount for texture quality of the halftones. By using additional secondary colours, we are able to further improve texture quality through reduction in texture visibility. Further on, we are able to provide a framework for multichannel printing and halftoning where the reproduction goals and decisions are made at colouration step on top of the dot locations distributed by monochrome DBS. The texture visibility is evaluated through two image quality metrics that are directly applicable to halftones: NQM and Graininess. It is shown that significant reduction on luminance axis is possible when two primary overlap is replaced with the secondary colour. The trend continues with three colour overprint (e.g. neutrals) where again the two primary colours are replaced with one secondary and then combined with third primary. Although two selected image quality metrics resemble well variation in luminance when channel replacement is introduced, they do not necessarily include all image quality attributes of a halftoning method. In future work, we will provide with more comprehensive set of image quality evaluation metrics. It should be noted here that as the number of overprints per addressable dot location exceeds three, the dot gain and physical limitation of both substrate and ink, unable any significant change in luminance and chrominance. Therefore, the physically imposed limitation guided us to constrain number of overprints to four. Similar limitation can be found in implementation of Cellular YNSN model or ink limitation algorithms.

To achieve the desired variability of options even for a single dot location we use method of printing NPs instead of primary colourants. If one observe printing system with NPs as a building blocks, for a multichannel printing system (e.g. seven channel), there are 128 NPs. For a two colour overprint, there is at least one “metamer” (another NP) that could be used instead. For three colours overprint there are three at least three metamers to select from. If we add that for e.g. 3x3 block which comprise “spatial NP” there are exponentially more metamers, the proposed multichannel hafltoning could be used to meet different reproduction goals.

Acknowledgements

This work was supported by the Marie Curie Initial Training Networks (ITN) CP7.0 N-290154 funding. Special thanks to Peter Nussbaum who helped with the work and Jon Yngve Hardeberg for guidance and to Caldera who provided with the RIP.

REFERENCES

[1] Zitinski,P.J., Nystrom, D., Gooran, S., "Multi-channel printing by Orthogonal and Non-Orthogonal Halftoning", in Proceedings 12th International AIC Congress, pp. 597-604, (2012)

[2] Slavuj, R. Coppel, L.G., Olen, M. and Hardeberg, J.Y., "Measuring or Estimating Neugebauer Primaries for Multi-channel Spectral Printing Modelling", accepted at MMRMA, SPIE Electronic Imaging, San Francisco, CA. (2014)

[3] Urban, P., Ink limitation for Spectral or Constant Colour Printing, 11th AIC congress, Sydney, Australia, (2009)

[4] Tzeng, D., and Berns, R. S.,"Spectral-Based Ink Selection for Multiple-Ink Printing I. Colourant Estimation of Original Objects", The Sixth Colour Imaging Conference: Colour Science, Systems and Applications, pp. 106 -111, (1998)

[5] Kipphan,H, Handbook of Print Media , Berlin - Heidelberg:Springer, (2001)

[6] Shaked, D, Arad, N., Fitzhugh,A., Sobel, I., Ink relocation for colour halftones US 5991512 A, (1997)

[7] Slavuj, R., Nussbaum, P., Hardeberg, J.Y., "Review of spectral characterization and halftoning for multichannel printing", in Proceedings of IARIGAI, Chemnitz, Germany, (2013)

[8] Emmel, P. and Hersch, R. D., "Modelling ink spreading for colour prediction", J. Imaging Sci. Technol. 46(2), pp. 237 – 246, (2002).

[9] Olen, M.; Padfield, J.; Parraman, C., "Reproducing the Old Masters": Applying colour mixing and painting methodologies to inkjet printing, Colour Imaging XIX: Displaying, Processing, Hardcopy, and Applications, San Francisco, CA., USA, February 02, 2014

[10] Urban, P., Berns, R.S., "Paramer Mismatch-based Spectral Gamut Mapping", IEEE Transactions on Image Processing, Vol.20, Issue 6, pp.1599 – 1610, (2011)

[11] Lieberman,D.J. and Allebach,J.P., "A dual interpretation for direct binary search and its implications for tone reproduction and texture quality," IEEE Trans. Image Process., vol. 9, no. 11, pp. 1950–1963, Nov. 2000.

[12] Lee, J.H., and Allebach, J.P., "CMYK Halftoning Algorithm Based on Direct Binary Search", in Proceedings IS&T/SID Ninth Colour Imaging Conference, Colour Science and Engineering: Systems, Technologies, Applications, November 6, 2001, Scottsdale, Arizona, USA

[13] Agar, A.U., and Allebach,J.P., "Model-Based Colour Halftoning Using Direct Binary Search", IEEE Transactions on Image Processing, Vol.14, No.12, December 2005, pp. 1945- 1959, 2005

[14] He,Z., "Hierarchical Colourant-Based Direct Binary Search Halftoning", IEEE Transactions on Image Processing, Vol. 19, No. 7, July 2010, pp. 1824-1836, (2010)

[15] Ortiz Segovia, M.V, Bonnier,N., and Allebach, J.P., "Ink Saving Strategy Based on Document Content Characterization and Halftone Textures", Proc. SPIE 8292, Colour Imaging XVII: Displaying, Processing, Hardcopy, and Applications, Jan. 2012

[16] Morovič, J., Morovič, P. and Arnabat, J., "HANS: Controlling Ink-Jet Print Attributes Via Neugebauer Primary Area Coverages", IEEE Transactions On Image Processing, Vol. 21, No. 2, FEBRUARY 2012

[17] Neugebauer, H. E. J., Die theoretischen Grundlagen des Mehrfarbenbuchdrucks. In Neugebauer Memorial Seminar on Colour Reproduction: 14-15 December 1989, Tokyo, Japan (Sayanagi, K., ed.), pp. xv, 203, SPIE, (1989)

[18] Pedersen, M., Image quality metrics for the evaluation of printing workflows, PhD thesis University of Oslo, Oct, 2011.

[19] Pappas, T.,N., " Model-Based Halftoning of Colour Images", IEEE TRANSACTIONS ON IMAGE PROCESSING, VOL. 6, NO. 7, pp. 1014-1024, (1997).

[20] Pedersen, M. and Amirshahi, S. A., "Framework for the Evaluation of Colour Prints Using Image Quality Metrics". 5th European Conference on Colour in Graphics, Imaging, and Vision (CGIV), Pages 75-82, Joensuu, Finland, June, 2010.

[21] Pedersen, M, Bonnier, N., Hardeberg, J. Y., and Albregtsen, F., "Image quality metrics for the evaluation of print quality". Image Quality and System Performance, Proceedings of SPIE/IS&T Electronic Imaging, SPIE, San Francisco, CA, USA, Jan, 2011.

[22] N. Damera-Venkata, T. D. Kite, W. S. Geisler, B. L. Evans, and A. C. Bovik., "Image quality assessment based on a degradation model", IEEE Transactions on Image Processing, 9:636–650, (2000)

[23] ISO 13660, Information technology - office equipment - measurement of image quality attributes for hardcopy output - binary monochrome text and graphic images (2001).

[24] Ortiz Segovia, M. V. , Bonnier, N., and Allebach, J. P. , "Print Quality Analysis for Ink-Saving Algorithms", Image Quality and System Performance IX, Proc. of SPIE-IS&T Electronic Imaging, SPIE Vol. 8293, 82930Q, (2012)

[25] Olen, M.; Parraman, C., "Exploration of alternative print methodology for colour printing through the multi-layering of ink", AIC, Newcastle, UK, (2013)

Chapter 11

Paper F

Print quality and colour accuracy of Spectral and Colorimetric reproduction with Multichannel DBS

Radovan Slavuj, Ludovic G. Coppel, Irina Ciortan, Peter Nussbaum, Jon Yngve Hardeberg

submitted to the Journal of Print and Media Technology Research

Chapter 11

Print quality and colour accuracy of Spectral and Colorimetric reproduction using Multichannel DBS halftoning

Radovan Slavuj, Ludovic G. Coppel, Irina Ciortan, Peter Nussbaum

The Norwegian Colour and Visual Computing Laboratory, Gjøvik University College, Norway

ABSTRACT

Two reproduction goals exist in every reproduction workflow; color accuracy and print quality. In order to provide a relation between these two different goals, spectral and colorimetric reproduction workflows are compared in terms of color accuracy and image quality. Evaluation of image quality is restricted to separation and halftoning as two key elements of a reproduction workflow. The color accuracy of the spectral reproduction used in this paper showed higher color accuracy but lower image quality. The image quality attribute that all parts of a reproduction workflow exhibit is noise. This was the objective metric that is applied to evaluate both colorimetric and spectral separation as well as full reproduction workflow with addition of halftoning. Due to less noise in the separation process, images printed using colorimetric workflows are strongly influenced by a halftoning noise. Using previously developed multichannel Direct Binary Search (DBS) halftoning method, image quality of both colorimetric and spectral reproduction workflow improves. Findings suggest that multichannel DBS halftoning is a good candidate to be used in spectral workflow and that the image quality can be improved until the point where it can match the image quality of colorimetric reproduction.

Chapter 11

1.INTRODUCION

A reproduction workflow is comprised of a series of steps before an input signal, in a form of spectral reflectance or colorimetric values, is estimated and sent to a printer as binary information. Typical reproduction workflow involves color space encodings, calibration, printer model estimates, gamut mapping and halftoning. The input signal, whether it is a spectral or a color, is aimed to be matched by printing specific ink combinations. The ink combination that is selected and amount of each ink in the combination is determined by the separation process or with the inverse model. The separation procedure usually involves an inversion of the forward printer characterization model and it is done either through previously build look-up table (LUT) inversion or more complex and time consuming, minima search optimization routines. Either way, such estimated ink combinations with specific ink amounts are then converted to binary map with halftoning and printed on the substrate.

Spectral and colorimetric printing workflows share a common goal of reproduction of the input signal with highest possible accuracy. However, colorimetric workflow by definition is concerned only for fixed, one illuminant condition, while spectral workflow in theory aims for illuminant independent spectral match (e.g. Tzeng and Berns, 1998, Gerhardt and Hardeberg, 2006, Taplin, 2001). The idea of spectral reproduction is to have a print that will appear the same as original (e.g. with color difference under 1 ΔE) when it is observed under any illuminant. In other words, a spectral print is a physical copy of the original's physical property to selectively reflect the light or to have the same spectral reflectance. It is well known that a single CIEL*a*b* value can be created out of the set of the reflectances, phenomenon called metamerism. If spectral match was possible, the problem of metamerism would be of lesser importance. In majority of the printing application however the spectral match is not possible due to the limited spectral gamut of today's printers (Urban and Berns, 2011, Morovic et al., 2012).

Although both reproduction workflows have an issue with limited gamut of the printer, with spectral reproduction workflow this problem is more prominent. As the spectral difference (e.g. spectral root mean squared error - RMS) does not correlate well with the perceptual difference (e.g. color difference), the most reasonable solution for gamut mapping of the spectral input is a transformation of the spectral data into a color space where conventional color gamut mapping can be applied (Urban and Berns, 2011). The benefit of having the spectral data on the input is that multiple color spaces (e.g. under different illuminations) can be computed (Derhak et al., 2015). In general, an issue with computing color space coordinates from the input spectral reflectance is that many different spectral reflectances can map to the same color space coordinate. These reflectances form a metamer set which can be significantly enlarged by allowing certain tolerance or a range in the color space. The tolerance of a single ΔE unit and lower is regarded to be a non-visible and is taken in paramer mismatch gamut mapping and separation proposed by Urban and Berns (2011). The problem of such solution for spectral reproduction is an image quality of the output where significant banding occurred on separation images (Samadzadegan and Urban, 2015).

The spectral reproduction workflow in this paper is also based on multi illuminant optimization, similar to one proposed by Urban and Berns (2011). Unlike work of Samadzadegan and Urban (2015) present work aims to evaluate image quality of whole

reproduction workflow; that is of the separation and halftoning combined. One unique feature which all parts of the reproduction workflow exhibit is a noise. Through the evaluation of noise, we could weight a contribution of different parts of the workflow to the overall noise of the reproduction workflow.

In halftoning, a well-known source of noise is when two dots with different luminance are placed next to each other. The effect is the most visible when dots overlap at low coverage. One solution for this problem is referred to as Minimal Brightness Variation Rendering (MBVR) (Shaked, et al., 1997) which reallocates dots in the channel independent halftoned separations (CI halftoning) to avoid overlaps. The overlapping dots produce high density dots on the output. These overlapping dots are the most visible if observed isolated on the substrate (e.g. in dot on dot halftoning). The effect is not that high but still obvious if the overlap is observed next to some of the printing primaries C, M, and Y. A common solution is to maximize dot of dot printing within processing block (Lee and Allebach, 2001, Agar and Allebach, 2005, Ortiz Segovia, et al., 2012). However, dot of dot algorithms are very computationally expensive (Tragery, et al., 2011). In Slavuj and Pedersen (2015) a different approach is taken where channel independent DBS halftoning is post processed with so called multichannel Direct Binary Search (MC DBS). This halftoning method takes just fraction of the time used by dot of dot algorithms and directly enables it to operate in multichannel printing environment. It is also shown that MC DBS improves image quality in comparison with channel independent DBS halftoning and that is a good candidate to be used with spectral reproduction workflow.

Spectral reproduction, despite its advantages (e.g. reduced metamerism), is yet to be widely used reproduction workflow. This is partly due to limited spectral gamut and non-optimal ink set for spectral reproduction (Tzeng and Berns, 1998, Alsam and Hardeberg, 2005). This fact makes it highly dependable on given application where one study (Slavuj, et al., 2014) suggests that more than a half of the printable colors (e.g. CIE L*a*b* values), have spectrum of colorants which are not printable on a current state of the art multichannel printer. Spectral and ICC based colorimetric reproduction workflows are different primarily in their inversion process where spectral usually use optimization routine while colorimetric uses look up tables (LUT). Therefore, selected CMYKRGB ink combination with which the target reflectance or the CIE L*a*b* value can be printed, is gained by minimizing a distance in CIE L*a*b* space under one illuminant for colorimetric workflow and multiple illuminants for spectral workflow. These two reproduction workflows are different in type of input data (spectral or color) and in ink selection criteria in separation process. These two different reproduction workflows, depicted on the Figure 1, might result in selecting different CMYKRGB combination for the same input pixel.

Subsequently, and what is a starting assumption of this work, is that image quality is potentially very different between colorimetric and spectral reproduction workflows.

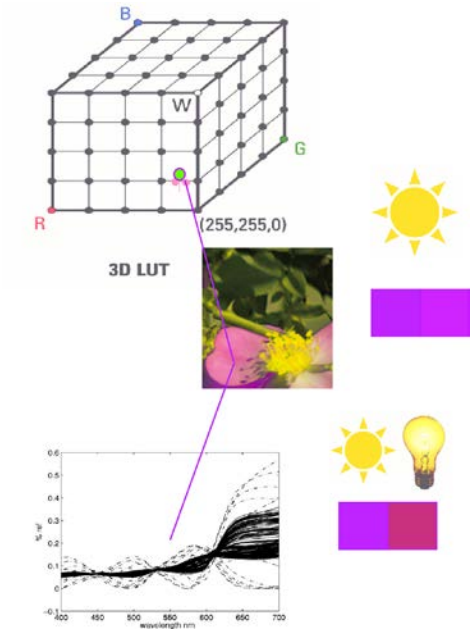

Figure 1. Simplification of the transformation process of LUT (up) in ICC colorimetric workflow and selection of paramers in optimization process of spectral workflow (down).

One can quantify a noise or smoothness of a separation (e.g. LUT based) without further application of halftoning (Samadzadegan and Urban, 2015, Wang, et al., 2010). Likewise, halftoning in absence of separation can be evaluated for similar image quality attributes (Lee and Allebach, 2001, Ortiz Segovia, et al., 2012). However, all these evaluations do not give a full description of the overall workflow image quality as both ideas assume ideal behaviors of another part of the workflow. On the other hand, the same noise or smoothness performance of final print is a resulting combination of separation and halftoning. In this work we quantify performance of spectral and colorimetric separation by evaluating a perceptual noise performance.

The underlying motivation of this work is to improve the print quality of spectral printing. In comparison with colorimetric workflow, we expect lower image quality but we aim to improve it using MC DBS halftoning. The evaluation is made of two parts. We first evaluate separation's color accuracy and image quality, and then we evaluate whole system's print quality by exercising different halftoning algorithms on separations. We start with an evaluation of the color accuracy of the spectral and colorimetric workflows by reproducing selected textile patches (Section 3.1). Following is an evaluation of the image quality (noise and graininess) of spectral and colorimetric separations by applying image quality metrics on the separation images (Section 3.2). The final comparison is made by halftoning separated images using different halftoning algorithms (Section 3.4). Note here that when image quality is referred, it is the separation image quality which is evaluated, while print quality is the image quality of the final print.

2. METHOD

The overall description of the method is shown in Figure 2. We compare the performance of the colorimetric and spectral workflows in terms of color accuracy and print quality for a set of spectral images of natural scenes, a painting and real textile patches. The spectral images or reflectance factors, either directly obtained from a database or measured are first used to compute the CIE L*a*b* under D_{50} and A illuminants.

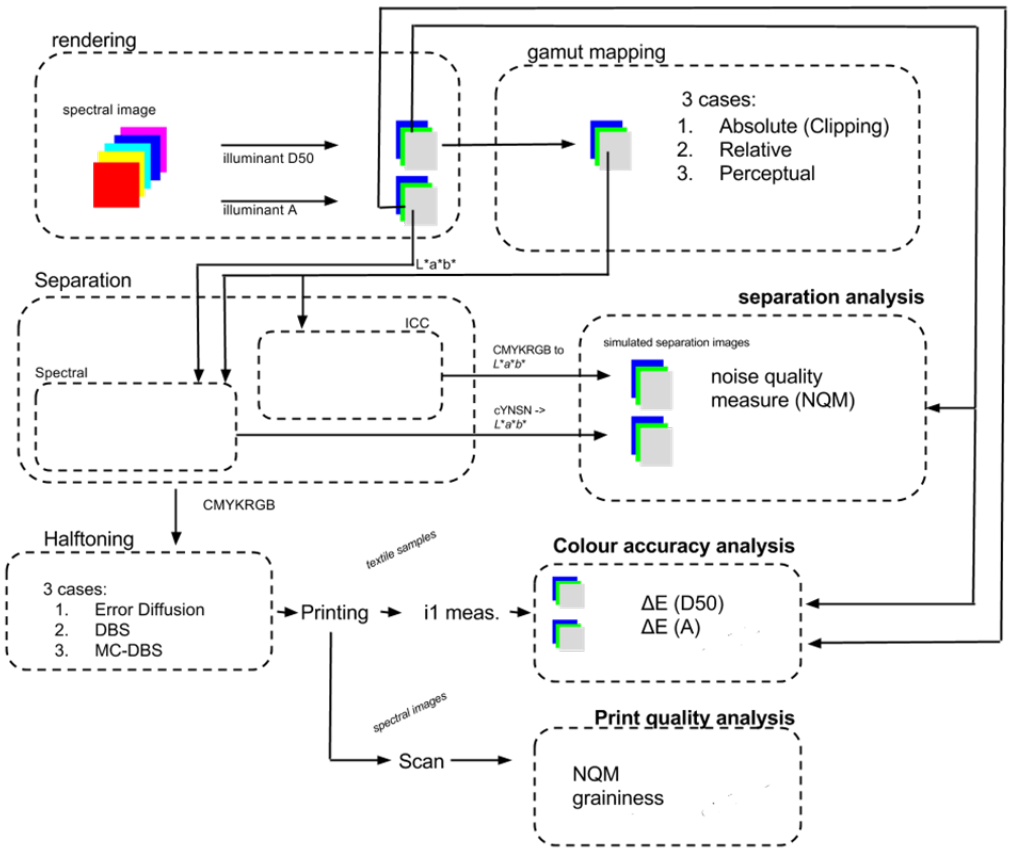

Figure 2. Overview of the reproduction workflows and of the print quality analyses. The dashed frames symbolize different steps of the reproducing workflow and our analysis. Bold letters mark our evaluation steps while normal letters mark different steps in a reproduction workflow.

The D_{50} rendering is then gamut mapped to the gamut of the printer. The colorimetric and spectral workflows differ in the next step where the separation from CIE L*a*b* to the seven CMYKRGB channels is made with help of an ICC profile (colorimetric workflow using only the D_{50} rendering) or with a multi illuminant separation and spectral gamut mapping algorithm (spectral workflow using both the D_{50} and A rendering). All colorimetric computations are performed using the 2° standard observer. At this stage, the quality of the two separation methods is evaluated in terms of induced noise in the simulated separation image (CMYKRGB to CIE L*a*b*) for three types of gamut mapping strategies (absolute, relative and perceptual colorimetric rendering). The first two gamut mapping strategies are clipping based while perceptual rendering is compression based. The rest of the evaluations are made only for the clipping gamut mapping of absolute color rendering table in the ICC profile. After the separation steps, the images are halftoned in channel independent manner prior to printing. The color accuracy of the colorimetric and spectral workflows are then assessed under both A and D_{50} illuminants using the measured reflectance factors of the textile samples (Figure 4) and their respective print reproductions. For this color accuracy evaluation we use channel independent (CI) DBS halftoning method. In order to evaluate the perceived quality of the prints, we choose the Noise Quality Metric (NQM) to assess noise, a graininess metric. To study the impact of halftoning on print quality and compare the performance of the MC DBS haltoning method to standard DBS and error diffusion halftoning, three prints are made for each image, one for each halftoning method. More details are given in the following subsections.

2.1 Material and measurements

In order to compare the print quality obtained with the colorimetric and spectral workflow, we choose spectral images of natural scenes from the Foster database (Foster, et al., 2006) and other images from Spectral Image Database for Quality (SIDQ) (Le Moan, et al., 2015). In addition, we also use a spectral acquisition of another painting to include an image with smooth gradation. As for the SIQD images, the spectral image of the painting was acquired using a HySpex line scanning hyperspectral camera VNIR 1600 (Norsk Elektro Optikk AS, Norway). The camera has a spectral resolution of 3.7 nm, interpolated to 10 nm steps for further processing. All used images are shown in Figure 3.

For the evaluation of color accuracy we use homogeneous textile samples made of wool and polyethylene (Figure 4). The dyes in colored fabrics have similar spectra as used ink set and most of them are printable with colorimetric workflow (Slavuj, et al., 2014) so we regard this set as a representative one for our experimentation.

Figure 3. Spectral images used in experiment: (1)Wool, (2) Painting - section, (3) Flower, (4) Building, (5) Print ramps, (6) Painting – full, (7) Cork, (8) Skin1, (9) Skin2, (10) Orange. (3-4) are from Foster [40] and the other except the painting in (6) are from SIQD [16].

Figure 4. Textiles sample set used for colour accuracy assessments.

The print reproductions are made with a 12 ink Z3200 PS multichannel printer (Hewlett-Packard) using seven Vivera inks (CMYKRGB) that are made for high endurance and large color gamut. For substrate we used HP Artist Matte Canvas which has shown to have optimal absorption balance, large color gamut and pleasing reproductions. The printer is directly controlled by supplying a pre halftoned 1200 dpi 7 channel Tiff binary image through a Caldera (Caldera, Strasbourg, France) Raster Image Processor (RIP) with all color management features off. Both the textile samples and their print reproductions are measured with an i1 spectrophotometer (X rite, Inc.). The printed images are scanned with an Epson Expression 10000XL scanner using a custom built ICC profile from a Kodak Q61 IT 8.7/2 target printed on our substrate. All prints are made with a 300dpi resolution while the scanner resolution is double that of the prints (600dpi). The scanned images are then converted to CIEL*a*b* space with previously created scanner profile. The scanning method is illustrated in Figure 5 and described in detail by Pedersen et al., 2010.

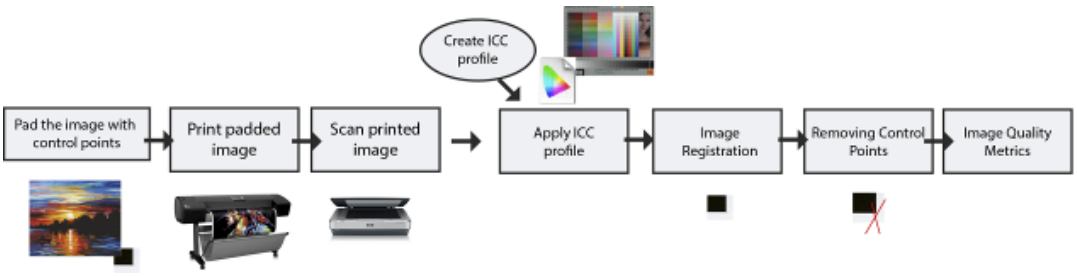

Figure 5. Framework for the scanning of the print reproductions.

2.2 Multi-illuminant separation

We use an implementation of a spectral gamut mapping and separation algorithm (Coppel, 2015, Tzeng, et al., 2000) that follows the work from Urban and Berns (2011). It is based on a sequence of colorimetric mappings within paramer mismatch gamuts. Given a set of illuminants in a prioritized order, the spectral gamut mapping aims at minimizing the color difference between the printer model estimate and the target under other illuminants (second or third in line), while keeping the difference under the first illuminant below 1 ΔE. We use ΔE_{94} as a measure of color difference since it is accurate enough for our purpose and less computationally expensive than ΔE_{00}. The printer is modelled with the cellular Yule Nielsen modified Neugebauer (cYNSN) model, described e.g. by Wyble and Berns (2000), using four cells. The calibration set includes all 4 ink combinations at 5 apparent ink coverages (0- 100% with 25% step). We consider only 4 ink combinations including K (e.g. CMYK, CKRG or MYKB) since it was observed that 5, 6 or 7 ink combinations do not contribute much to the spectral variability of the printouts (Coppel, et al., 2013). In this work, we apply the separation algorithm with D_{50} as the first illuminant and A as the second illuminant. This means that for each pixel in the images, the search is performed for the CMYKRGB combination that leads to $\Delta E_{94} < 1$ under D_{50} and minimal color difference under A. Note that a gamut mapping is performed under D_{50} prior to the separation.

2.3 Colorimetric separation

The colorimetric workflow is based on the ICC architecture (ICC, 2010). The ICC profile is made with a X rite iProfiler software. We use 3000 calibration patches to provide high accuracy with acceptable computation time. Profiles have seven channel outputs corresponding to seven (assumed independent) channels of the printer we use. We use then the ICC profile to convert the CIE L*a*b* values of the spectral images, computed for D_{50} / 2° condition, to CMYKRGB, and from CMYKRGB to CIE L*a*b*. Different profiles are generated for the three gamut mapping (absolute, relative and perceptual rendering intent) and for different halftoning methods. The profiles has a Grey Component Replacement algorithm (GCR) applied but to a lower extent. The gamut mapping is the same as for the multi illuminant separations.

2.4 Halftonings

We aim at comparing the impact of halftoning on multi illuminant (spectral) reproduction. We restrain our analysis to iterative halftoning methods that have been shown to give the least visible textures (Lieberman and Allebach, 2000). As a reference, we first test the widely used Floyd Steinberg Error Diffusion (ED) method described by (Ulichney, 1987). Error Diffusion in all its versions is a pixel neighborhood altering algorithm, where error accumulated at processing pixel is diffused at neighboring pixels. We shortly describe at this point the Digital Binary Search (DBS) halftoning method, which we apply channel independently for all ink channels (CI DBS) and with an extension to multichannel color halftoning (MC DBS) proposed by Slavuj and Pedersen (2015).

The DBS is one of the model based algorithms for halftoning where a Human Visual System (HVS) model and printer model are taken into account when performing optimization. Optimization yields best possible dot distribution on the area. The input original image is pre halftoned where the initial halftone is generated. Series of iterations are done, and with every iteration and through the HVS filter, the halftone is compared with the original. The changes on the halftone image are done through toggling (turning pixel location on or off) and swapping pixels within defined block. By comparison the error metric is calculated and algorithm converges when this metric reaches a minimum. A more detailed description of this halftoning algorithm can be found in (Lieberman and Allebach, 2000). The MC DBS uses a hierarchical scale of the dot luminance (Figure 6), starting from the lowest luminance dot (e.g. of black ink) to the highest luminance dot (yellow ink).

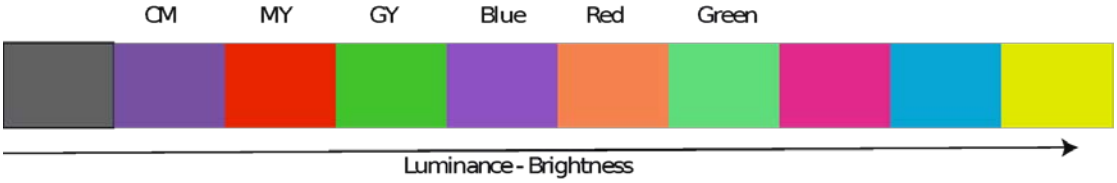

Figure 6. Primary colorants and overlap by visibility with decreasing luminance from right to left.

Therefore, dots with the lowest luminance should have the most optimal spatial distribution while dots with highest luminance are not of the concern as they are the least perceivable on white paper. In color halftoning, yellow channel is usually neglected due to its similar luminance to the white paper (Lee and Allebach, 2001). On the other hand, He argued that although yellow is not significantly disturbing when printed alone, it can be when overlapping with other inks (He, 2010). In MC DBS, yellow channel is taken into account in replacement of the primary channel's overlaps. This rather simple change reduces halftone noise and graininess (Slavuj and Pedersen, 2015). It is worth noting that these overlap replacements reduce the need for complex dot of dot structures as in (Lee and Allebach, 2001, He, 2010). Therefore, each ink keeps its optimal dot distribution as determined by monochrome DBS. Seven channel separations are first halftoned independently with monochrome DBS using. Merging these channels constitutes a channel independent DBS halftoning (CI DBS). The four binary images are then summed for

identification of the overlaps of CM, CY and MY combinations. These overlaps are replaced with some of RGB inks and the CMY overlaps are changed to one of the BY, RC, GM complementary color combinations. In contrast to ICC where Gray Component Replacement (GCR) is used, K is treated separately here as many ink combinations can map to near black colors. We therefore replace black in light and mid – tones (corresponding to black apparent coverage up to 75%), with some of the two color complementary color combinations (GM, RC, BY). These combinations are lighter than K alone and thus their halftone pattern is less perceptible. Note here that this change is only done when used with spectral workflow as colorimetric workflow has GCR already applied on profile.

2.5 Print quality evaluation

As shown in Figure 2, the multi illuminant (spectral) and the ICC based colorimetric workflows differ only in the separation step. We want to evaluate the impact of this separation on perceived print quality and of its interaction with the preceding gamut mapping and subsequent halftoning steps. Noise has many sources but in this work we limit our evaluation to the noise of separation error (e.g. error of interpolation or rounding), pixel wise processing (in contrast to neighborhood based operations), and halftoning induced noise.

To quantify noise of a reproduction workflow, we use the Noise Quality Measure (NQM) which corresponds to a perceived noise (Damera Venkata, et al., 2000). The NQM is taken from luminance channel only as most of the changes in relation with halftoning are evident there. The metric is computed on the Y channel in CIE XYZ space, and both original image and scanned print are filtered with HVS model to account for the viewing conditions. The assumed viewing distance is set to 50 cm.

For evaluation of the separations we use images number 1-5 and image number 10 shown on Figure 3. In order to ensure that it is only the separation that has been compared, we applied the same gamut mapping on both spectral and colorimetric workflow. These three gamut mapping strategies are performed with another, highly accurate ICC profile (calibrated with 5000 patches) and the LUTs for absolute, relative and perceptual color rendering are extracted and used as a means for gamut mapping. For the image quality of the separation and halftoning, all images from Figure 3 are used. The procedure of the printing, scanning and the metrics application is shown on Figure 5. To add to the evaluation of the halftoning, the graininess metric is added and described below.

Graininess is defined as aperiodic fluctuations of the optical density at a spatial frequency greater than 0.4 cycles per millimeter in all directions (Hains, 2003). However, this applies to monochrome reproductions. For color reproduction, we instead quantify graininess as the standard deviation of the ΔE_{00} differences as proposed by Ortiz Segovia et al. (2012).

3. RESULTS AND DISCUSSION

3.1 Color accuracy

The $L^*a^*b^*$ values of the textile patches are compared to the gamut of the printer in Figure 7. The sample set has around 30% samples out of the HPz3200 multichannel printer gamut**.** The color difference between the textile patches and their print reproduction obtained with the spectral and colorimetric workflows are given in Table 1 for both D_{50} and A illumination conditions. Color difference in Table 1 point to rather different performance of spectral and

colorimetric workflow, where spectral is clearly better. Part of that performance difference is attributed to the use of different models in separation; cYNSN with spectral and interpolation based LUT with colorimetric workflow. As expected, model based spectral workflow is more accurate under both illuminants, but LUT based interpolation show a significant error of the estimation. The large maximum error is spotted at a few of dark samples is believed to come as a function of the Grey Component Replacement algorithm on the RIP, while in spectral workflow GCR was not used.

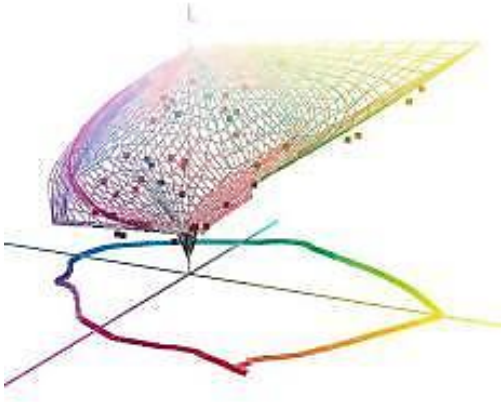

Figure 7. Gamut plot in D_{50} / 2° CIE L*a*b* space of the HP Z3200 multichannel printer (wireframe) and measurements of textile patches.

Table 1. Color difference between measurements on real textile samples and print reproductions for the spectral and colorimetric workflows.

	ΔE_{00} / D_{50}					ΔE_{00} / A			
	mean	median	max	95th perc.		mean	median	max	95th perc.
Spectral	4.04	4.32	6.21	5.61		3.89	4.35	6.66	6.14
ICC	8.73	8.00	23.62	18.05		8.29	7.59	23.89	17.84

3.2 Separation analysis

The NQM scores are shown in Figure 8 for the rendering intent gamut mapping case. For the 5 images used, the ICC separation leads to larger NQM scores than the spectral separation except for the orange image, which on the other hand gets low NQM for both separations. Overall, NQM scores are very different for different images, and the difference between different images is larger than the difference between spectral and color separation (Figure 8).

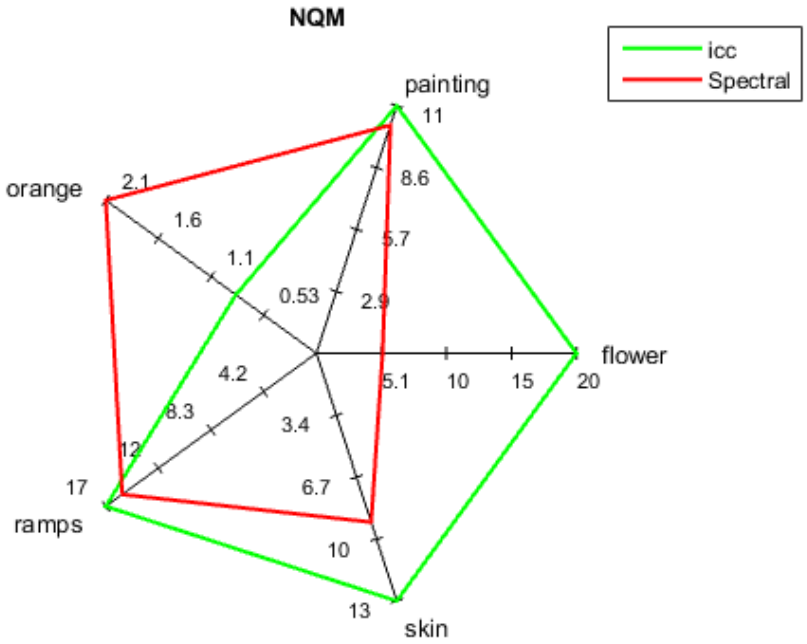

Figure 8. NQM score of spectral and colorimetric separations with for absolute rendering intent.

The mean NQM (from all NQM scores of all used images) of for the different rendering intents (Table 2) indicates nonetheless that more noise is generated in the spectral separation than in the ICC separation. From Table 1 and Table 2 it is obvious that spectral modeling and gamut mapping has the advantage in color accuracy but lower image quality (e.g. higher noise) of the separation.

Table 2. NQM scores of spectral and colorimetric separations using gamut mapping with three different rendering intents

	Absolute RI	Relative RI	Perceptual RI
ICC	9.62	8.14	6.25
Spectral	6.43	5.29	4.89

The source of this noise comes mostly as the result of gamut mapping (GM) but it is also from the separation. Therefore, for all gamut mappings applied, spectral shows lower score

that colorimetric separation. On the other hand, perceptual rendering intent, which alters values of the points even within the gamut, leads to the lowest perceptual score of all three gamut mappings.

3.3 Effect of halftoning on print quality

In this part we evaluate image quality performance of the MC DBS. First we compare MC DBS with Floyd Steinberg Error Diffusion. Error Diffusion due to its neighborhood filtering creates artefacts if input dot area coverages are not smooth (e.g. like spectral transformations) (Figure 10).

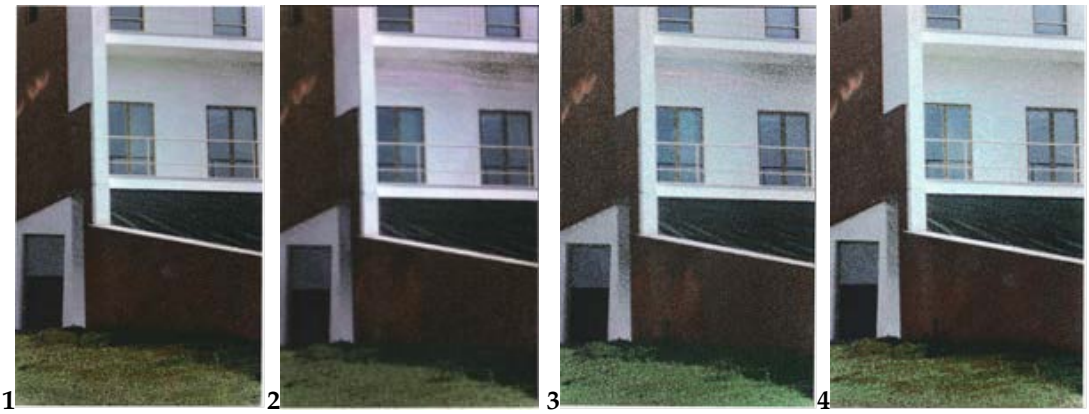

Figure 10. Spectral Separation with simulated image (1), CI ED (2), CI DBS (3), MC DBS (4). To emphasize the differences, prints are made with 150dpi resolution. CI ED in combination with spectral separation produces banding artefacts while CI DBS have optimized spatial distribution which reduces banding artefacts. The MC DBS is the same as CI DBS but also improves texture uniformity in shadow and dark areas and increase detail level in these areas as well.

Channel independent Error Diffusion show significant artifact in light areas of the image passing thought the area of subtle gradient. Similar behavior was reported in (Gerhardt and Hardeberg, 2006) where due to error filter passing through the area of rapid light to dark transitions (noise area), error is accumulated and released toward the end of scan line (assuming raster direction). When two inks overlap, the dot gain or ink spreading increases and is larger from the single dot on the paper (Hersch and Crete, 2005). It is not just that overlap replacement with single ink reduce visibility of the halftone, it also helps to reduce the ink amount and spreading in the certain areas which would otherwise lead to the saturation and undesired tone reduction (Figure 11). Also it helps for the high coverage patches (or halftone cells) that contain black ink, as these areas get saturated with ink faster.

1 2

Figure 11. Spectral reproduction of painting using Error Diffusion halftoning (1) and MC DBS (2).

Overall NQM score of spectral vs colorimetric workflow using MC DBS is shown on Figure 13.The results confirm that halftoning plays a significant role in print quality that the impact of halftoning is different for spectral and colorimetric workflow. In colorimetric workflow, which has smoother or less noisy separation than spectral workflow, halftoning is important parameter in determining image quality.

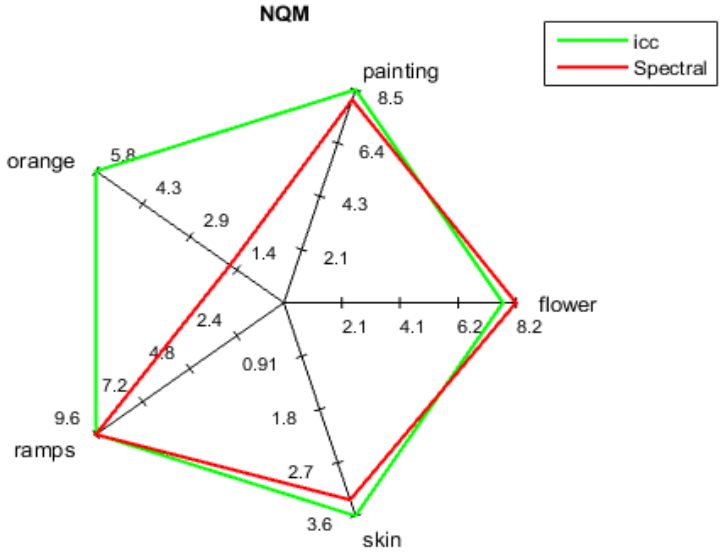

Figure 12. Performance of colorimetric and spectral workflow with MC DBS halftoning.

From Table 2, where only separation noise is evaluated, colorimetric workflow is significantly better than spectral. However, after halftoning spectral workflow is very close to achieve quality of the colorimetric workflow. Table 3 provides the mean of the image quality metrics used to compare spectral and colorimetric workflow with different halftoning applied.

Table 3. Mean score for all images for image quality metrics of the colorimetric and spectral reproduction workflow with different halftoning methods. All reproductions are gamut mapped using absolute rendering intent.

Image quality	NQM	Graininess
ICC CI ED	5,3	2.8
ICC CI DBS	6,2	2.5
ICC MC DBS	7,3	1.6
Spectral CI ED	4,4	2.9
Spectral CI DBS	5,8	2.3
Spectral MC DBS	7,1	1.7

As expected, NQM score is lower than after separation, for both spectral and colorimetric workflow. The halftoning adds significant perceptual noise which lowers the NQM score, and this is true for all halftoning algorithms used. However NQM score can be increased by using MC DBS over CI DBS and CI ED. The NQM score for spectral workflow is similar to colorimetric workflow for printed images. This suggests that the colorimetric workflow is more influenced by the halftoning noise than the spectral workflow is. The overall conclusion is that the halftoning has more influence to the NQM score than the separation process (Table 2 and Table 3). However it is possible to increase the score of the perceptual noise by selection of the halftoning algorithm. The DBS algorithm in all cases shows better performance than ED but with using MC DBS halftoning method, the NQM score is further increased. It is worth noting that although the NQM metric is the one that is applicable to both separation and halftoning other metrics could be a part of the analysis of the future work.

Graininess is the metric solely attributed to the halftoning. It is clear that reduced graininess is achieved with MC DBS than with other two tested halftonings. Also, the graininess is very similar for both colorimetric and spectral workflow, no matter what halftoning is used.

4. CONCLUSIONS

We evaluated the image quality of a colorimetric and a spectral separation combined with halftoning. We show that colorimetric separation integrated in the ICC profile yield less noise than a custom in spectral separation. In case of the spectral separation, the image quality will depend on the halftoning used. For both colorimetric and spectral workflow, using MC DBS halftoning will lead to less noise or better image quality. When combined with halftoning, spectral workflow yield similar image quality performance to colorimetric which leads toward the conclusion that halftoning has much more impact on image quality when applied after colorimetric separation.

Acknowledgements
This work was supported by the Marie Curie Initial Training Networks (ITN) CP7.0 N-290154 funding. Special thanks to Caldera who provided the RIP.

REFERENCES

Agar, A.U., and Allebach, J.P., 2005. Model-Based Color Halftoning Using Direct Binary Search, IEEE Transactions on Image Processing, Vol.14, No.12, December 2005, pp. 1945-1959.

Alsam, A. and Hardeberg, J.Y., 2005. Optimal colorant design for spectral colour reproduction, Color Imaging: Processing, Hardcopy, and Applications X, SPIE Proceedings 5667, pp. 38-46.

Coppel, L.G., 2015, Spectral gamut mapping and ink separation with fluorescing substrates, Proc. IEEE Color and Visual Computing Symposium, Gjovik, Norway.

Coppel, L.G., Le Moan, S., Zitinski Elias, P.S., Slavuj, R. and Hardeberg J.Y., 2013. Next generation printing - Towards spectral proofing, in Advanced in Printing and Media Technology, vol 41, M. Lovreˇcek and N. Enlund, Eds. IARIGAI, pp. 19–24., 2013.

Damera-Venkata, N., Kite, T.D., Geisler, W.S., Evans, B.L., and Bovik. A.C., 2000. Image quality assessment based on a degradation model, IEEE Transactions on Image Processing, pp. 9:636–650.

Derhak, Maxim W.; Green, Phil & Lianza, Tom. 2015. Introducing iccMAX: new frontiers in color management, Color Imaging XX: Displaying, Processing, Hardcopy, and Applications, Proceedings of SPIE/IS&T Electronic Imaging, SPIE, Volume 9395, pp. 9395-20, San Francisco, CA, USA.

Foster, D.H., Amano, K., Nascimento, S.M.C. and Foster, M.J., 2006. Frequency of metamerism in natural scenes. Journal of the Optical Society of America A, 23, pp. 2359-2372.

Gerhardt, J. and Hardeberg, J.Y., 2006, Spectral colour reproduction by vector error diffusion. In Proceedings CGIV 2006, pp. 469–473.

Hains, C., Wang, S.G., Knox, K., and Sharma, G., 2003. Digital Color Imaging Hand-book, chapter 6 Digital Color Halftones, pages 385–490. CRC Press.

He,Z., 2010. Hierarchical Colorant-Based Direct Binary Search Halftoning, IEEE Transactions on Image Processing, Vol. 19, No. 7, July 2010, pp. 1824-1836.

Hersch, R., Crete, F., 2005, Improving the Yule-Nielsen modified spectral Neugebauer model by dot surface coverages depending on the ink superposition conditions, IS&T/SPIE

Electronic Imaging Symposium, Conf. Imaging X: Processing, Hardcopy and Applications, SPIE Vol. 5667, pp. 434-445.

Lee, J.H., and Allebach, J.P., 2001. CMYK Halftoning Algorithm Based on Direct Binary Search", in Proceedings IS&T/SID Ninth Color Imaging Conference, Color Science and Engineering: Systems, Technologies, Applications, Scottsdale, Arizona, USA.

Le Moan, S., George, S., Pedersen, M., Blahova, J., and Hardeberg, J.Y., 2015. A database for spectral image quality, in Image Quality and System Performance XII, San Francisco, CA, USA, vol. 9396, p. 25, IS&T/SPIE.

Lieberman,D.J. and Allebach,J.P., 2000. A dual interpretation for direct binary search and its implications for tone reproduction and texture quality, IEEE Trans. Image Process., vol. 9, no. 11, pp. 1950–1963.

Morovic, P., Morovic, J., Arnabat, J., 2012. Revisiting Spectral Printing: A Data Driven Approach, 20th Color and Imaging Conference Final Program and Proceedings, IS&T, pp. 335–340.

Ortiz Segovia, M. V. , Bonnier, N., and Allebach, J. P. , 2012. Print Quality Analysis for Ink-Saving Algorithms, Image Quality and System Performance IX, Proc. of SPIE-IS&T Electronic Imaging, SPIE Vol. 8293.

Ortiz Segovia, M.V, Bonnier,N., and Allebach, J.P., 2012. Ink Saving Strategy Based on Document Content Characterization and Halftone Textures", Proc. SPIE 8292, Color Imaging XVII: Displaying, Processing, Hardcopy, and Applications.

Pedersen, M., Bonnier, N., Harderberg, J.Y., and Albregtsen, F., 2010. Attributes of image quality for color prints, Journal of Electronic Imaging 19(1), pp. 11–16.

Samadzadegan, S. and Urban, P., 2013. Spatially resolved joint spectral gamut mapping and separation," In Color and Imaging Conference, Society for Imaging Science and Technology 2013(1), pp. 2–7.

Shaked, D., Arad, N., Fitzhugh, A., and Sobel, I., Ink Relocation for Color Halftones 1996 [Online]. Available: HP Labs. Tech. Rep., HPL-96- 127R1.

Slavuj, R.; Marijanovic, K.; Hardeberg, J., Y., 2014. Colour and spectral simulation of textile samples onto paper; a feasibility study, Journal of AIC.

Slavuj, R. and Pedersen, M., 2015. Multichannel DBS halftoning for improved texture quality, Proc. SPIE, Color Imaging: Displaying, Processing, Hardcopy, and Applications, San Francisco, CA, USA.

Specification ICC.1:2010, Image technology colour management - Architecture, profile format, and data structure, International Color Consortium, 2010.

Taplin, L. A., 2001. Spectral Modeling of a Six-Color Inkjet Printer, Msc Thesis , RIT.

Tragery, B., Wah Wuy,C., Stanich, M., Chandu, K., 2011. GPU-enabled parallel processing for image halftoning applications, 2011 IEEE International Symposium on Circuits and Systems (ISCAS),pp. 1528-1531, Rio de Janeiro, Brazil.

Tzeng, D., and Berns, R. S., 1998. Spectral-Based Ink Selection for Multiple-Ink Printing I. Colorant Estimation of Original Objects, The Sixth Color Imaging Conference: Color Science, Systems and Applications, pp. 106 -111.

Tzeng, D. S., Berns, R. S. and York, N., 2000. Spectral-Based Six-Color Separation Minimizing, in IS&T 8th Color and Imaging Conference, Scottsdale, USA, pp. 342–347.
Ulichney, R., Digital Halftoning. Cambridge, MA: MIT Press, 1987.

Urban, P. and Berns, R., 2011. Paramer Mismatch-Based Spectral Gamut Mapping, IEEE Transactions on Image Processing, Vol. 20, No. 6, 2011.

Wang, Zhaohui; Aristova, Anna & Hardeberg, Jon Yngve. Quantifying Smoothness of the LUTs-based Color Transformations. 31st International Congress on Imaging Science (ICIS), Beijing, China, May, 2010.

Wyble, D. R. and Berns, R. S., 2000. A critical review of spectral models applied to binary color printing, Color Research & Application, vol. 25, no. 1, pp. 4–19.

Chapter 12

Paper G

Colour and spectral simulation of textile samples onto paper; a feasibility study

Radovan Slavuj, Kristina Marijanovic, Jon Yngve Hardeberg

Published in

Journal of International Colour Association,

Vol. 12.

Pages 36-43

Chapter 12

Colour and spectral simulation of textile samples onto paper; a feasibility study

Radovan Slavuj, Kristina Marijanovic, Jon Yngve Hardeberg

The Norwegian Colour and Visual Computing Laboratory, Gjøvik University College

ABSTRACT

This study has investigated how the growing technology of multichannel printing and area of spectral printing in the graphic arts could help textile industry to communicate accurate colour. In order to reduce the cost, printed samples that serve for colour judgment and decision in the design process are required. With the increased colour gamut of multichannel printing systems we are expecting to include most of the colours from textile samples. The results show that with careful control of ink limits and with bypassing the colour management limitations imposed on printing system; we are able to include more than 90% of colour textile samples into the multichannel printer gamut. Also we evaluated how much textile spectra we can print with multichannel printers. This gives a basis for the area of the spectral printing and where this study aims on particular application of such systems. We also conclude here that it is possible to print around 75% of all reflectance from textile colours.

Chapter 12

1. INTRODUCION

A fundamental requirement for any colour management paradigm is unambiguous colour communication. Due to the different physical nature of materials and colourants used in different industries, different colour management workflows have been adopted. In the graphic arts (printing) industry, the dominant colour management workflow is that standardized by the International Colour Consortium (ICC) and based on metameric reproduction [1]. This trichromatic based workflow has recently been enhanced by the introduction of multichannel printing. Additional channels (beyond the common CMYK) are introduced to extend the colour gamut where conventional printing systems have shortcomings.

In previous preliminary work [2,3] we evaluated whether it was possible to include all textile colours within the printable colour gamut. A particular challenge in that study was to evaluate whether it would be possible to reproduce textile samples within a given range of colour accuracy and how much textile spectra we can print. These samples were 5 cm x 5 cm pieces of fabric that are normally produced within 0.8 ΔE_{CMC} tolerance from a reference set. The colour difference was evaluated for UL3000 store illuminant and 10 degrees colorimetric observer. Designers use these physical samples when they are deciding which shade an item of garment product will be, or which shade needs to be placed next to each other in a printed or yarn dyed pattern on a garment product. The existing set of roughly 4000 colours is supporting the design process within the colour set that designers are able to pick from. Once their colours for a season and brand are chosen, fabric samples are ordered to work with. The possibility of printing these colour samples versus purchasing them from a dyeing company would significantly save in cost.

With four channel printing technology, such reproduction is not feasible [2]. With the addiction of red, green and blue printing channels, the expansion of the gamut was found to be significant and many more textile colours were included in the printable gamut [3]. However this is still not sufficient to be acceptable for such an application. Many dark colours are still out of the gamut and the particular ink configuration was not optimal for reproduction of the textile colours.

When "spectral printing" was introduced [4,5,6,7], a new set of possibilities for printing has emerged. Aims of the spectral printing are to increase spectral and colour accuracy, reduce the metamerism and where possible, extend the application of printing into new fields. These application areas of the spectral printing ranges from: highly accurate industrial colour communication in terms of colour swatches, catalogues and samples (e.g. textile and paint industry), spectral proofing, fine art reproduction, and security [8]. All these applications would require optimal colourant set to comprise the gamut of original. The main aim is to have spectral match or at least colour match between original and reproduction under certain set of illumination sources [9]. For achieving this step is to have most of the original's colours and spectra within the printable gamut. Therefore, the aim of this study is to evaluate how much of the textile sample colours and spectra we can include into the available gamut of the current print technologies and substrates.

2. METHOD

The comparison of the printer gamut was performed with 4872 textile colour samples and spectra with the multichannel printer colour and spectral gamut. We used Colour Think software to visualize gamuts in CIELab space, in both two and three dimensions. To represent the spectral gamut we first use PCA to reduce the dimensionality of input spectra that define printer spectral space [3,10]. Here we used rotated Principal Components that could be observed as colourants of a particular device [11]. Our multichannel printer utilizes seven independent channels and subsequently we obtain first seven basis vectors from PCA and then compute the convex hull. From the borders of each intersection within hyper-plane, the target reflectance is found as a distance or vector position relative to the borders. To evaluate if the target vector distance (position) is within the convex hull, we use *inhull* Matlab function [12]. As function does not include spectra that are lying on the border of the convex hull, we further set the limit and "desaturate" target spectra to obtain full in-gamut information. Although we are not considering any gamut mapping within this work, we report the distance or how far from the spectral gamut borders certain point is located.

2.1 Experimental part

To establish process of spectral printing one must have control of all independent channels of a given printer. The ONYX RIP was employed to drive our twelve channel printer (HP Z3200 ink - jet) where we could control ink limits and run each channel to its maximum in order to have real physical capabilities of this device. Although the printer is equipped with light/diluted inks and special colours, for our purposes we consider that it has essentially seven independent channels (CMYKRGB). The printer is driven through the information from a 7-channel tiff file where digital values for each channel are encoded. The substrates used for printing were HP Artists Matte Canvas and HP Premium Matte Photo Paper. The former has surface structure that best resembles texture of the textile-like material, where latter has largest gamut, especially in dark areas (using Photo Black colour).

In order to have controlled comparison between textile and paper printed samples we have to compensate for the differences in measurement methodology. In graphic arts the dominant measurement geometry is 0:45, where in textile industry, the standard instrumentation has d:8 geometry. The latter integrates incoming light and effectively neglects the texture of the textile material. Instruments used in our study were Gretag Macbeth i1 and Datacolour 6500 which has much more sensitivity in dark region.

Sample preparation for measurement of textile assumes double folded material. Due to the nature of sample preparation for a measurement and the texture of surface, when two textile samples are compared, the most commonly used colour difference formula is ΔE_{CMC} where L channel is normalized by factor 2. The same could be applied to the comparison of the coloured textile and paper printed sample. In fact we are referring that the measurements of an anisotropic, porous surface need to be scaled in order to compare with uniformly coloured patch (textile versus paper).

3. RESULTS AND DISCUSSION

The colour comparison starts with gamut plots obtained after establishing custom printing workflow, where each channel of the printer is controlled and where ink limitation setup allowed for each channel to go to its maximum for a given substrate. Further on we have included primaries ramps (CMYKRGB) measured with Datacolour 6500 d:8 instrument. This allowed us to visualize the difference produced by these measurements geometries.

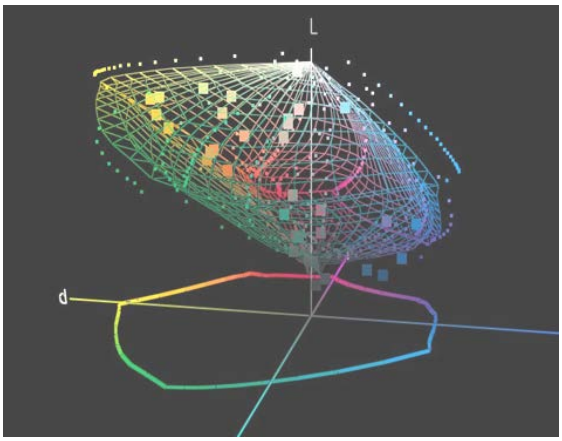

Figure 1. The plot of the basic gamut with ink limitation control and measurement with 0:45 geometry (wireframe), gamut regions measured with d:8 geometry (smaller squares) and sampled textile colour (bigger squares).

It can be seen from *Figure 1* that most of the textile colours that are outside of the printable gamut are located in the section of low lightness. All the sample colours are within a* and b* dimension of the gamut volume but they tend to be out of the printable gamut in lower part of the lightness (L*) dimension.

The paper surface that is used for this evaluation has high scattering properties and low ink penetration. Also, the structure of the canvas type material leaves some unprinted part of the elevated surface and this can cause the full gamut volume to rise up in the lightness direction. Therefore some of the dark samples cannot be reproduced with this material. Alternative would be to use different substrate for this group of the samples or to meet them with colour dyed paper. On the below figure, we plot all colours in hue-saturation direction using both canvas and photo-paper. Photo – paper provides wider gamut range, even in dark areas, but measurements here neglects gloss effect which would induce appearance change that makes it unsuitable for simulation of textile material.

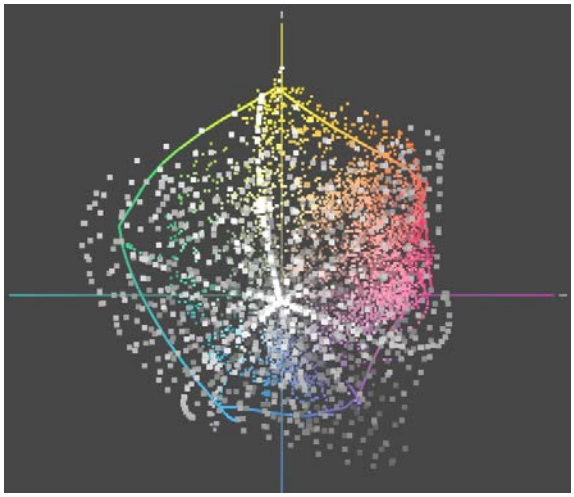

Figure 2. 2D plot of 4872 textile colours (colour points), HP Canvas matte substrate (line frame), white points (photo-paper).

From Figure 2 we can conclude that there are some issues in orange-red region where even with photo paper we are not able to meet this section. Addition of orange colour (to all others) that is present in some multichannel systems would improve simulation. Also, exclusion of the GCR increases variability in dark region, and even if this is not feasible in terms of ink consumption, spectral or multichannel printing should not be concerned by that. On Table 1, we summarise this comparison in terms of ΔE_{CMC} colour difference.

Table 1. ΔE_{CMC} Colour difference between printed and textile samples after application of ink limitation on each controlled channel and measurements with d:8 geometry

ΔE_{CMC}			
illuminant	*Min*	*Max*	*Avg.*
D50	*0.13*	*5.5*	*1.1*
D65	*0.13*	*4.9*	*1.28*
A	*0.13*	*4.4*	*1.2*
C	*0.1*	*5.6*	*1.2*
F2	*0.1*	*4.2*	*1.05*
UL 3000	*0.1*	*3.9*	*1.02*

With the exception of dark colours and orange sector, the differences are between colours seems to not be visible. This would effectively mean that this process is feasible after some adjustments. However we can have no such claims on overall appearance of the samples where texture might play large roll.

Now we perform spectral analysis where printer space is represented as a seven dimensional convex hull constrained with basis vectors. These basis vectors are derived through PCA and they reduce dimensionality from e.g. 36 (380-730 in 10nm step) to 7. Therefore, we selected first seven PC that corresponds to the number of independent colourants within our multichannel printing system. To make the analysis more intuitive, we have performed varimax rotation of the basis vectors which yields spectral curves that closely resembles seven channel systems (Figure 3).

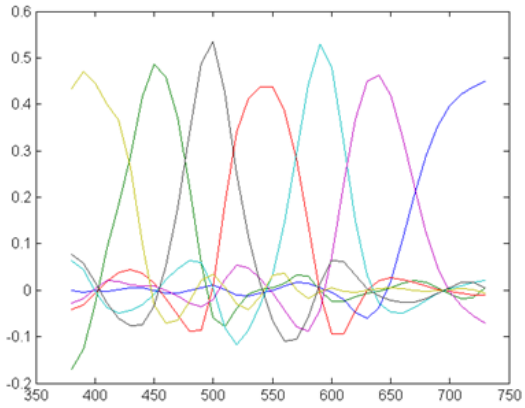

Figure 3. First seven basis vectors spanning the printer space with varimax rotation applied to reduce negative components of the PC.

The cross sections through the seven dimensional convex hull are represented as three dimensional objects projected on two dimensional plane. It is rather convenient way to visualize spectral gamut and corresponds with some of the previous attempts [5,10]. Slices that are represented here combine two basis vectors (1st and 2nd , 3rd and 4th , 5th and 6th) where *convhulln* function has been used to obtain indices of the hull (Figure 4 to 6). Approximated spectral gamut can then be compared with reflectance (textile samples) transformed to the same PCA space.

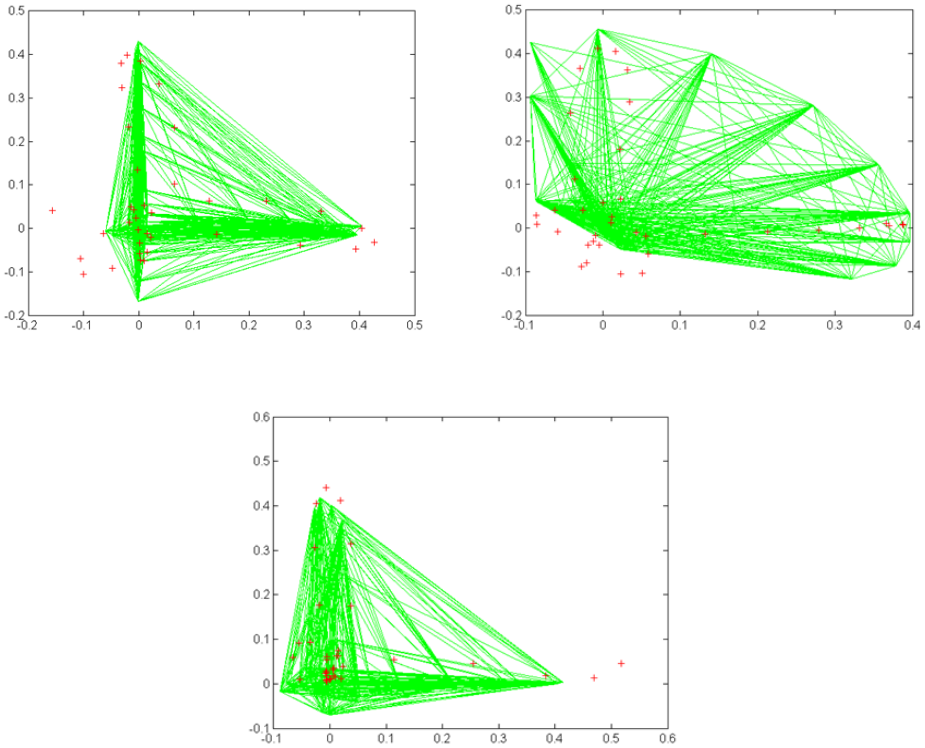

Figure 4(top right),5(top left),6(bottom centred) – Convex hull of two basis vectors (green object) and test points (red pluses). The figures show two dimensional projection (cross section) of 3D objects where two basis vectors combine.

Further on, we used *inhull* function to evaluate number and percentage of spectra we can include in spectral printer gamut. Out of the 4872 evaluated textile reflectances, it is possible to include 3939 within spectral printer gamut. This corresponds to around 75% of evaluated reflectances with maximum RMS = 0.22 for out of gamut reflectances. As it was case previously (colour gamut comparison), the most error occurs within low reflective area and orange sector. This can be seen from Figure 7 which is the combination of 5th and 6th PC that are corresponds to orange – red sector.

Additional analysis can be found in Table 2 where we evaluated how spectral gamut coverage is changed with dimensions added. Generally, adding more basis vectors will improve recovery of the spectra within the data set. However, more dimensions do not necessarily imply better representation of other data set. For this reason there is a decrease in overall spectral coverage of the multidimensional gamut where the variability and spectral error within data set improves.

Table 2. Spectral and dimensionality analysis printable reflectance of textile colours

PCA	%variability included	%in gamut	Mean RMS (in-gamut)	Max RMS (out of gamut)
3D	98.3	88%	0.041	0.22
4D	99.9	76%	0.033	0.21
5D	100	73%	0.028	0.15
6D	100	65%	0.025	0.15
7D	100	52%	0.022	0.14

This counters idea that increases in dimension within the PCA analysis better characterize the data set if more PC are included. One way to explain this is when we have all colours within 2D gamut (e.g. hue, saturation – Figure 3) and not in 3D (when lightness added – Figure 2). Different substrates used for printing will require different number of basis vectors to accurately represent the data. As four basis vectors are sufficient to represent our multichannel printer with given substrate, adding more dimensions will result in more samples out of the gamut [5]. The difference between percentage spectral and colour coverage lies in fact that multiple reflectances can map to the same colour (metamerism). Other reason why more spectra are outside the gamut that it is colour (75% vs 90%) is in representation of the spectral gamut and in the nature of colorants. Namely we are dealing here with essentially different chemicals used for colouration (ink vs dye) that have different spectral properties but can map to same colour. Also when we increase dimensions to represent the gamut, there is always possibility of match in lower dimensions that would not match in higher dimensions. However, as metamerism is one of the biggest problems in textile industry, spectral analysis is gaining importance and should be included in reproduction chain. Other option would be to use reproduction chain within given set of illuminants used in graphic arts and textile industry and to perform gamut mapping in these restricted multi-illuminant spaces [9]. Also evaluation of the difference should be performed in multi-illuminant metric (MIPE) [5] as working in spectral space not correlates very well with visual space. Spectral gamut analysis could be further used as a base for spectral gamut mapping [10]. In this study we have been more concerned with in gamut spectra but there is a possibility to determine distance of the point (reflectance) from the gamut boundary.

4. CONCLUSIONS

In this work we presented two alternatives for the reproduction of the textile colour onto paper substrates. With multichannel ink-jet systems, it is much more likely that we can accurately reproduce textile colours and spectra. To maximize the capabilities of these devices, the full spectral printing workflow should be established. There the maximum potential of the available inks will be used as well as the control of the individual channels. Also the colourant selection process should be performed in order to address the shortcomings that current multichannel systems have for this application.

Reduced dimensionality of the spectral space of a printer leads to possibility of representing multidimensional gamut as a convex hull. Approximated spectral gamut can then be compared with reflectance transformed to the same PCA space where multiple cross sections can lead to the visualization of the spectral gamut. Spectral analysis shows that 75 % of textile colours spectra can be included in printable spectral gamut. As many of

these colours (25% at least) have its metamers that maps to the same point in colour space, alternative approach to the reproduction should be used. In colour workflow, it is feasible to use multichannel printers for simulation of textile colours where in pure spectral workflow is still not satisfying. Although the texture has and its influence to colour perception of the sample is not evaluated here, it will be addressed in future work.

REFERENCES

1. Green, P.J. (2010), Colour Management : Understanding and Using ICC Profiles, Wiley, Feb. 2010.

2. Marijanovic, K. (2011). Spectral print reproduction - modelling and feasibility. Master thesis, Gjøvik University College, 2012.

3. Slavuj, R., Marijanovic, K., Hardeberg, J.Y. (2013). Feasibility study for textile colour simulation with multichannel printing technology, AIC, Newcastle, UK.

4. Gerhardt, J. and Hardeberg, J.Y. (2006), Spectral colour reproduction by vector error diffusion, In Proceedings CGIV 2006, pp. 469–473.

5. Morovic, P, Morovic, J. , Arnabat, J. (2012), Revisiting Spectral Printing: A Data Driven Approach, 20th Colour and Imaging Conference Final Program and Proceedings, pp. 335–340.

6. Taplin, L. A. (2001), Spectral Modelling of a Six-Colour Inkjet Printer, Msc Thesis, Rochester Institute of Technology, NY, USA.

7. Tzeng, D., & Berns, R. S. (1998), Spectral-Based Ink Selection for Multiple Printing Colourant Estimation of Original Objects, The Sixth Colour Imaging Conference: Colour Science, Systems and Applications, pp. 106 -111.

8. Urban, P. (2013), Spectral Image Reproduction Workflow: From Pixel to Print, ROND, Spectral Printing – Opportunities, Challenges and Outlook, MIUN, Sweden

9. Urban, P., Berns, R.S. (2011). Paramer Mismatch – based Spectral Gamut Mapping, IEEE Transactions on Image Processing, Vol.20, Issue 6, pp.1599 – 1610.

10. Bakke, A.M., Hardeberg, J.Y. and Farup, I. (2005), Multispectral gamut mapping and visualization: a first attempt. SPIE Proceeding on Colour Imaging X: Processing, Hardcopy, and Applications, pp 193-200, San Jose, California, USA, Jan, 2005.

11. Alsam A. and Hardeberg Y. (2005). Optimal colourant design for spectral colour reproduction, Colour Imaging: Processing, Hardcopy, and Applications X, SPIE Proceedings 5667, pp. 38-46.

12. J.D'Errico, "Inhull" http://www.mathworks.com/matlabcentral/fileex change /10226-inhull.

Erratum

This version of the thesis has been corrected for the page numbers mismatches that are present in the original (printed version).

The first page has been replaced with more appropriate, high resolution logo of the HiG. Other changes are visible in the Table of Contents which now corresponds to the page numbers in the document.

Remaining corrections are concerned on font and size of the page numbers and on uniform alignments of the headers and footers.

23.12.2015. Radovan Slavuj